ENCLOSURE 4
ATTACHMENT 6

H.B. ROBINSON STEAM ELECTRIC PLANT, UNIT NUMBER 2
Westinghouse WCAP-18944-NP, Revision 1,
"H.B. Robinson Unit 2 Subsequent License Renewal: Reactor Vessel Upper Shelf Energy Equivalent Margins Analysis," December 2024

WCAP-18944-NP
Revision 1

December 2024

H.B. Robinson Unit 2 Subsequent License Renewal: Reactor Vessel Upper Shelf Energy Equivalent Margin Analysis

Westinghouse

*** This record was final approved on 12/06/2024 08:42:18. (This statement was added by the PRIME system upon its validation)

WCAP-18944-NP
Revision 1

H.B. Robinson Unit 2 Subsequent License Renewal: Reactor Vessel Upper Shelf Energy Equivalent Margin Analysis

December 2024

Gordon Z. Hall*
Structural Design and Analysis
(All Except Appendix A)

J. Brian Hall*
Materials Innovation
(Appendix A)

Verifier: B. Reddy Ganta*
Structural Design and Analysis
(All Except Appendix A)

Gordon Z. Hall*
Structural Design and Analysis
(Appendix A)

Reviewers: Thomas E. Demers*
Structural Design and Analysis

Approved: Gerrie W. Delport* for Stephen P. Rigby, Manager
Structural Design and Analysis

*Electronically approved records are authenticated in the electronic document management system.

Westinghouse Electric Company LLC
1000 Westinghouse Drive
Cranberry Township, PA 16066, USA

© 2024 Westinghouse Electric Company LLC
All Rights Reserved

*** This record was final approved on 12/06/2024 08:42:18. (This statement was added by the PRIME system upon its validation)

FOREWORD

This document contains Westinghouse Electric Company LLC proprietary information and data which has been identified by brackets. Coding [(a,c,e)] associated with the brackets sets forth the basis on which the information is considered proprietary.

The proprietary information and data contained in this report were obtained at considerable Westinghouse expense and its release could seriously affect our competitive position. Westinghouse has policies in place to identify proprietary information. Under that system, information is held in confidence if it falls in one or more of several types, the release of which might result in the loss of an existing or potential competitive advantage, as follows:

(a) The information reveals the distinguishing aspects of a process (or component, structure, tool, method, etc.) where prevention of its use by any of Westinghouse's competitors without license from Westinghouse constitutes a competitive economic advantage over other companies.

(c) Its use by a competitor would reduce his expenditure of resources or improve his competitive position in the design, manufacture, shipment, installation, assurance of quality, or licensing a similar product.

(e) It reveals aspects of past, present, or future Westinghouse or customer funded development plans and programs of potential commercial value to Westinghouse.

The document herein is bracketed and marked to indicate the bases for withholding. The justification for withholding is indicated in both proprietary and non-proprietary versions by means of lower-case letters (a) (c) and (e) located as a superscript immediately following the brackets enclosing each item of information being identified as proprietary or in the margin opposite such information. These lower-case letters refer to the types of information Westinghouse customarily holds in confidence identified above.

The proprietary information in the brackets is provided in the proprietary version of this report (WCAP-18944-P, Revision 1).

*** This record was final approved on 12/06/2024 08:42:18. (This statement was added by the PRIME system upon its validation)

RECORD OF REVISIONS

Revision	Date	Revision Description
0	August 2024	Original issue.
1	See PRIME	Addressing additional customer comments for Appendix A. The main body of report is unchanged. Changes are marked with change bars.

*** This record was final approved on 12/06/2024 08:42:18. (This statement was added by the PRIME system upon its validation)

TABLE OF CONTENTS

ACRONYMS v

EXECUTIVE SUMMARY vi

1 INTRODUCTION 1-1
2 REGULATORY REQUIREMENTS 2-1
2.1 REGULATORY REQUIREMENTS 2-1
2.2 COMPLIANCE WITH 10 CFR 50 APPENDIX G AND ACCEPTANCE CRITERIA 2-1
2.2.1 ASME Section XI Code Reconciliation 2-2
2.3 ACCEPTANCE CRITERIA 2-2
2.3.1 Levels A and B Service Loadings 2-2
2.3.2 Level D Service Loadings 2-3
3 EQUIVALENT MARGINS ANALYSIS INPUTS 3-1
3.1 FINITE ELEMENT STRESS ANALYSIS 3-1
3.1.1 Mechanical Loads 3-4
3.1.2 Reactor Coolant System Transients 3-5
3.2 J-INTEGRAL RESISTANCE MODELS 3-7
3.2.1 Reactor Vessel Nozzle-to-Shell Weld 3-7
3.2.2 Reactor Vessel Nozzle Forging Base Metal 3-9
3.2.3 Reactor Vessel Upper/Intermediate Shell Plates 3-13
4 FRACTURE MECHANICS ANALYSIS 4-1
4.1 METHODOLOGY DISCUSSION 4-1
4.1.1 Nozzle-to-Shell Welds and Upper/Intermediate Shell Forging 4-1
4.1.2 Nozzle Corner K_I Closed-Form Solution 4-3
4.1.3 Calculation of J for Small-Scale Yielding 4-3
4.1.4 Postulated Flaws 4-4
4.1.5 Weld Residual Stress 4-4
4.1.6 Stress due to Mechanical Loads 4-4
4.2 APPLIED J-INTEGRAL RESULTS AND COMPARISON WITH J-R CURVE ALLOWABLES 4-5
4.2.1 Nozzle-to-Shell Welds Levels A/B 4-5
4.2.2 Nozzle-to-Shell Welds Level D 4-7
4.2.3 RV Nozzle Forgings Levels A/B 4-10
4.2.4 RV Nozzle Forgings Level D 4-13
4.2.5 Upper and Intermediate Shell Plates Levels A/B 4-17
4.2.6 Upper and Intermediate Shell Plates Level D 4-19
5 CONCLUSIONS 5-1
6 REFERENCES 6-1

Appendix A Upper Shelf Fracture Toughness Testing of Robinson Reactor Pressure Vessel Steel Plate A-1

*** This record was final approved on 12/06/2024 08:42:18. (This statement was added by the PRIME system upon its validation)

ACRONYMS

ASME	American Society of Mechanical Engineers
ASTM	American Society for Testing and Materials
CMTR	certified material test report
CVN	Charpy v-notch
DW	deadweight
eLBB	extended loss of coolant accident
EMA	equivalent margin analysis
EOLE	end-of-license-extension
FEA	finite element analysis
FEM	finite element model
HAZ	heat affected zone
J	J-integral due to the applied loads, in-lb/in^2 (or lbf/in^2)
J_1	applied J-integral at a flaw depth of a_0 + 0.1 in., in-lb/in^2 (or lbf/in^2)
J-R	J-integral fracture resistance for the material, or J-material, or J_R
J-R curve	J-integral fracture resistance vs. crack-extension curve
$J_{0.1}$	J-integral fracture resistance for the material at a ductile flaw extension of 0.1 in
LOCA	loss of coolant accident
NRC	Nuclear Regulatory Commission
OBE	operating basis earthquake
RG	regulatory guide
RNP	H.B. Robinson Nuclear Plant
RPV or RV	reactor pressure vessel
SF	structural factor (dimensionless)
SIF	stress intensity factor, ksi√in
LSB	large steam line break
SLR	subsequent license renewal
SRSS	square root sum of squares
SSE	safe shutdown earthquake
USE	upper shelf energy
WRS	weld residual stress, ksi

*** This record was final approved on 12/06/2024 08:42:18. (This statement was added by the PRIME system upon its validation)

EXECUTIVE SUMMARY

At the start of the 80-year subsequent license renewal (SLR) project of the H.B. Robinson Nuclear Plant (RNP) Unit 2, several locations of the reactor vessel (RV) were identified as being at risk to potentially drop below the upper shelf energy (USE) limit of 50 ft-lb per 10 CFR 50, Appendix G. Materials with end-of-license-extension (EOLE) USE below 50 ft-lb are required to be evaluated per paragraph IV.A.1.a of 10 CFR 50, Appendix G. This report presents the methodology and results of the equivalent margins analysis (EMA) for the following locations for the 80-year SLR:

- Intermediate Shell Plates
- Upper Shell Plates
- RV Inlet and Outlet Nozzle Forgings
- Nozzle-to-Shell Welds

[

]^{a,c,e}

Levels A and B Conditions

For all evaluated locations, the J for the postulated flaw plus a 0.1-inch flaw extension (J_1) with a structural factor (SF) of 1.15 for accumulation pressure, and SF of 1.0 for thermal are below the J-material at 0.1-inch flaw extension ($J_{0.1}$). Therefore, the acceptance criteria in ASME Section XI, K-2200 (a)(1) [6] is satisfied.

The slope of J (with a SF=1.25 for accumulation pressure, SF=1 for thermal) is less than the J-integral resistance (J-R) curve at the intersection of both curves (i.e., when J = J-R). Therefore, the stability acceptance criteria in ASME Section XI, K-2200 (a)(2) [6] is satisfied.

Levels C and D Conditions

There is no Level C or Level D transient defined in the reactor vessel design specification. The Level D large steam line break transient per the current design basis, generic 60-year EMA, WCAP-13587, Rev. 1, Figure 3-2 [2] is analyzed to bound Levels C/D conditions.

For the evaluated locations, the J_1 with a SF of 1.0 are below the $J_{0.1}$. Therefore, the acceptance criteria in ASME Section XI, K-2400 (a) [6] is satisfied.

The slope of J is less than the J-R curve at the intersection of both curves (i.e., when J = J-R). Therefore, the stability acceptance criteria in ASME Section XI, K-3400 [6] is satisfied. Using this approach, Level D loadings are shown to satisfy the more limiting Level C acceptance criteria established by K-2300 [6].

Per K-2400 of [6], all flaws evaluated for Level D assumed a flaw depth equal to 1/10 of the base metal thickness, plus the cladding thickness, but not exceeding 1 inch, plus a 0.1-inch flaw extension. All flaws evaluated herein have been shown to exhibit ductile and stable flaw extension when compared to $J_{0.1}$ for all Level D loading conditions. This satisfies the 75% of wall thickness requirement, per K-2400 (c) [6], as the final flaw size, after extension, is much less than 75% of the wall thickness.

Additionally, the maximum Level D internal pressure is less than the tensile instability pressures calculated per K-5300 (b) [6] for all evaluated locations and flaws.

*** This record was final approved on 12/06/2024 08:42:18. (This statement was added by the PRIME system upon its validation)

1 INTRODUCTION

The purpose of this report is to document the equivalent margins analysis (EMA) for H.B. Robinson Nuclear Plant (RNP) Unit 2 reactor vessel (RV) to support an 80-year subsequent license renewal (SLR), per the Duke Energy contract RNP-2077-04-SLR-001, Task 3(j) [1]. It is noted that the current analysis of record for RNP Unit 2 is the generic Westinghouse EMA in WCAP-13587 [2].

Per paragraph IV.A.1.a of 10 CFR 50, Appendix G, RV beltline materials with end-of-license extension (EOLE) Upper Shelf Energy (USE) below 50 ft-lb limit are required to be evaluated for margins of safety against fracture equivalent to those required by Appendix G of Section XI of the ASME Code. Several locations were identified in [1] at the start of the project as being at risk to potentially drop below the minimum USE of 50 ft-lb. These following locations are addressed for the 80-year SLR by the EMA provided herein:

- Intermediate Shell Plates
- Upper Shell Plates
- RV Inlet and Outlet Nozzle Forgings
- Nozzle-to-Shell Welds

The RNP Unit 2 intermediate shell and upper shell plates are considered beltline materials per WCAP-18766-NP [4]. The RV extended beltline is defined as the region of materials that meet or exceed a neutron fluence exposure of 1.0 E+17 n/cm^2 (E> 1.0 MeV). As discussed in Section 3 and Tables 5-2 and 5-3 of WCAP-18766-NP [4], the RV inlet/outlet nozzles and nozzle welds were considered as extended beltline material conservatively assuming fluence value of 2.0 E+17 n/cm^2 (E> 1.0 MeV). The 10 CFR 50, Appendix G paragraph IV.A.1.a requirements for beltline material is applied to the extended beltline materials herein.

For the EMA, Table 5-3 of WCAP-18766-NP [4] provides USE values for the reactor vessel, including the upper and intermediate shell plates, nozzle-to-shell welds and nozzle forgings. Due to lack of test orientation information in the nozzle forging certified material test reports (CMTR), PWROG-23006-NP [3] provided conservative USE values for the inlet and outlet nozzle forgings for the purpose of EMA. [

]^{a,c,e}

*** This record was final approved on 12/06/2024 08:42:18. (This statement was added by the PRIME system upon its validation)

2 REGULATORY REQUIREMENTS

2.1 REGULATORY REQUIREMENTS

In accordance with 10 CFR 50, Appendix G, IV.A.1, [5] Reactor Vessel Upper Shelf Energy Requirements are as follows.

(a) "Reactor Vessel beltline materials must have Charpy upper-shelf energy in the transverse direction for base material and along the weld for weld material according to the ASME Code, of no less than 75 ft-lb (102 J) initially and must maintain Charpy upper-shelf energy throughout the life of the vessel of no less than 50 ft-lb (68 J), unless it is demonstrated in a manner approved by the Director, Office of Nuclear Reactor Regulation, that lower values of Charpy upper-shelf energy will provide margins of safety against fracture equivalent to those required by Appendix G of Section XI of the ASME Code. This analysis must use the latest edition and addenda of the ASME Code incorporated by reference into 10 CFR 50.55a (b)(2) at the time the analysis is submitted.

(b) Additional evidence of the fracture toughness of the beltline materials after exposure to neutron irradiation may be obtained from results of supplemental fracture toughness tests for use in the analysis specified in section IV.A.1.a.

(c) The analysis for satisfying the requirements of section IV.A.1 of this appendix must be submitted, as specified in § 50.4, for review and approval on an individual case basis at least three years prior to the date when the predicted Charpy upper-shelf energy will no longer satisfy the requirements of section IV.A.1 of this appendix, or on a schedule approved by the Director, Office of Nuclear Reactor Regulation."

In accordance with NRC Regulatory Guide 1.161 [13], the NRC has determined that the analytical methods described in ASME Section XI, Appendix K, provide acceptable guidance for evaluating reactor pressure vessels when the Charpy USE falls below the 50 ft-lb limit of Appendix G of 10 CFR Part 50. However, the staff noted that Appendix K does not provide information on the selection of transients and provides very little detail on the selection of material properties. Consistent with PWROG-19047-NP-A [17], the cooldown transient for RNP with a constant pressure of 2750 psia assumed throughout the transient bounds all Levels A/B conditions. This is consistent with and based on the ASME Section XI, Appendix K 100°F/hour cooldown rate guidance coincident with the use of a high pressure value. The Level C/D transient selection is based on the guidance in Regulatory Guide 1.161 Section 4.0 [13]. Based on [8], there is no Level C or D transient defined in the design specification. The level D large steam line break (LSB) transient per the current design basis, WCAP-13587, Rev. 1, Figure 3-2 [2] is analyzed to bound Levels C/D conditions. For clarity, this report will refer to this loading condition as Level D instead of Level C/D. Additional transient discussions are contained in Section 4.1.

2.2 COMPLIANCE WITH 10 CFR 50 APPENDIX G AND ACCEPTANCE CRITERIA

The analyses reported herein are performed in accordance with the code of record, 2007 Edition with 2008 Addenda of the ASME Code Section XI, Appendix K [6]. Per the design input request response [7], Duke Energy concurs that NRC has authorized use of the 2007 Edition and 2008 Addenda of Section XI through 10CFR50.55a. The material properties used for the finite element stress analysis are based on the original RV construction code. See Section 3.1 for detailed discussion on material properties for the finite element analysis (FEA).

*** This record was final approved on 12/06/2024 08:42:18. (This statement was added by the PRIME system upon its validation)

2.2.1 ASME Section XI Code Reconciliation

In accordance with 10 CFR 50.60, Appendix G, IV, 1., low values of USE require an analysis (EMA) to demonstrate adequate margins of safety against fracture equivalent to those required by Appendix G of Section XI of the ASME Code. The analysis must use the latest NRC approved edition and addenda of the ASME Code, which is 2019 Edition. The EMA herein is performed in accordance to ASME Section XI Appendix K. There has been no substantive change of ASME Section XI Appendix K between 2007 Edition through 2008 Addenda [6] and 2019 Edition [9]. Therefore, the RNP ASME XI code of record, 2007 Edition through 2008 Addenda [6] is reconciled to the current NRC approved ASME Code 2019 Edition.

2.3 ACCEPTANCE CRITERIA

ASME Section XI, Appendix K [6] provides the acceptance criterial for the Level A, B, C and D conditions. These criteria summarized in the following subsections are consistent with Regulatory Guide 1.161.

The EMA is performed in accordance with ASME Section XI [6], Appendix K. This is consistent with previous SLR EMAs, such as B&W designed plants Surry and Turkey Point [15 and 16], and Westinghouse designed plant, North Anna [17] which had been accepted by NRC. As discussed in Section 4.1, detailed FEA thermal transient, pressure, mechanical and residual stresses were used in the calculation of K_I and J. This is more rigorous than the K_I formulas in K-4200 which uses generic stress calculations for cylinders.

Based on previous EMAs such as North Anna [17], the Appendix K approach was also applied to the locations of the nozzle corners in a manner consistent with the other locations evaluated herein. This includes the ¼ wall thickness flaw assumption for Level A and B conditions, which is reasonable for the reactor vessel shell but results in a postulated flaw of more than 3 inches for the nozzle forging at the nozzle corners (due to the nozzle corner having a larger thickness than the reactor vessel shell). This postulated flaw size is very large, and therefore this approach is considered conservative for the nozzle corner locations. This conservatism is acceptable and appropriate as the nozzle corner is evaluated and shown to be acceptable using the Appendix K criteria.

2.3.1 Levels A and B Service Loadings

Per ASME Section XI, K-2200 [6]:

(a) Postulated axial and circumferential flaws are interior semi-elliptical surface flaws with a depth of ¼ of the wall thickness and a length to depth (l/a) aspect ratio of 6.

  (1) J with a SF of 1.15 for accumulation pressure, and an SF of 1.0 for thermal (cooldown) shall be less than the J-integral of the material (J-R curve) at a ductile flaw extension of 0.1 inch. Accumulation pressure is defined in K-1300 as 1.1 times design pressure which is 2.5x1.1=2.75ksi.

  (2) J with a SF of 1.25 for accumulation pressure and a SF of 1.0 for thermal (cooldown) shall be ductile and stable. The flaw stability criteria is per K-3400 [6]: $\frac{\partial J}{\partial a} < \frac{dJ_R}{da}$ at J ≡ JR.

(b) The J-R curve shall be a conservative representation for the vessel material under evaluation.

As noted above, the flaw stability criteria per K-3400 is: $\frac{\partial J}{\partial a} < \frac{dJ_R}{da}$ at J ≡ JR. This is further explained in K-4310. The J-R curve shall be plotted on the crack driving force diagram and shall intersect the horizontal axis at the initial flaw depth, a_0. Flaw stability at a given applied load is verified when the slope of the J curve is less than the slope of the J-R curve at the point on the J-R curve where the two curves intersect.

*** This record was final approved on 12/06/2024 08:42:18. (This statement was added by the PRIME system upon its validation)

2.3.2 Level D Service Loadings

Per ASME Section XI [6], K-2400, the Level D postulated flaws shall be the same as those specified for Level C in K-2300.

(a) Postulated axial and circumferential flaws are interior semi-elliptical surface flaws with depths up to 1/10 of the wall thickness of the base metal plus cladding, with total depth not exceeding 1 inch. For cases where 1/10 wall thickness plus cladding exceeded 1 inch, 1 inch is used for the postulated flaws for Level D. The length to depth (ℓ/a) aspect ratio is 6.

(1) J with a SF of 1.0 for thermal and pressure shall be less than the J-R curve at a ductile flaw extension of 0.1 inch. Note that the K-2300(a)(1) criteria for Level C is conservatively considered herein for Level D conditions.

(2) J with a SF of 1.0 for thermal and pressure shall be ductile and stable.

(b) The J-R curve shall be a conservative representation for the vessel material under evaluation.

(c) The total flaw depth after stable flaw extension shall be less than or equal to 75% of the vessel wall thickness, and the remaining ligament shall not be subject to tensile instability.

The flaw stability criteria is detailed in K-5300.

(a) Stability is verified per K-3400: $\frac{\partial J}{\partial a} < \frac{dJ_R}{da}$ at J ≡ JR.

(b) For Level D Service Loadings, demonstrate that total flaw depth after stable flaw extension is less than or equal to 75% of the vessel wall thickness, and the remaining ligament is not subjected to tensile instability. The internal pressure shall be less than the instability pressure (P_I), calculated by the equations below:

(1) For axial flaw, $P_I = 1.07\sigma_o \left[\frac{1 - A_c/A}{\frac{R_i}{t} + \frac{A_c}{A}}\right]$

(2) For circumferential flaw, $P_I = 1.07\sigma_o \left[\frac{1 - A_c/A}{\frac{R_i^2}{2R_m t} + \frac{A_c}{A}}\right]$

P_I is limited to $P_I = 1.07\sigma_o \left[\frac{t}{R_i}\right]$

where,

σ_o	=	Flow stress, average of yield strength and ultimate tensile strength
A	=	An area parameter = t (ℓ + t)
A_c	=	Area of the flaw = $\pi a \, \ell / 4$
R_i	=	Inner radius of the vessel
R_m	=	Mean radius of the vessel
t	=	Wall thickness of the vessel
a	=	Flaw depth
ℓ	=	Flaw length

*** This record was final approved on 12/06/2024 08:42:18. (This statement was added by the PRIME system upon its validation)

3 EQUIVALENT MARGINS ANALYSIS INPUTS

3.1 FINITE ELEMENT STRESS ANALYSIS

The general procedures for J-integral calculation are described in ASME Section XI, Appendix K [6]. As discussed in Section 2.1, the cooldown transient was analyzed to bound Levels A/B. The Level D transient is SLB. Figure 3-1 through Figure 3-3 illustrates the finite element model (FEM) of the Robinson reactor vessel. Geometry and dimensions are taken from design drawings. The applied loadings consist of pressure, thermal and attached piping and support reactions at the RV nozzles. Multiple cutlines for each location of interest were placed to extract through-wall stress profiles as a function of time. J integrals are then calculated as described in 4.1 using the FEA through-wall stresses for all time points. The most limiting values are reported in Section 4.2.

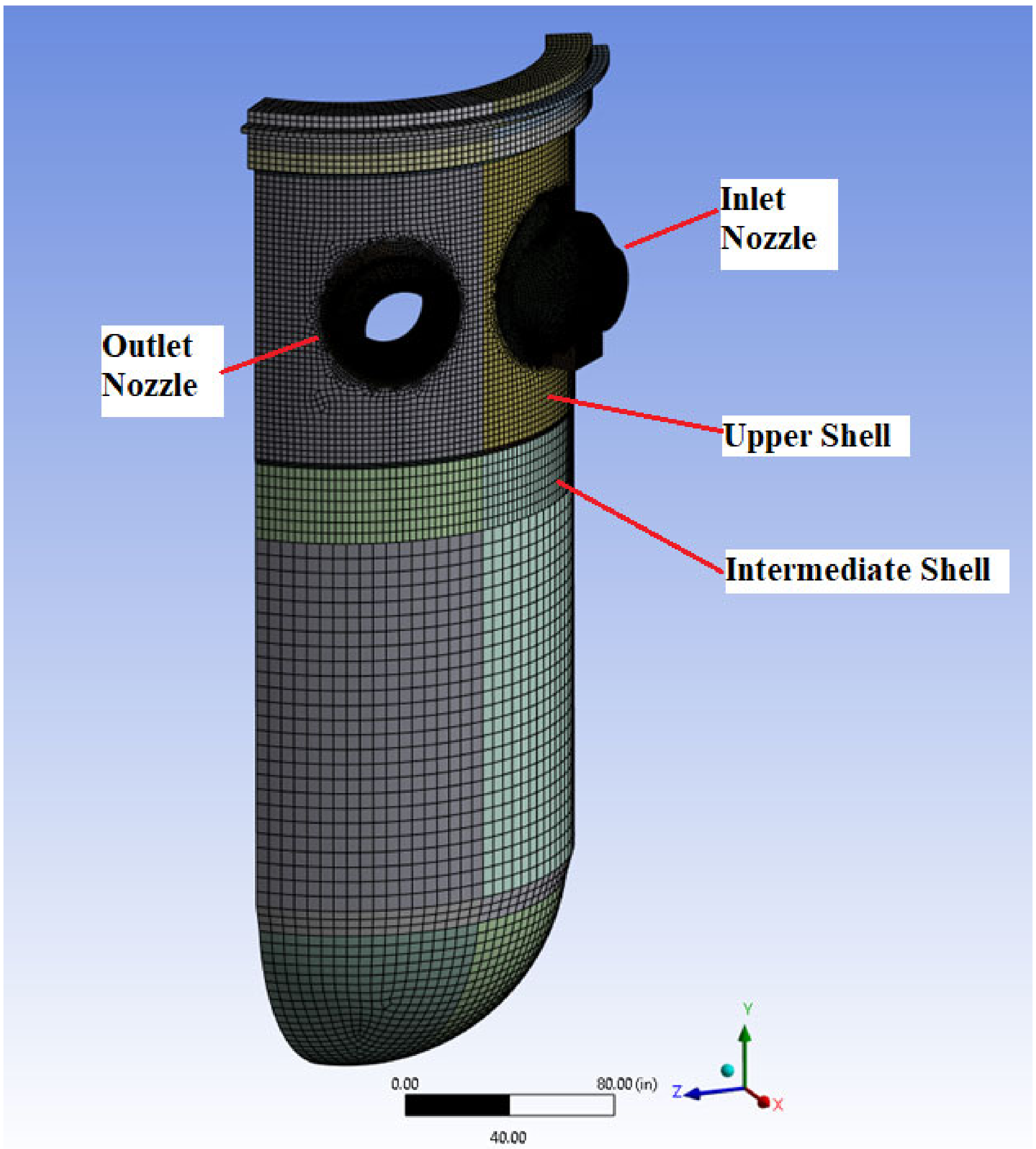

Figure 3-1: Robinson Reactor Vessel Finite Element Model Overview

*** This record was final approved on 12/06/2024 08:42:18. (This statement was added by the PRIME system upon its validation)

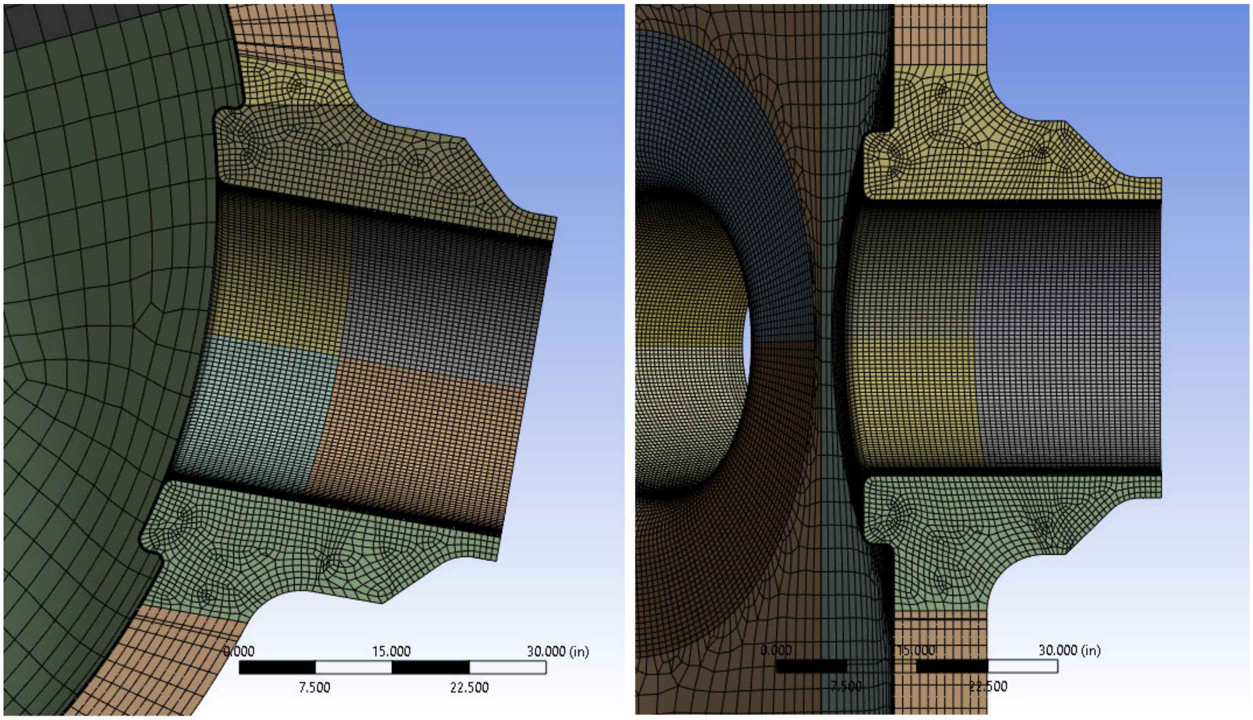

Top View **Side View**

Figure 3-2: Robinson Reactor Vessel Finite Element Model Outlet Nozzle Details

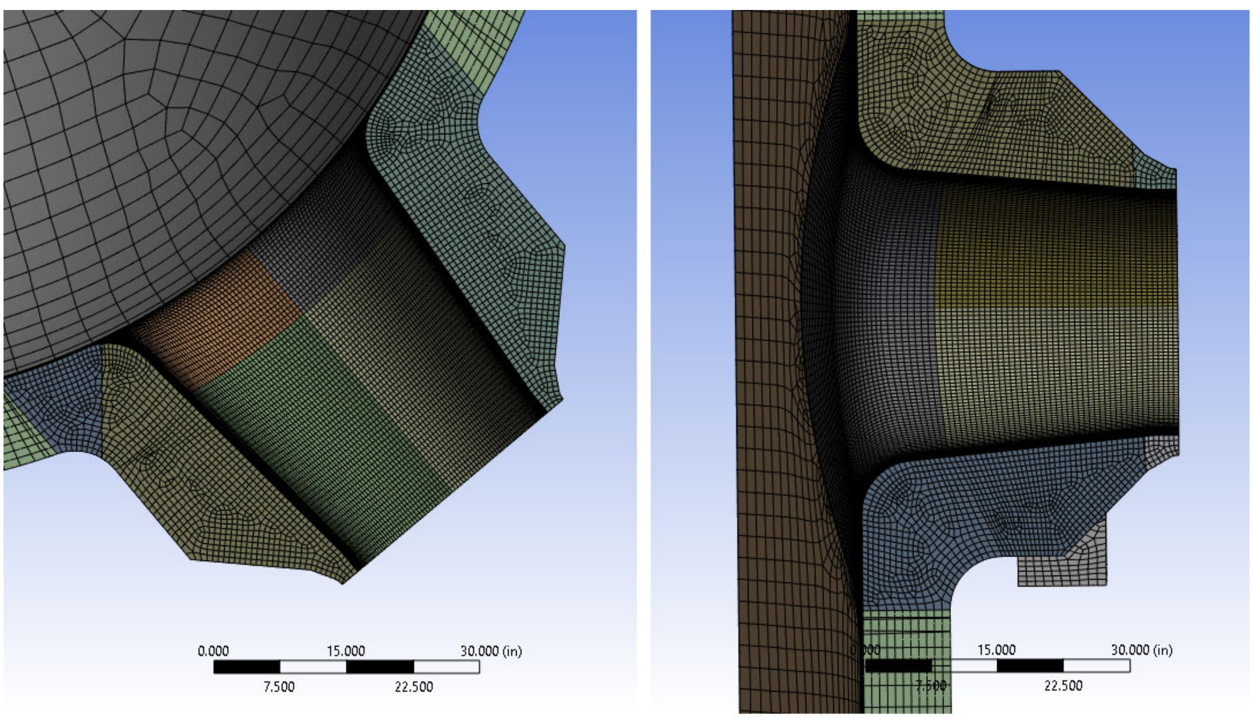

Top View **Side View**

Figure 3-3: Robinson Reactor Vessel Finite Element Model Inlet Nozzle Details

*** This record was final approved on 12/06/2024 08:42:18. (This statement was added by the PRIME system upon its validation)

The RNP RV base metal for the upper shell plate, intermediate (middle), lower shell plates, and lower head are SA-302 Gr. B. The inlet and outlet nozzle forgings are SA-336. Per design specification [21], internal cladding is austenitic stainless steel with a corrosion resistance equal to or better than Type 304. Therefore, Type 304 stainless steel properties are used for the cladding in the FEA. This is typical of RVs and same as the North Anna EMA [17].

The material properties used in the FEA are based on the original RV construction code, ASME Boiler and Pressure Vessel Code, Section III, 1965 Edition [18.a]. As the 1965 ASME Section III does not provide thermal properties, they are taken from the next code year, 1974 ASME Section III [18.b]. Poisson's ration and density are not specified in earlier ASME Codes, they are taken from Table PRD of 2010 ASME Section II Part D [18.c]. All material properties are listed in Table 3-1 and Table 3-2.

Table 3-1: Base Metal Material Properties (SA-302 Gr. B and SA-336)

Temperature [°F]	E Modulus [x10^6 psi]	α Thermal Expansion Coef. [x10^{-6} in/(in·°F)]	K Thermal Conductivity [BTU/(hr·ft·°F)]	C_p Specific Heat Capacity [BTU/(lb_m·°F)]	ρ Density [lb_m/in^3]	ν Poisson's Ratio
70	27.9	6.10	31.5	0.1144	0.28	0.3
100	-	-	31.0	0.1163		
150	-	-	30.5	0.1163		
200	27.7	6.38	30	0.1182		
250	-	-	29.5	0.1201		
300	27.4	6.60	29.1	0.1220		
350	-	-	28.6	0.1239		
400	27.0	6.82	28.1	0.1258		
450	-	-	27.6	0.1277		
500	26.4	7.02	27.2	0.1296		
550	-	-	26.7	0.1315		
600	25.7	7.23	26.2	0.1333		
650	-	-	25.8	0.1362		
700	24.8	7.44	25.3	0.1390		

Table 3-2: Cladding Material Properties (Type 304 Stainless Steel)

Temperature [°F]	E Modulus [x10^6 psi]	α Thermal Expansion Coef. [x10^{-6} in/(in·°F)]	K Thermal Conductivity [BTU/(hr·ft·°F)]	C_p Specific Heat Capacity [BTU/(lb_m·°F)]	ρ Density [lb_m/in^3]	ν Poisson's Ratio
70	27.4	9.20	8.35	0.1112	0.29	0.3
100	-	-	8.40	0.1121		
150	-	-	8.67	0.1135		
200	27.1	9.34	8.90	0.1147		
250	-	-	9.12	0.1160		
300	26.8	9.47	9.35	0.1174		
350	-	-	9.56	0.1192		
400	26.4	9.59	9.80	0.1200		
450	-	-	10.00	0.1218		
500	26.0	9.70	10.23	0.1231		
550	-	-	10.45	0.1238		
600	25.4	9.82	10.70	0.1251		
650	-	-	10.90	0.1264		
700	24.9	9.94	11.10	0.1276		

*** This record was final approved on 12/06/2024 08:42:18. (This statement was added by the PRIME system upon its validation)

3.1.1 Mechanical Loads

The RNP RV nozzle mechanical loads include deadweight (DW), thermal, operation basis earthquake (OBE), safe shutdown earthquake (SSE) loads. Loss of coolant accident (LOCA) loads for the Level C/D is based on extended leak before break (eLBB). The OBE, SSE, and LOCA loads are unsigned and are assumed to act in the positive or negative direction.

Table 3-3 and Table 3-4 also list the nozzle load combinations used in the analysis. The Level A/B summation is based on pressure plus DW plus thermal plus or minus OBE loads, and the Level C/D summation is based on DW plus thermal plus or minus the square root sum of the squares (SRSS) of SSE and LOCA loads. The inlet and outlet local coordinate systems are as follows: +X is along the axis of the nozzle oriented towards RV centerline, +Y is vertical oriented towards the RV head, and +Z is lateral following the right-hand rule.

The support pad loads are listed in Table 3-5. As previously mentioned, LOCA is based on eLBB. The vertical support pad loads are signed and act in the vertical direction only. The lateral support pad loads are unsigned and are assumed to act in positive or negative direction. The Level A/B summation is based on pressure plus DW plus thermal plus or minus OBE loads, and the Level C/D summation is based on DW plus thermal plus or minus the square root sum of the squares (SRSS) of SSE and LOCA loads.

Individual load cases are run to test the effect of mechanical loads on both nozzles simultaneously; the goal of these cases is to develop summations that produced maximum tensile stresses on the nozzle welds.

Table 3-3: Level A/B Inlet/Outlet Nozzle Mechanical Load Cases

Load		Forces [kips]			Moments [in·kips]		
		F_x	F_y	F_z	M_x	M_y	M_z
		Inlet					
DW		0.00	0.00	0.00	0.00	0.00	0.00
Thermal		-4.45	-92.00	10.26	-2802.30	1831.00	7439.90
OBE		124.00	51.00	59.00	2491.00	12126.00	2871.00
SSE		243.00	89.00	119.00	4472.00	23655.00	5421.00
LOCA		1,337.00	1,437.00	1,473.00	0.00	61,750.00	0.00
		Outlet					
DW		0.00	0.00	0.00	0.00	0.00	0.00
Thermal		-5.00	230.00	-10.00	-320.00	-1830.00	27084.00
OBE		65.00	90.00	71.00	1572.00	11248.00	7282.00
SSE		113.00	92.00	124.00	1343.00	19569.00	7371.00
LOCA		1485.00	380.00	0.00	0.00	0.00	80300.00
Load Cases							
Inlet	Load Case 1	119.55	-41.00	69.26	-311.30	13,957.00	10,310.90
	Load Case 2	-128.45	-143.00	-48.74	-5,293.30	-10,295.00	4,568.90
Outlet	Load Case 1	60.00	320.00	61.00	1,252.00	9,418.00	34,366.00
	Load Case 2	-70.00	140.00	-81.00	-1,892.00	-13,078.00	19,802.00

Note:

(1) Pressure is not included in this summation and is run as a separate load.

*** This record was final approved on 12/06/2024 08:42:18. (This statement was added by the PRIME system upon its validation)

Table 3-4: Level C/D Inlet/Outlet Nozzle Mechanical Load Cases with eLBB

Load		Forces [kips]			Moments [in·kips]		
		F_x	F_y	F_z	M_x	M_y	M_z
		Inlet					
DW		0.00	0.00	0.00	0.00	0.00	0.00
Thermal		-4.45	-92.00	10.26	-2802.30	1831.00	7439.90
OBE		124.00	51.00	59.00	2491.00	12126.00	2871.00
SSE		243.00	89.00	119.00	4472.00	23655.00	5421.00
LOCA		178.58	95.28	282.90	127.13	2,987.57	823.56
		Outlet					
DW		0.00	0.00	0.00	0.00	0.00	0.00
Thermal		-5.00	230.00	-10.00	-320.00	-1830.00	27084.00
OBE		65.00	90.00	71.00	1572.00	11248.00	7282.00
SSE		113.00	92.00	124.00	1343.00	19569.00	7371.00
LOCA		245.74	16.54	50.82	123.68	3207.94	1367.19
Load Cases							
Inlet	Load Case 3	297.12	38.38	317.17	1,671.51	25,673.92	12,923.10
	Load Case 4	-306.01	-222.38	-296.65	-7,276.11	-22,011.92	1,956.70
Outlet	Load Case 3	265.48	323.47	124.01	1,028.68	18,000.20	34,580.72
	Load Case 4	-275.48	136.53	-144.01	-1,668.68	-21,660.20	19,587.28

Note:

(1) Pressure is not included in this summation and is run as a separate load.

Table 3-5: Inlet Pad Load Cases

Condition	Case	Forces [kips]	
		F_y	F_z
Level A/B	Load Case 1	-237.50	245.40
	Load Case 2	237.50	-245.40
Level C/D	Load Case 3	726.50	447.89
	Load Case 4	-726.50	-447.89

3.1.2 Reactor Coolant System Transients

The transients evaluated for Level A/B is plant cooldown and large steam line break for Level C/D. As discussed in the design input transmittal [8], the current licensing basis EMA for RPN is the Westinghouse generic EMA in WCAP-13587 [2]. The bounding Large Steamline Break (LSB) thermal transient defined in Figure 3-2 of WCAP-13587 [2] will be used for the Levels C/D of the EMA. The digitized LSB transient per WCAP-13587 is reproduced in Figure 3-4. The plant cooldown is a 100°F/hour ramp from 557°F to 70°F shown in Figure 3-5. This transient assumes zero power conditions initially, therefore, applicable to both the inlet and outlet nozzles.

*** This record was final approved on 12/06/2024 08:42:18. (This statement was added by the PRIME system upon its validation)

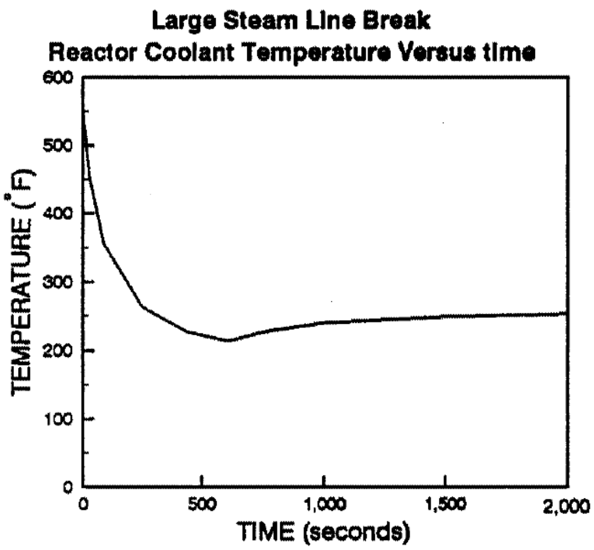

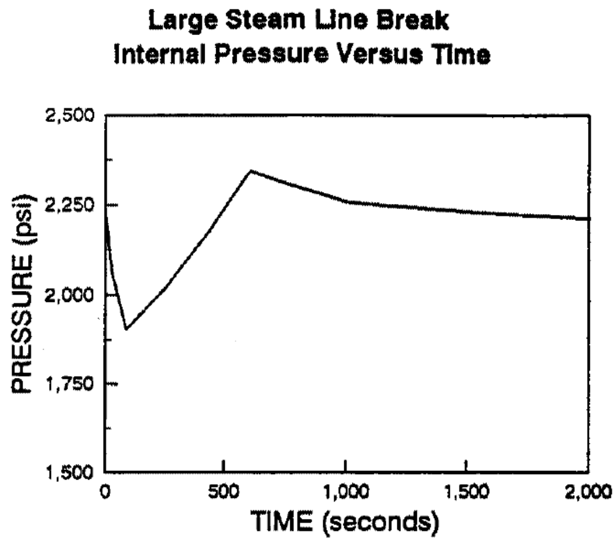

Figure 3-4: Temperature and Pressure History for Large Steam Line Break Transient [2]

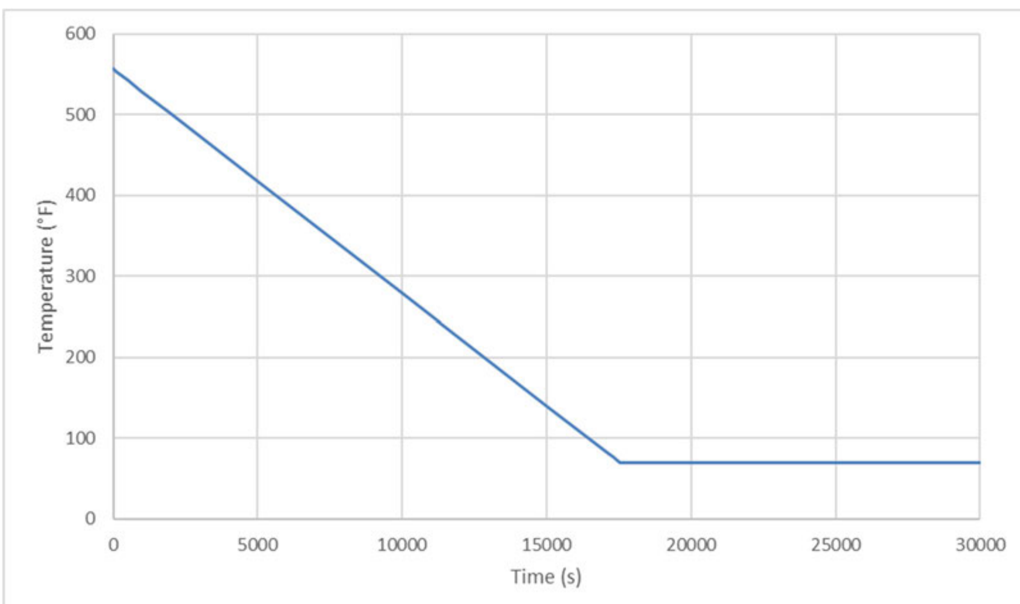

Figure 3-5: Temperature History for Plant Cooldown Transient

*** This record was final approved on 12/06/2024 08:42:18. (This statement was added by the PRIME system upon its validation)

3.2 J-INTEGRAL RESISTANCE MODELS

The J-integral resistance (J-R) curves are conservative representations for the RV material property as a function of flaw extension. As actual fracture toughness for RNP RV nozzle forging and welds are not available, guidance in NUREG/CR-5729 [12] and Regulatory Guide (RG) 1.161 [13] are used. The RV shell J-R curve is based on test data reported in Appendix A.

3.2.1 Reactor Vessel Nozzle-to-Shell Weld

The J-R curves for the RV nozzle-to-shell welds are calculated based on Charpy models based on equations from NUREG/CR-5729 and provided in RG 1.161. Per RG 1.161, Section 3, the general form for J-R is:

$$J_R = (MF)\{C1(\Delta a)^{C2}\exp\,[C3(\Delta a)^{C4}]\}$$

Per RG 1.161, Section 3.2, the parameters are defined as follows:

C1 = exp[-4.12 + 1.49 ln (CVN) - 0.00249T], where T is temperature in °F

C2 = 0.077 + 0.116 lnC1

C3 = -0.0812 – 0.0092 lnC1

C4 = -0.5

MF = 0.629 for Levels A, B, C; MF = 1.0 for Level D.

CVN is the Charpy V-notch Impact Energy in ft-lbs. For the nozzle weld, the conservatively projected 80-year (70 EFPY) SLR upper shelf energy (USE) of [ ][a,c,e] in [4] is used. The J-R curves for the nozzle welds are shown in Figure 3-6 and Figure 3-7 and listed in Table 3-6.

Table 3-6: Nozzle-to-Shell Weld J-R Curves

a,c,e

*** This record was final approved on 12/06/2024 08:42:18. (This statement was added by the PRIME system upon its validation)

a,c,e

Figure 3-6: RV Nozzle-to-Shell Weld J-R, Levels A/B, MF = 0.629

a,c,e

Figure 3-7: RV Nozzle-to-Shell Weld J-R, Level D, MF = 1.0

3.2.2 Reactor Vessel Nozzle Forging Base Metal

The J-R curves for the RV nozzle forging base metal is calculated based on the Charpy models in Table 11 of NUREG/CR-5729. When the specimen net thickness, Bn = 1 inch, ln(Bn) = 0. The equations in NUREG/CR-5729 simplifies to RG 1.161, Section 3.3. The same the general form for J-R defined in RG 1.161, Section 3 is applicable. The parameters for RV base metal are defined in RG 1.161, Section 3.3.1:

$C1 = \exp[-2.44 + 1.13 \ln(CVN) - 0.00277T]$, where T is temperature in °F

$C2 = 0.077 + 0.116 \ln C1$

$C3 = -0.0812 - 0.0092 \ln C1$

$C4 = -0.409$

MF = 0.749 for Levels A, B, C; MF = 1.0 for Level D.

PWROG-23006-NP [3] provides the RV nozzle USE for the purpose of the EMA. These values are based on the data study of initial unirradiated USE of RV nozzles. [

] a,c,e As discussed in PWROG-23006-NP, while the orientation is identified as "unknown" data, this value is consistent with Watts Bar USE data and would bound RNP inlet nozzles. The J-R curves for the RV inlet and outlet nozzles are illustrated in Figure 3-8 through Figure 3-11, and listed in Table 3-7.

*** This record was final approved on 12/06/2024 08:42:18. (This statement was added by the PRIME system upon its validation)

Table 3-7: Reactor Vessel Nozzle Forging J-R Curves

a,c,e

*** This record was final approved on 12/06/2024 08:42:18. (This statement was added by the PRIME system upon its validation)

a,c,e

Figure 3-8: RV Inlet Nozzle Forging J-R, Levels A/B, MF = 0.749

a,c,e

Figure 3-9: RV Inlet Nozzle Forging J-R, Level D, MF = 1.0

a,c,e

Figure 3-10: RV Outlet Nozzle Forging J-R, Levels A/B, MF = 0.749

a,c,e

Figure 3-11: RV Outlet Nozzle Forging J-R, Level D, MF = 1.0

3.2.3 Reactor Vessel Upper/Intermediate Shell Plates

The J-R curves for the RV Upper and Intermediate shell plates are calculated based on the J-R curve test documented in Appendix A. The J-R curve is described by the following power law equation.

$$J_R = C^* \Delta a^n$$

where

C = constant, with unit of in-lb/in^2 (or lbf/in)

Δa = flaw extension with unit of inch

n = exponent, unitless

Levels A/B

Appendix A provides the values for C and n parameters for mean values minus 2 σ (2 standard deviation). These values represent the bounding 95% of the measured data, i.e., 5 percentile. Therefore, it is applicable to Levels A/B. The C and n parameter used for the RNP RV shell plates are listed in Table 3-8. The values for C and n at 1/10 wall thickness (1/10T) are chosen to conservatively bound all postulated flaw depths.

Level D

The mean value for the parameter C per Appendix A is used for Level D. The C and n parameter used for the RNP RV shell plates are listed in Table 3-8. These are applicable to 390°F to 556°F (199°C to 291°C) per Appendix A. The J-R curves for the RV shell plates are illustrated in Figure 3-12 and listed in Table 3-9.

a,c,e

Figure 3-12: Robinson Reactor Vessel Shell Plate J-R, Levels A/B and D

Table 3-8: Robinson Reactor Vessel Shell Plate J-R Parameters at 70 EFPY

a,c,e

Table 3-9: Reactor Vessel Upper and Intermediate Shell Plate J-R Curves

a,c,e

*** This record was final approved on 12/06/2024 08:42:18. (This statement was added by the PRIME system upon its validation)

4 FRACTURE MECHANICS ANALYSIS

The EMA methodology that was used for the RNP RV locations with the projected USE below 50 ft-lbs is consistent with previously NRC approved methodologies for WCAP-13587, Rev. 1 [2] and PWROG-19047-NP-A [17]. The respective NRC Safety Evaluation Reports are in [19 and 20]. The EMA methodology is discussed further in Section 4.1. [

] a,c,e

4.1 METHODOLOGY DISCUSSION

The J are calculated per ASME Section XI, Appendix K [6], which is consistent with the NRC approved EMA reports, WCAP-13587 [2] and PWROG-19047-NP-A [17]. The maximum J values at the critical time points for service Leves A/B and Level D, along with plots of J vs. flaw depth, are compared with the J-R curves for the EMA. The Levels A/B service loadings required by ASME XI, Appendix K, are based on accumulation pressure (internal pressure load) and a cooldown rate (thermal load). For Levels A/B, K-1300 and K-4000 of [6] conservatively defined the accumulation pressure as 1.1 times the design pressure, which is a constant pressure of 2,750 psia applied throughout the 100°F/hour cooldown transient.

The actual design thermal transients are used for the FEA stress and input for the K_I and J calculations, instead of the generic design pressure and cooling rate in the ASME Section XI, Appendix K. As discussed in Section 2.1 of this report, the plant cooldown transient is used to bound all Levels A/B conditions. This is also consistent with the Appendix K guidance of 100°F/hour cooldown rate. The Level D SLB transient per the current design basis, WCAP-13587, Rev. 1 [2] is analyzed to bound Levels C/D conditions.

ASME Section XI, Appendix K [6] provides various postulated flaw depths, locations, and orientations, as well as the J and stability criteria. Per K-2000 of [6], the postulated flaws shall be oriented along the major axis of the weld of concern. Therefore, only circumferential flaws are applicable to the RV inlet and outlet nozzle welds. Both axial and circumferential flaws will be postulated for the nozzle forging and upper/intermediate shell plates.

4.1.1 Nozzle-to-Shell Welds and Upper/Intermediate Shell Forging

For an axial or circumferential flaw of depth "*a,*" the stress intensity factor (SIF) due to radial thermal gradients can be calculated per K-4210(c) of [6]. However, since the thermal stresses are based on FEA, the procedure from ASME Section XI, Appendix A [6] is used to calculate SIFs. This method accurately captures the stress states of the actual geometry by representing the through-wall stress distribution as a polynomial equation. The same methodology is used for SIF due to pressure and mechanical loads.

The stress profile representation prescribed in A-3200 of [6] is for location over the flaw depth (x/a) for which the A_i coefficients need to be recalculated for every flaw depth analyzed. The term "x" is defined as distance through the wall measured from the flawed surface. In order to simplify the calculation, the analysis herein uses through-wall stress profiles (x/t) in a similar fashion. The procedure in A-3320 of [6] is modified for the use of through-wall stress representation. This x/t approach is consistent with methods prescribed in publications such as API-579-1 [14] and A-3212 and A-3411(c) of the 2019 Edition of ASME Section XI [9]. Note that in Appendix A of the 2019 Edition of ASME Section XI, the same G_i coefficient tables are applicable for both the "x/a" and "x/t" method. This is an NRC accepted approach for previous

*** This record was final approved on 12/06/2024 08:42:18. (This statement was added by the PRIME system upon its validation)

EMAs for a number of SLR plants such as the North Anna EMA [17]. Additionally, 2021 Edition of ASME Section XI Appendix A includes the x/t methods consistent with the description herein.

The closed-form solution in K-4210 of [6] for SIF due to pressure loading, K_{Ip} is generic for cylinder geometry, which is appropriate for the RV. However, the closed-form solution for cylinder is overly conservative for the nozzle weld locations. Therefore, the method described in A-3200 of [6], including crack face pressure, with an actual FEA pressure stress profile will be used for the SIF calculations.

The through-wall stress profile is represented as follows by a cubic polynomial:

$$\sigma = A_0 + A_1\left(\frac{x}{t}\right) + A_2\left(\frac{x}{t}\right)^2 + A_3\left(\frac{x}{t}\right)^3$$

$$K_I = \left[(A_0 + A_p)\,G_0 + A_1G_1\left(\frac{a}{t}\right) + A_2G_2\left(\frac{a}{t}\right)^2 + A_3G_3\left(\frac{a}{t}\right)^3\right]\sqrt{\frac{\pi a}{Q}}$$

$$Q = 1 + 4.593\left(\frac{a}{l}\right)^{1.65} - q_y$$

$$q_y = \frac{1}{6}\left[\frac{A_0G_0 + A_1G_1\left(\frac{a}{t}\right) + A_2G_2\left(\frac{a}{t}\right)^2 + A_3G_3\left(\frac{a}{t}\right)^3}{\sigma_y}\right]^2$$

Where:

σ = the stress perpendicular to the plane of the crack

x = the distance from the inner surface where the crack initiates

a = flaw depth, [in]

t = wall thickness, [in]

l = flaw length, [in]

A_i = coefficients from the cubic polynomial stress profile, i= 0, 1, 2, 3

A_p = 0 for thermal K_{It}; A_p = internal vessel pressure for pressure K_{Ip}

G_i = free surface correction factors from Table A-3320-1 of [6] for point 1, the deepest point

q_y = plastic zone correction factor

The plastic zone correction factor, q_y, in this application is set to zero because K-4210 of [6] uses the effective flaw depth, "a_e," which already includes ductile flaw extension and a plastic zone correction.

*** This record was final approved on 12/06/2024 08:42:18. (This statement was added by the PRIME system upon its validation)

4.1.2 Nozzle Corner K_I Closed-Form Solution

The nozzle corner flaws are considered using the quarter-circular crack in a quarter-space crack geometry shown in Figure 4-1 for which solutions are available in [10]. Crack tip K_I values are computed using:

$$\sigma = A_0 + A_1 x + A_2 x^2 + A_3 x^3$$

$$K_I = \sqrt{\pi a}\left[0.723 A_0 + 0.551\left(\frac{2a}{\pi}\right)A_1 + 0.462\left(\frac{a^2}{2}\right)A_2 + 0.408\left(\frac{4a^3}{3\pi}\right)A_3\right]$$

Where:

σ = the stress perpendicular to the plane of the crack, and A_0, A_1, A_2, and A_3 are the polynomial
coefficients for the stress profile

x = the distance from the inner surface where the crack initiates

a = flaw depth

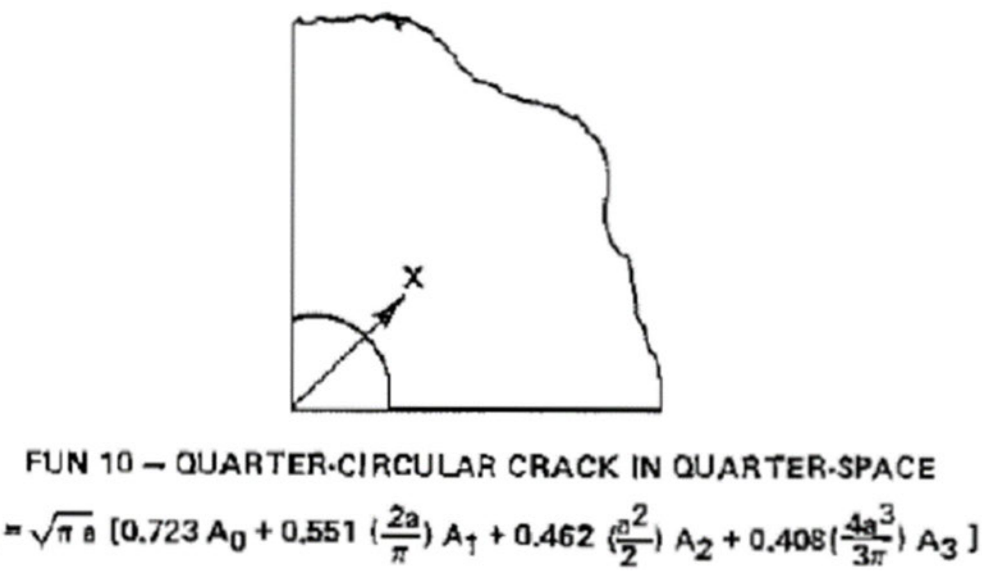

Figure 4-1: K_I Solution for Quarter-Circular Crack in Quarter-Space [10, page 5]

4.1.3 Calculation of J for Small-Scale Yielding

The calculation of J due to applied loads accounts for a material's elastic-plastic behavior. When elastic fracture mechanics with small-scale yielding applies, J may be calculated using crack tip SIF formulae with a plastic zone correction.

The effective flaw depth for small-scale yielding, a_e, shall be calculated per K-4210 of [6]:

$$a_e = a + \left[\frac{1}{6\pi}\right]\left[\frac{K_{Ip}+K_{It}}{\sigma_y}\right]^2, \text{[in]}$$

Where, K_{Ip} and K_{It} are SIFs due to pressure and thermal stresses, respectively.

σ_y = material yield strength, ASME temperature-dependent value is used, [ksi]

*** This record was final approved on 12/06/2024 08:42:18. (This statement was added by the PRIME system upon its validation)

Both axial and circumferential K'_{Ip} and K'_{It} are calculated the same way as K_{Ip} and K_{It} as described in Sections 4.1.1 and 4.1.2, except that the flaw depth, *a,* is substituted with the effective flaw depth, a_e. Then, the J for small-scale yielding is calculated using the following formula:

$$J_1 = 1000\frac{(K'_{Ip}+K'_{It})^2}{E'}, \text{[lbf/in]}$$

Where:

$E' = E/(1-\nu^2)$, [ksi]

E = Young's modulus, [ksi]

ν = Poisson's ratio = 0.3

4.1.4 Postulated Flaws

The procedures for the J calculation for Levels A/B are described in ASME Section XI, K-4000 [6]. The J calculation procedure for Level D is described in ASME Section XI, K-5000, which is the same as those for Levels A/B in K-4000, except that the effect of cladding/base metal differential thermal expansion needs to be considered for Levels C/D per K-5210(a). Therefore, stress data from the FEM with cladding is included for the Level D evaluation. Further details of the postulated flaw requirements per ASME Section XI, K-2200, K-2300 and K-2400 are summarized in Section 2.3.

4.1.5 Weld Residual Stress

The weld residual stress (WRS) is to be included for nozzle-to-shell welds and shell plates. The normalized WRS profile is from [11, Section 4.1.3.4, Figure 30]. The WRS is directly added to FEA thermal stresses for the calculation of K_{It}. This is an NRC accepted approach for previous EMAs for a number of SLR plants such as the North Anna EMA [17].

4.1.6 Stress due to Mechanical Loads

Since the structural factor (SF) is only applicable to pressure, the mechanical stress is directly added to the FEA thermal stress in the stress intensity factor calculations. The maximum through-thickness mechanical stress for design conditions is added to the corresponding thermal stresses. K_I and J are calculated for all transient time points. The limiting J values for postulated flaws plus a 0.1-inch flaw extension, J_1 are reported herein.

*** This record was final approved on 12/06/2024 08:42:18. (This statement was added by the PRIME system upon its validation)

4.2 APPLIED J-INTEGRAL RESULTS AND COMPARISON WITH J-R CURVE ALLOWABLES

The detailed methodology of the J evaluation is described in Section 4.1. As discussed in Section 2.1, the cooldown transient is evaluated for Levels A/B. FEA through-wall stress profiles were fitted to 3rd order polynomials, and A-3200 of [6] was used for the calculation of K_{It} and K_{Ip} instead of the generic closed-form solution in Appendix K of [6]. As discussed in Section 4.1, this is more accurate and is an NRC approved method. Unit pressure (1 ksi) FEA stress profiles were scaled to pressure transients and K_{Ip} was then calculated in the same manner as K_{It} using the 3rd order polynomial method. As described in Section 4.1.1, the crack face pressure was applied, and the double counting of the plastic zone correction was removed by setting the q_y term in A-3200 of [6] to zero. The plastic correction was accounted for in the a_e term per K-4210 of [6]. All K_I and J are calculated for all transient time points. The limiting J values for the postulated flaws plus a 0.1-inch flaw extension are reported.

4.2.1 Nozzle-to-Shell Welds Levels A/B

The J values for the postulated flaw plus a 0.1-inch flaw extension, J_1 (from K-1300 nomenclature) with pressure SF = 1.15 and J with SF =1.25 for Level A/B are presented in Table 4-1. The applied J_1 for both inlet and outlet nozzle welds are below the J-R at 0.1-inch flaw extension, $J_{0.1}$ from Table 3-6. The acceptance criteria in ASME Section XI, K-2200 (a)(1) [6] is satisfied.

As shown in Figure 4-2 and Figure 4-3, the slope of J is less than the J-R curve at the intersection of both curves (i.e., when J = J-R). Therefore, the stability acceptance criteria in ASME Section XI, K-2200 (a)(2) [6] is satisfied.

The most limiting J is compared to the J-R curve for 600°F. This is conservative since 600°F bounds the maximum temperature during the cooldown transient.

Table 4-1: Inlet and Outlet Nozzle Welds Level A/B, Circumferential Flaw, Limiting J

a,c,e

*** This record was final approved on 12/06/2024 08:42:18. (This statement was added by the PRIME system upon its validation)

a,c,e

Figure 4-2: Outlet Nozzle Weld, Circumferential Flaw, Level A/B J vs. J-R, SF=1.25

a,c,e

Figure 4-3: Inlet Nozzle Weld, Circumferential Flaw, Level A/B J vs. J-R, SF=1.25

*** This record was final approved on 12/06/2024 08:42:18. (This statement was added by the PRIME system upon its validation)

4.2.2 Nozzle-to-Shell Welds Level D

The J and J_1 values for nozzle-to-shell weld flaw extensions for Level D are presented in Table 4-2. As discussed in Section 2.3.2, SF = 1 for thermal and pressure. Since the 1/10 base metal wall thickness plus cladding exceeded 1 inch for all evaluated locations, the postulated flaw depth is 1 inch. The applied J_1 for both inlet and outlet nozzle welds are below the J-R value, $J_{0.1}$ from Table 3-6. The acceptance criteria in ASME Section XI, K-2300 (a)(1) [6] is satisfied.

As shown in Figure 4-4 and Figure 4-5, the slope of J is less than the J-R curve at the intersection of both curves (i.e., J = J-R). Therefore, the stability acceptance criteria in ASME Section XI, K-2300 (a)(2) [6] is satisfied.

The most limiting J is compared to the J-R curve for 400°F. This is conservative since 400°F bounds the Level D transient metal temperature at the time point that results in the most limiting J.

Table 4-2: Inlet and Outlet Nozzle Welds Level D, Circumferential Flaw, Limiting J

a,c,e

Additionally, as discussed in Section 2.3.2, K-5300(b) also requires that the remaining ligament is not subjected to tensile instability. As shown in Table 4-3, the Level D, SLB transient internal pressure of 2.5 ksi is significantly less than the tensile instability pressures, P_I, calculated per K-5300(b). Therefore, the remaining ligament is not subjected to tensile instability.

*** This record was final approved on 12/06/2024 08:42:18. (This statement was added by the PRIME system upon its validation)

Table 4-3: K-5300 Tensile Instability Check for Nozzle Welds Circumferential Flaws

a,c,e

a,c,e

Figure 4-4: Outlet Nozzle Weld, Circumferential Flaw, Level D J vs. J-R, SF=1

*** This record was final approved on 12/06/2024 08:42:18. (This statement was added by the PRIME system upon its validation)

a,c,e

Figure 4-5: Inlet Nozzle Weld, Circumferential Flaw, Level D J vs. J-R, SF=1

*** This record was final approved on 12/06/2024 08:42:18. (This statement was added by the PRIME system upon its validation)

4.2.3 RV Nozzle Forgings Levels A/B

The nozzle corner is the limiting location for the nozzle forging due to the wall thickness and the stress concentration effect. The J values for the postulated flaw plus a 0.1-inch flaw extension, J_1 with pressure SF = 1.15 and J with SF =1.25 for Level A/B are presented in Table 4-4. All J_1 are below the nozzle forging Levels A/B J-R, $J_{0.1}$ from Table 3-7. The acceptance criteria in ASME Section XI, K-2200 (a)(1) [6] is satisfied.

As shown in Figure 4-6 to Figure 4-9, the slope of J is less than the J-R curve at the intersection of both curves (i.e., when J = J-R). Therefore, the stability acceptance criteria in ASME Section XI, K-2200 (a)(2) [6] is satisfied.

The most limiting J is compared to the J-R curve for 600°F. This is conservative since 600°F bounds the maximum temperature during the cooldown transient.

Table 4-4: Nozzle Corner Level A/B, Limiting J

a,c,e

a,c,e

Figure 4-6: Outlet Nozzle Corner, Circumferential Flaw, Level A/B J vs. J-R, SF=1. 25

a,c,e

Figure 4-7: Inlet Nozzle Corner, Circumferential Flaw, Level A/B J vs. J-R, SF=1.25

*** This record was final approved on 12/06/2024 08:42:18. (This statement was added by the PRIME system upon its validation)

a,c,e

Figure 4-8: Outlet Nozzle Corner, Axial Flaw, Level A/B J vs. J-R, SF=1.25

a,c,e

Figure 4-9: Inlet Nozzle Corner, Axial Flaw, Level A/B J vs. J-R, SF=1.25

*** This record was final approved on 12/06/2024 08:42:18. (This statement was added by the PRIME system upon its validation)

4.2.4 RV Nozzle Forgings Level D

The J and J_1 values for RV forging flaw extensions for Level D are presented in Table 4-5. As discussed in Section 2.3.2, SF = 1 for thermal and pressure. Since the 1/10 base metal wall thickness plus cladding exceeded 1 inch for all evaluated locations, the postulated flaw depth is 1 inch. The applied J-integral for the postulated flaw plus a 0.1-inch flaw extension, J_1 for nozzle circumferential and axial flaws are below the J-R value, $J_{0.1}$ at 600°F for the inlet and outlet nozzle forgings from Table 3-7.

As shown in Figure 4-10 through Figure 4-13, the slopes of J is less than the J-R curve at the intersection of both curves (i.e., when J = J-R). Therefore, the stability acceptance criteria in ASME Section XI, K-2300 (a)(2) [6] is satisfied.

The most limiting J is compared to the J-R curve for 600°F. This is conservative since 600°F bounds the maximum temperature during the Level D, SLB transient.

Table 4-5: Nozzle Corner Level D, Limiting J

a,c,e

Additionally, as discussed in Section 2.3.2, K-5300(b) also requires that the remaining ligament is not subjected to tensile instability. As shown in Table 4-6, the Level D, SLB transient internal pressure of 2.5 ksi is significantly less than the tensile instability pressures, PI, calculated per K-5300(b). Therefore, the remaining ligament is not subjected to tensile instability.

*** This record was final approved on 12/06/2024 08:42:18. (This statement was added by the PRIME system upon its validation)

Table 4-6: K-5300 Tensile Instability Check for Nozzle Forgings Circumferential and Axial Flaws

a,c,e

*** This record was final approved on 12/06/2024 08:42:18. (This statement was added by the PRIME system upon its validation)

a,c,e

Figure 4-10: Outlet Nozzle Corner, Circumferential Flaw, Level D J vs. J-R, SF=1

a,c,e

Figure 4-11: Inlet Nozzle Corner, Circumferential Flaw, Level D J vs. J-R, SF=1

*** This record was final approved on 12/06/2024 08:42:18. (This statement was added by the PRIME system upon its validation)

a,c,e

Figure 4-12: Outlet Nozzle Corner, Axial Flaw, Level D J vs. J-R, SF=1

a,c,e

Figure 4-13: Inlet Nozzle Corner, Axial Flaw, Level D J vs. J-R, SF=1

*** This record was final approved on 12/06/2024 08:42:18. (This statement was added by the PRIME system upon its validation)

4.2.5 Upper and Intermediate Shell Plates Levels A/B

The J values for the postulated flaw plus a 0.1-inch flaw extension, J_1 with pressure SF = 1.15 and J with SF =1.25 for Level A/B are presented in Table 4-7. The applied J_1 for both circumferential and axial flaws are below the shell plate Level A/B J-R, $J_{0.1}$ from Table 3-9. The acceptance criteria in ASME Section XI, K-2200 (a)(1) [6] is satisfied.

As shown in Figure 4-14 and Figure 4-15, the slope of J is less than the J-R curve at the intersection of both curves (i.e., when J = J-R). Therefore, the stability acceptance criteria in ASME Section XI, K-2200 (a)(2) [6] is satisfied.

The shell plate FEA stresses were taken at the intersection of upper shell to the intermediate shell. It captured the stress concentration effect; therefore, the results are applicable to both upper and intermediate shell plates.

Table 4-7: Upper and Intermediate Shell Plates Level A/B, Limiting J

a,c,e

*** This record was final approved on 12/06/2024 08:42:18. (This statement was added by the PRIME system upon its validation)

a,c,e

Figure 4-14: RV Shell, Circumferential Flaw, Level A/B J vs. J-R, SF=1.25

a,c,e

Figure 4-15: RV Shell, Axial Flaw, Level A/B J vs. J-R, SF=1.25

*** This record was final approved on 12/06/2024 08:42:18. (This statement was added by the PRIME system upon its validation)

4.2.6 Upper and Intermediate Shell Plates Level D

The J and J_1 values for the upper and intermediate shell plates for Level D are presented in Table 4-8. As discussed in Section 2.3.2, SF = 1 for thermal and pressure. Since the 1/10 base metal wall thickness plus cladding exceeded 1 inch for all evaluated locations, the postulated flaw depth is 1 inch. The applied J-integral for the postulated flaw plus a 0.1-inch flaw extensions, J_1 for both circumferential and axial flaws are below the J-R value, $J_{0.1}$ from Table 3-9. The acceptance criteria in ASME Section XI, K-2300 (a)(1) [6] is satisfied.

As shown in Figure 4-16 and Figure 4-17, the slope of J is less than the J-R curve at the intersection of both curves (i.e., J = J-R). Therefore, the stability acceptance criteria in ASME Section XI, K-2300 (a)(2) [6] is satisfied.

Table 4-8: Upper and Intermediate Shell Plates Level D, Limiting J

a,c,e

Additionally, as discussed in Section 2.3.2, K-5300(b) also requires that the remaining ligament is not subjected to tensile instability. As shown in Table 4-9, the Level D, SLB transient internal pressure of 2.5 ksi is significantly less than the tensile instability pressures, PI, calculated per K-5300(b). Therefore, the remaining ligament is not subjected to tensile instability.

*** This record was final approved on 12/06/2024 08:42:18. (This statement was added by the PRIME system upon its validation)

Table 4-9: K-5300 Tensile Instability Check for Nozzle Forgings Circumferential and Axial Flaws

a,c,e

a,c,e

Figure 4-16: RV Shell, Circumferential Flaw, Level D J vs. J-R, SF=1.0

*** This record was final approved on 12/06/2024 08:42:18. (This statement was added by the PRIME system upon its validation)

a,c,e

Figure 4-17: RV Shell, Axial Flaw, Level D J vs. J-R, SF=1.0

*** This record was final approved on 12/06/2024 08:42:18. (This statement was added by the PRIME system upon its validation)

5 CONCLUSIONS

The RNP Unit 2 RV nozzle-to-shell welds, nozzle forgings and upper/intermediate shell plates were evaluated for equivalent margins of safety per ASME Code Section XI [6]. The flaw extension and stability criteria of ASME Section XI, Appendix K are satisfied for all locations evaluated herein.

Levels A/B

For all evaluated locations, the J for the postulated flaw plus a 0.1-inch flaw extension (J_1) with a structural factor (SF) of 1.15 for pressure and SF of 1.0 for thermal are below the J-material at 0.1-inch flaw extension ($J_{0.1}$). Therefore, the acceptance criteria in ASME Section XI, K-2200 (a)(1) [6] is satisfied.

The slope of J (with a SF=1.25) is less than the J-material (J-R curve) at the intersection of both curves (i.e., when J = J-R). Therefore, the stability acceptance criteria in ASME Section XI, K-2200 (a)(2) [6] is satisfied.

Level D

For all the evaluated locations, the J_1 with a SF of 1.0 are below the $J_{0.1}$. Therefore, the acceptance criteria in ASME Section XI, K-2400 (a) [6] is satisfied.

The slope of J is less than the J-R curve at the intersection of both curves (i.e., when J = J-R). Therefore, the stability acceptance criteria in ASME Section XI, K-3400 [6] is satisfied. Using this approach, Level D loadings are shown to satisfy the more limiting Level C acceptance criteria established by K-2300 [6].

Per K-2400 of [6], all flaws evaluated for Level D assumed a flaw depth equal to 1/10 of the base metal thickness, plus the cladding thickness, (not exceeding 1 inch), plus a 0.1-inch flaw extension. All flaws evaluated herein have been shown to exhibit ductile and stable flaw extension when compared to $J_{0.1}$ for all Level D loading conditions. This satisfies the 75% of wall thickness requirement, per K-2400 (c) [6], as the final flaw size, after extension, is much less than 75% of the wall thickness.

Additionally, the maximum Level D internal pressure is less than the tensile instability pressures calculated per K-5300 (b) [6] for all evaluated locations and flaws.

*** This record was final approved on 12/06/2024 08:42:18. (This statement was added by the PRIME system upon its validation)

6 REFERENCES

1. RNP-2077-04-SLR-0001, Rev. 0, "Reactor Coolant Systems Class 1 Component Analysis Required for RNP Unit 2 Subsequent License Renewal (80 years)," June 28, 2022.
2. WCAP-13587, Rev. 1, "Reactor Vessel Upper Shelf Energy Bounding Evaluation for Westinghouse Pressurized Water Reactors," September 1993.
3. PWROG-23006-NP, Rev. 0, "H.B. Robinson Unit 2 Inlet and Outlet Nozzle Initial Upper-Shelf Energy Determination," July 2023.
4. WCAP-18766-NP, Rev. 0, "H.B. Robinson Unit 2 Subsequent License Renewal: Time-Limited Aging Analyses (TLAAs) on Reactor Vessel Integrity (RVI)," June 2024.
5. Code of Federal Regulations, 10 CFR Part 50, Appendix G, "Fracture Toughness Requirements," U.S. Nuclear Regulatory Commission, Washington D.C., Federal Register, Volume 77, No. 14, January 23, 2012.
6. ASME Boiler and Pressure Vessel Code, Section XI, "Rules for Inservice Inspection of Nuclear Power Plant Components," 2007 Edition, with 2008 Addenda. (*Code of Record confirmed per [7]*)
7. DUKE-RNP-SLR-22-004, Rev. 0, "Design Input Request (DIR) Appendix L Evaluations," August 25, 2022.
8. DUKE-RNP-SLR-22-010, Rev. 0, "Design Input Request (DIR) Reactor Vessel (RV) Integrity – EMA (WS02h)," November 21, 2022.
9. ASME Boiler and Pressure Vessel Code, Section XI, "Rules for Inservice Inspection of Nuclear Power Plant Components," 2019 Edition.
10. S. A. Delvin and P. C. Riccardella, "Fracture Mechanics Analysis of JAERI Model Pressure Vessel Test," ASME Paper No. 78-PVP-91, Proceedings of the 1978 ASME Pressure Vessels and Piping Conference, June 25-30, 1978, Montreal, Quebec, Canada.
11. Fracture Analysis of Vessels – Oak Ridge FAVOR, v05.1, Computer Code: Theory and Implementation of Algorithms, Methods, and Correlations, ORNL/NRC/LTR-05/18 (*ADAMS Accession Number ML063350323*).
12. NUREG/CR-5729, "Multivariable Modeling of Pressure Vessel and Piping J-R Data," May 1991.
13. U.S. Nuclear Regulatory Commission Regulatory Guide 1.161, "Evaluation of Reactor Pressure Vessels with Charpy Upper-Shelf Energy Less Than 50 Ft-Lb," June 1995.
14. API 579-1/ASME FFS-1, "Fitness-For-Service," Annex 9B, "Compendium of Stress Intensity Factor Solutions," June 2016.
15. BAW-2192NP Supplement 1, Rev. 0, "Low Upper-Shelf Toughness Fracture Mechanics Analysis of Reactor Vessels of B&W Owners Reactor Vessel Working Group for Levels A & B Service Loads," December 2017 (*ADAMS Accession Number ML17354A012*).

*** This record was final approved on 12/06/2024 08:42:18. (This statement was added by the PRIME system upon its validation)

16. BAW-2178NP Supplement 1, Rev. 0, “Low Upper-Shelf Toughness Fracture Mechanics Analysis of Reactor Vessels of B&W Owners Reactor Vessel Working Group for Levels C & D Service Loads,” December 2017 (*ADAMS Accession Number ML18029A199*).

17. PWROG-19047-NP-A, Rev. 0, “North Anna Units 1 and 2 Reactor Vessels Low Upper-Shelf Fracture Toughness Equivalent Margin Analysis,” September 2021 (*ADAMS Accession Number ML21264A535*).

18. Material Properties for Finite Element Model in accordance to:

    a. ASME Boiler & Pressure Vessel Code, Section III, 1965 Edition

    b. ASME Boiler and Pressure Vessel Code, Section III, 1974 Edition

    c. ASME Boiler and Pressure Vessel Code, Section II-D, 2010 Edition

19. NRC SE Report, “Safety Assessment of Report WCAP-13587, Revision 1, “Reactor Vessel Upper Shelf Energy Bounding Evaluation For Westinghouse Pressurized Water Reactors,” September 1993”, April 21, 1994.

20. NRC SE Report, “Final Safety Evaluations for BAW-2192, Supplement 1NP, Revision, “Low Upper-Shelf Toughness Fracture Mechanics Analysis of Reactor Vessels of B&W Owners Reactor Vessel Working Group for Level A&B Service Loads” and BAW-2178, Supplement 1NP, Revision 0, “Low Upper-Shelf Toughness Fracture Mechanics Analysis of Reactor Vessels of B&W Owners Reactor Vessel Working Group for Level C&D Service Loads,” April 29, 2019 (*ADAMS Accession Number ML19106A196*).

21. 676367, Rev. 0, “Reactor Vessel - Reactor Coolant System,” June 8, 1966, modified by:

    a. 676487, Rev. 0, “Addendum to Equipment Specification 676376, Rev. 0, Reactor Vessel - Reactor Coolant System,” February 21, 1967.

    b. DS-MRCDA-12-2, Rev. 0, “Addendum to H.B. Robinson Unit 2 Reactor Vessel Equipment Specification 676367, Rev. 0,” April 25, 2012.

*** This record was final approved on 12/06/2024 08:42:18. (This statement was added by the PRIME system upon its validation)

APPENDIX A

Upper Shelf Fracture Toughness Testing of

Robinson Reactor Pressure Vessel Steel Plate

*** This record was final approved on 12/06/2024 08:42:18. (This statement was added by the PRIME system upon its validation)

A.1 Background and Purpose

Several of the H. B. Robinson Unit 2 Reactor Pressure Vessel (RPV) shell plates have sulfur above the A-302 Grade B plate cutoff of 0.018% set in Regulatory Guide (RG) 1.161[A1] for validity of the NUREG/CR-5729 [A2] Charpy prediction model. Therefore, upper-shelf fracture toughness ($J_{material}$) has been measured rather than only depending on the closed form model in RG 1.161 and NUREG/CR-5729. Westinghouse performed J-R curve tests per ASTM E 1820 [A3] determining $J_{material}$ using available unirradiated archive plate W10201-4. Several 0.5-inch-thick compact tension fracture toughness (0.5TC(T)) specimens were machined from the archive plate and tested according to ASTM E 1820 to ensure four fully valid tests were obtained with at least 2 valid tests at 390°F and 2 at 550°F.

The specimens were pre-cracked and tested per the requirements of ASTM E 1820. Full $J_{material}$ curves were developed as far as the capacity of the specimen permits. After testing the specimens were heat-tinted, broken open, the fracture surfaces measured, and photographed. The resulting lower bound $J_{material}$ toughness curve has been adjusted for reduction in fracture toughness due to neutron irradiation to the applicable 80-year fluence needed for the equivalent margins analysis (EMA). Plate W10201-5 also has high sulfur (S) but is not available in archives. The adjusted W10201-4 results bound the properties and chemistry of plate W10201-5. The bounding adjusted J-R curve for the measured unirradiated plate W10201-4 can be used for $J_{material}$ for all the beltline plates in the EMA.

*** This record was final approved on 12/06/2024 08:42:18. (This statement was added by the PRIME system upon its validation)

A.2 Summary of Results and Conclusions

The results of the ASTM E1820-15 ductile fracture toughness testing of unirradiated archive plate W10201-4 are summarized in Table A2-2. Figure A2-1 through Figure A2-7 show the plots of the fracture toughness J-R (J versus Δa where Δa is the stable crack extension) curves.

Extra J-R curve tests were conducted as part of this test program to ensure valid results were obtained. Some tests were also conducted with specimen orientation of L-T (strong) in case the analysis cannot pass with the conservative weak direction (T-L) results. Please note that test L-TB4 is not valid and is an approximate value. The L-T orientation is expected to have higher toughness than T-L, however, test L-TB3 has a lower measured J_{Ic} value than the T-L tests at the 288°C test temperature. For the other tests shown in Table A2-2, some had minor E1820 validity criteria violations but can be considered reliable and valid tests.

Conservatively, a mean - 2σ (2 standard deviations) lower bound and mean J-R curve was determined which is lower than the lowest T-L J_{Ic}, C (J@1 mm) and J at 2.54 mm (0.1 inch) values measured and should be used for all temperatures from 199°C to 291°C as shown in Table A2-1a and Table A2-1b, respectively. Typically, one would expect a lower upper-shelf toughness at higher temperature. This measured unirradiated toughness is adjusted to the fluence of interest applicable to subsequent license renewal (SLR) as shown in Table A2-1a and Table A2-1b, which is bounding for all the upper and intermediate shell plates. J_{Ic} is the onset of stable crack extension, and the J-R curve is described by the following power law equation with C and n values shown in Table A2-1a, Table A2-1b and Table A2-2:

$$J = C * \Delta a^n$$

Table A2-1a: Predicted Lower Bound Toughness Values for EMA at 70 EFPY for Upper and Intermediate Shell Plates for 199°C to 291°C

Vessel Location	Fluence (x 10^{19} n/cm^2, E > 1.0 MeV)	Projected RG1.99R2 USE Decrease (%)	J_{Ic}		C		n
			kJ/m^2	in-lb/in^2	kJ/m^2	in-lb/in^2	
Unirradiated	0.0	0%	110	627	184	4225	0.43
1/10T	7.077	32%	75	426	125	2873	0.43
1/4T	5.061	30%	77	439	129	2958	0.43

Table A2-1b: Predicted Mean Toughness Values for EMA at 70 EFPY for Upper and Intermediate Shell Plates for 199°C to 291°C

Vessel Location	Fluence[(b)] (x 10^{19} n/cm^2, E > 1.0 MeV)	Projected RG1.99R2 USE Decrease (%)	J_{Ic}		C		n
			kJ/m^2	in-lb/in^2	kJ/m^2	in-lb/in^2	
Unirradiated	0.0	0%	150	856	216	4969	0.43
1/10T	7.077	32%	102	582	147	3379	0.43
1/4T	5.061	30%	105	599	151	3479	0.43

*** This record was final approved on 12/06/2024 08:42:18. (This statement was added by the PRIME system upon its validation)

Table A2-2: Summary of Plate W10201-4 Upper Shelf Toughness 0.5TCT Test Results

Orientation, Thickness Location	Test Temperature (°C)	J_{Ic} (kJ/m^2)	J_{Ic} Validity Violation	C	n	J-R Curve Validity Violation	Specimen ID
L-T, 3/4T	200	256[1]	multiple[1]	311	0.26	multiple[1]	L-TB4
	291	132	A9.9.2.2[2]	251	0.59	none	L-TB3
T-L, 1/4T	288	150	none	216	0.35	none	T-LU3
	288	174	none	233	0.30	9.1.4.2[3]	T-LU4
	199	140	none	203	0.36	9.1.4.2[3]	T-LU5
	199	162	none	230	0.36	9.1.4.2[3]	T-LU6
T-L, 3/4T	199	123	A9.9.2.2[2]	200	0.44	none	T-LB8

Notes:

[1] Not valid; therefore, reported as J_Q. Significant difference between compliance and optically measured Δa (E1820 9.1.5.2) slightly exceeded allowable limit and significant noise in blunting line (E1820 A9.9.2.2).

[2] Slightly higher noise in blunting line than allowed (E1820 A9.9.2.2); result not significantly affected.

[3] Small final crack length straightness violation

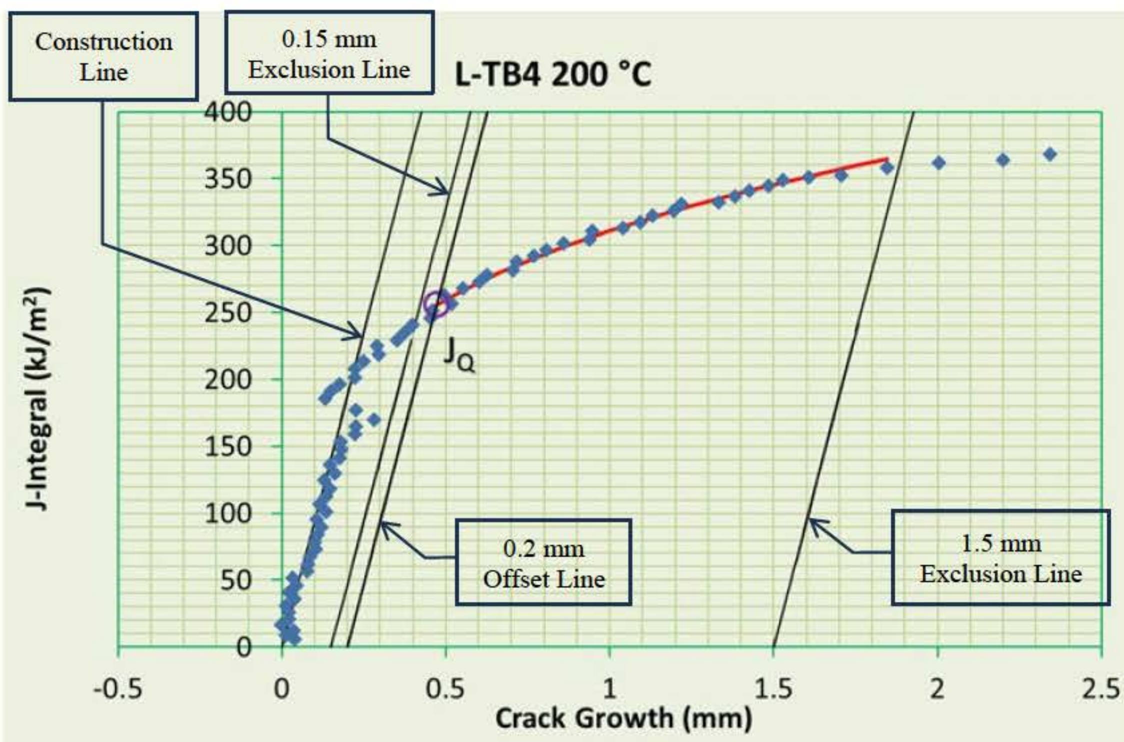

Figure A2-1: Plate W10201-4 L-T Specimen L-TB4 J-R Curve

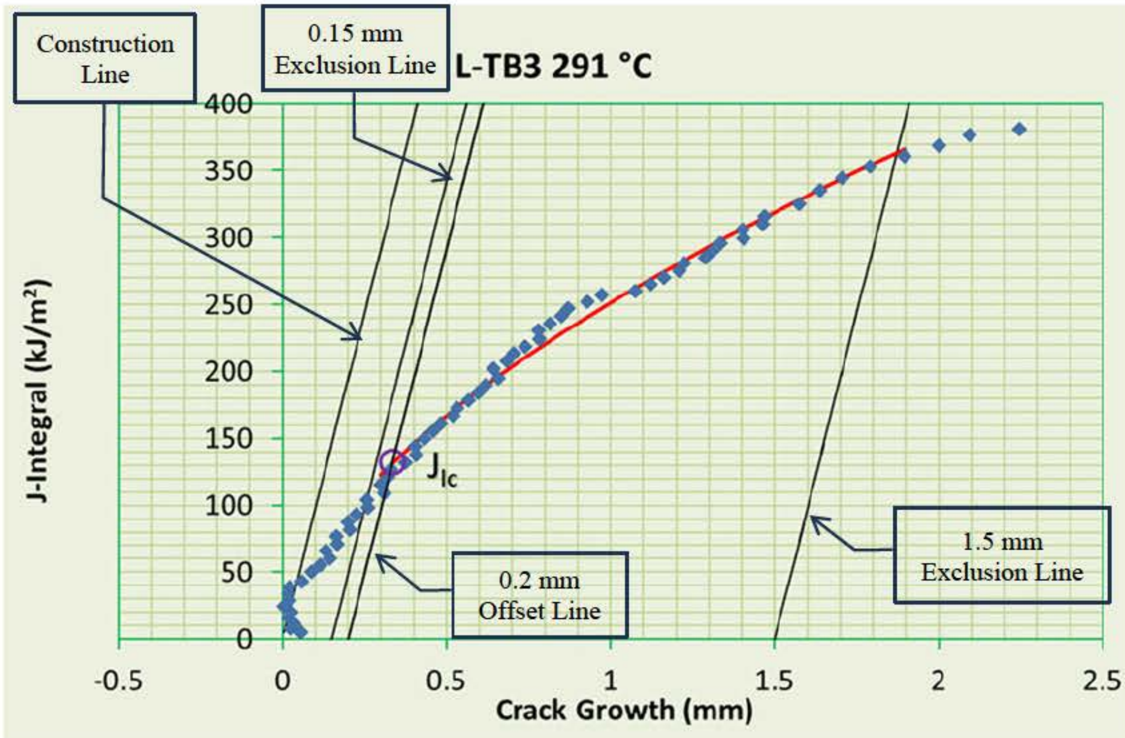

Figure A2-2: Plate W10201-4 L-T Specimen L-TB3 J-R Curve

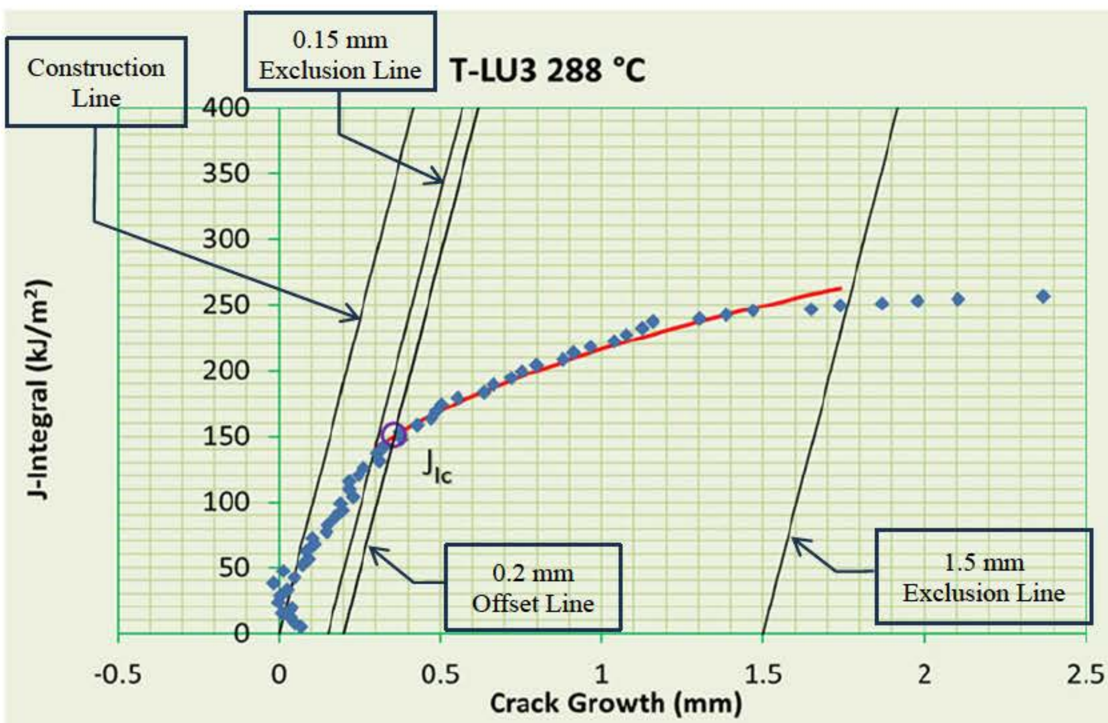

Figure A2-3: Plate W10201-4 T-L Specimen T-LU3 J-R Curve

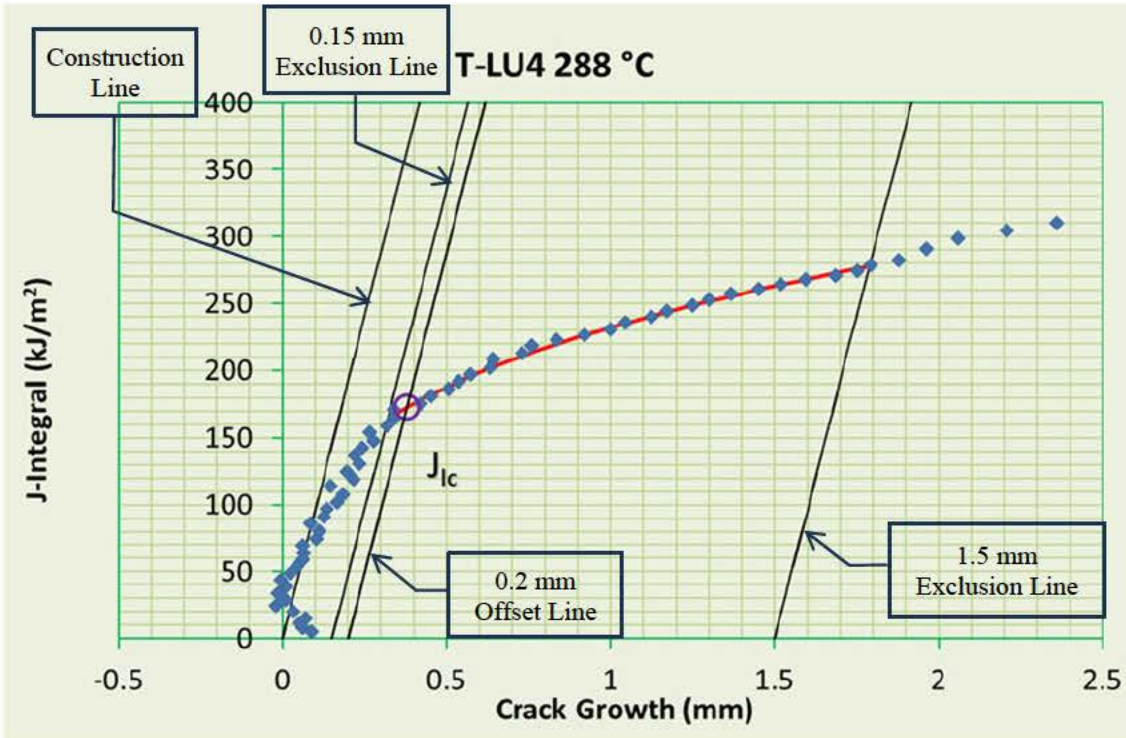

Figure A2-4: Plate W10201-4 T-L Specimen T-LU4 J-R Curve

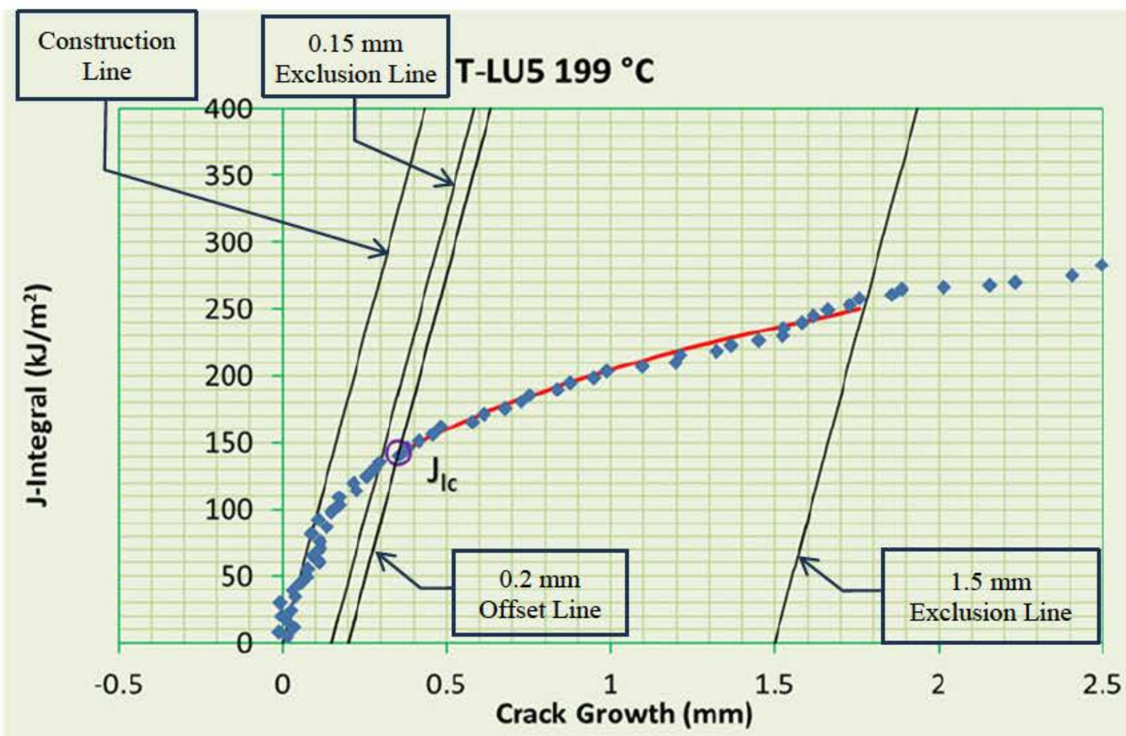

Figure A2-5: Plate W10201-4 T-L Specimen T-LU5 J-R Curve

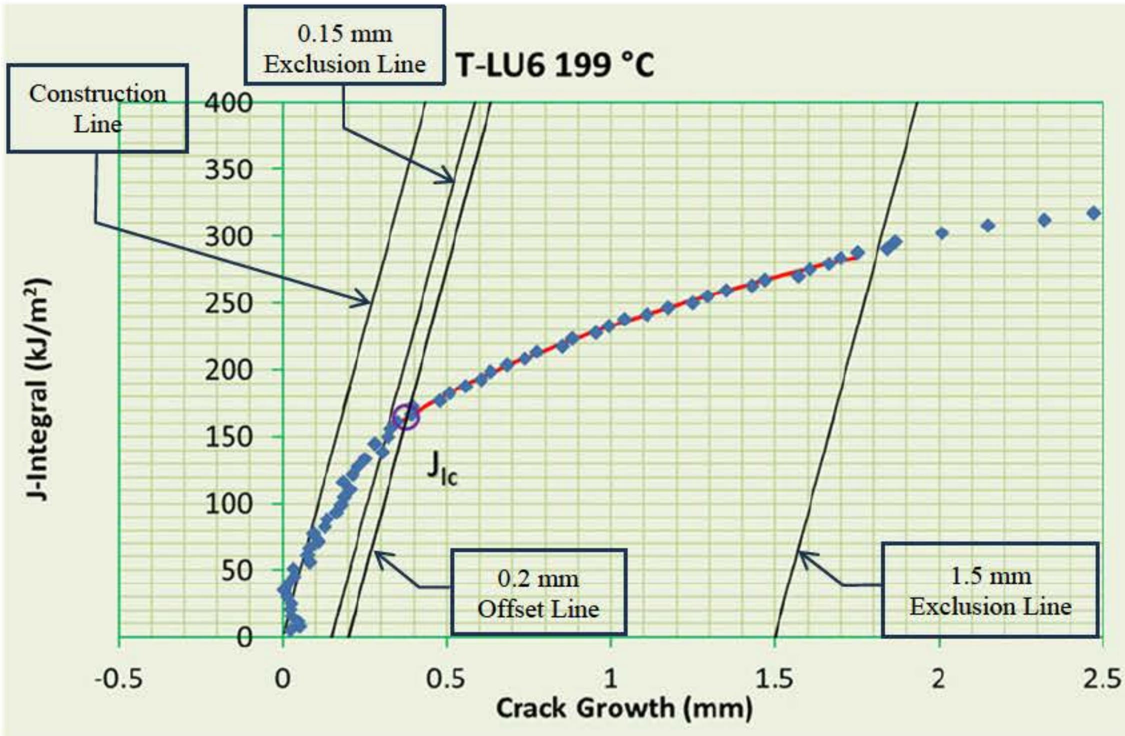

Figure A2-6: Plate W10201-4 T-L Specimen T-LU6 J-R Curve

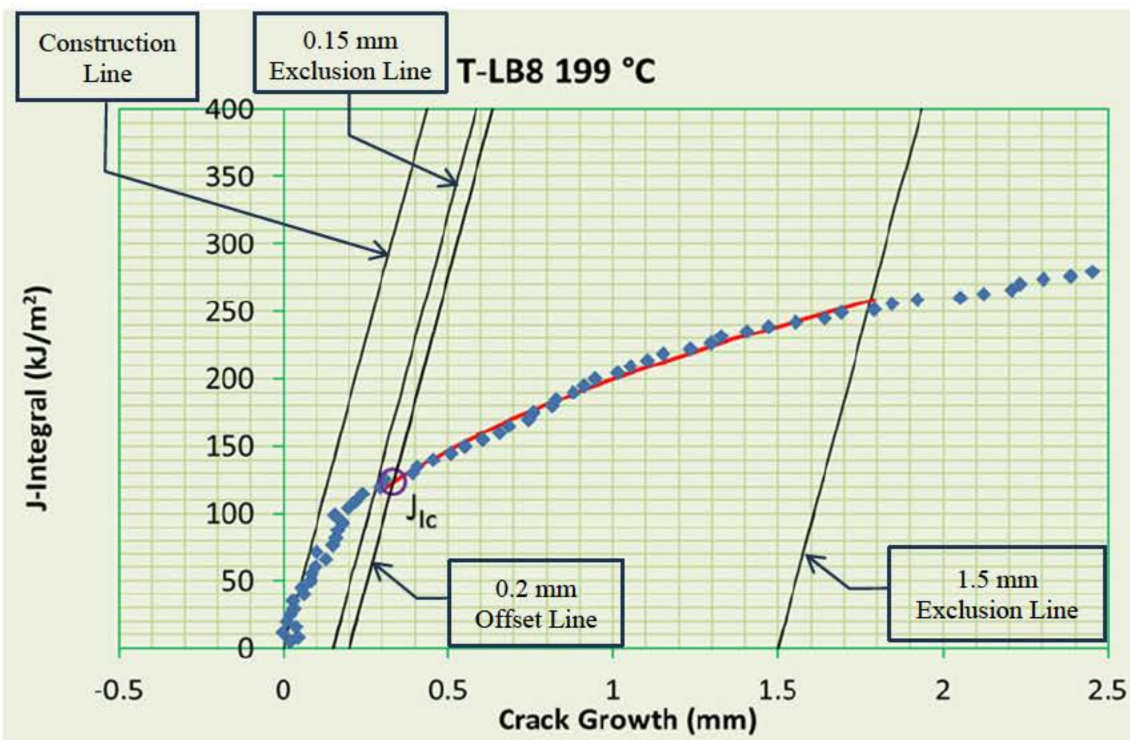

Figure A2-7: Plate W10201-4 T-L Specimen T-LB8 J-R Curve

A.3 References

[A1] U.S. Nuclear Regulatory Commission Regulatory Guide 1.161, “Evaluation of Reactor Pressure Vessels with Charpy Upper-Shelf Energy Less Than 50 Ft-Lb,” June 1995.

[A2] E. D. Eason, L. E. Wright, and E. E. Nelson, “Multivariable Modeling of Pressure Vessel and Piping J-R Data,” NUREG/CR-5729, US Nuclear Regulatory Commission, May 1991.

[A3] ASTM E 1820-15, “Standard Test Method for Measurement of Fracture Toughness,” ASTM International, 2015.

[A4] WCAP-7373, “Carolina Power and Light Co. H. B. Robinson Unit No. 2 Reactor Vessel Radiation Surveillance Program”, S.E. Yanichko, January 1970.

[A5] SA-302, “Specification for Manganese-Molybdenum and Manganese-Molybdenum-Nickel Steel Plates for Pressure Vessels,” ASME B&PV Section II, 1966 Winter Addenda.

[A6] NUREG/CR-5265, “Size Effects on J-R Curves for A 302-B Plate,” U.S. Nuclear Regulatory Commission, January 1989.

[A7] WCAP-17651-NP, Revision 0, “Palisades Nuclear Power Plant Reactor Vessel Equivalent Margins Analysis,” February 2013.

[A8] PWROG-20043-NP, Revision 0, “PBN Unit 1 IS Plate A9811-1 Equivalent Margins Analysis for SLR,” October 2020.

[A9] WCAP-13554, Revision 0, “Effects of Section Size and Cleanliness on the Upper Shelf and Transition Range Toughness of Three Nuclear Pressure Vessel Steels,” August 1992.

[A10] *“Radiation Embrittlement of Reactor Vessel Materials*,” Regulatory Guide 1.99, Revision 2 (Washington, DC: U.S. Nuclear Regulatory Commission, 1988).

[A11] T. Ogawa, J. B. Hall, B. E. Mays, and T. C. Hardin, “Upper Shelf Energy Prediction Model for Irradiated Reactor Pressure Vessel Steels,” Proceedings of the ASME 2017 Pressure Vessel & Piping Conference, ASME 2017.

[A12] WCAP-18766-NP, Rev. 0, “H.B. Robinson Unit 2 Subsequent License Renewal: Time-Limited Aging Analyses (TLAAs) on Reactor Vessel Integrity (RVI),” June 2024.

[A13] T. Ogawa, J. B. Hall, and B. E. Mays, *Prediction Model for the Decrease in Upper Shelf Energy of Reactor Vessel Steel Due to Neutron Embrittlement*, MRP-414 (Palo Alto, CA: EPRI, 2016).

*** This record was final approved on 12/06/2024 08:42:18. (This statement was added by the PRIME system upon its validation)

A.4 Testing Methods and Acceptance Criteria

All the specimens were precracked at room temperature in the irradiated condition in the low-level cell at Churchill in accordance with ASTM E1820-20. The number of cycles ranged from 49,000 to 64,000. All precrack loads are acceptable with maximum precrack load being 6.1kN. A sine wave generator was used for precracking with a frequency around 20 Hz and a minimum/maximum ratio of between 0.1 and 0.2.

An inboard clip gage was used to measure displacement on the load-line. The gauge knife edges were integrally machined into the specimen load-line as shown in Figure A5-1. The specimen temperature was controlled by a split tube furnace. Two thermocouples were placed specimens to record the specimen temperature. One was spot welded to the specimen and the other was magnetically attached as an independent check.

Before performing each test, precycles were conducted to measure crack depth by measuring load vs. CMOD compliance to ensure the clip gage is properly seated and to enable calculation of crack depth and consistency according to Section 8.6.3.1 of E1820.

The calculation methodology is according to ASTM E1820-15 Annex A9. The various acceptance criteria in E1820 are checked as applicable.

A.5 Input

Plate W10201-4 is reported as SA-302-B in the certified material test report (CMTR) versus SA 302 Grade A in WCAP-7373 [A4]. The chemistry reported in [A4] is consistent between the CMTR and is shown in Table A5-1. Both grade specifications from SA-302 from the 1966 ASME Code [A5] for comparison are shown in Table A5-1.

Table A5-1: Plate W10201-4 Chemistry and Tensile Properties

Specification or Heat Measurement	C %	Mn %	P %	S %	Si %	Mo %	Yield (ksi)	Tensile (ksi)	Elong. (%)	Red. Area (%)
SA-302-A Spec.	0.25 max	0.90-1.35	0.035 max	0.040 max	0.13-0.32	0.41-0.64	45	75-95	15	19
SA-302-B Spec.	0.25 max	1.10-1.55	0.035 max	0.040 max	0.13-0.32	0.41-0.64	50	80-100	15	18
Heat A6604-1 Plate W10201-4	0.19	1.35	0.007	0.019	0.23	0.48	55.0	77.5[1]	33.0	62.7

Note:

[1] The tensile strength tested for the RV surveillance program in both TL and LT orientations are greater than 80 ksi [A4].

Plate W10201-4 meets the requirements for both Grade A and Grade B and is therefore considered as SA-302 Grade B consistent with the CMTR, hereafter.

Figure A5-1 illustrates the W10201-4 plate material removed from archival storage. The plate was stamped identifying it at Lukens Heat No. A6604-1 and plate W10201-4 consistent with the CMTR and

*** This record was final approved on 12/06/2024 08:42:18. (This statement was added by the PRIME system upon its validation)

WCAP-7373 as indicated in Figure A5-1. All stampings are as expected definitively identifying it as the plate stated. The thickness of the plate is consistent with that stated in the CMTR of 10-3/4".

A 1.5" wide piece was cut from the block as shown in Figure A5-2. This cut was far away from the quenched edges which were clearly labeled. The middle of the specimens were removed about 7-3/4" from one of the quenched edges which is less than 1 x thickness required by ASME. However, since the distance is close to 1 x thickness, the impact is expected to be minimal. Also 1" of material from the flame cut edge shown as the surface in the foreground in Figure A5-2 was not used. Twelve (12) specimens total were machined from the 1.5"x9.5" block shown in Figure A5-2. Eight were fabricated in the TL (weak direction) and four (4) in the LT (strong direction) as shown in Table A5-2. The working direction is shown in Figure A5-2. The following IDs for the TL specimens: TLU1, TLU2, TLU3, TLU4, TLU5, TLU6, TLB7, TLB8, and for the LT specimens: LTB1, LTB2, LTB3, and LTB4. "U" in the specimen ID = Upper layer being 1/4T (~3") from the top surface and "B" in the specimen ID = Bottom layer being 1/4T (~3") from the bottom surface. The specimen isometric drawing is shown in Figure A5-3. The specimens were side-grooved 10% of thickness each side. The dimensions were measured for each specimen.

Figure A5-1: Photographs of the W10201-4 Plate Section As-Received and the Plate Stamp Identification

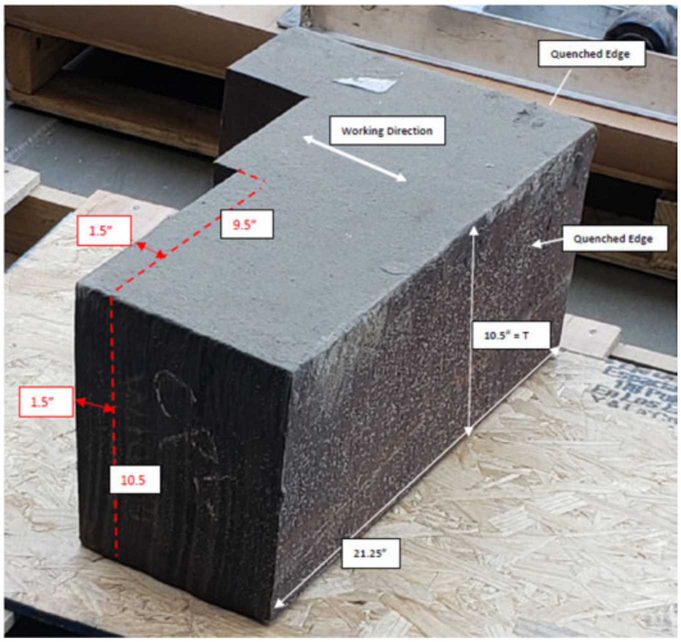

Figure A5-2: Photograph of the Archival Block Showing the Location of Extraction of the Test Material

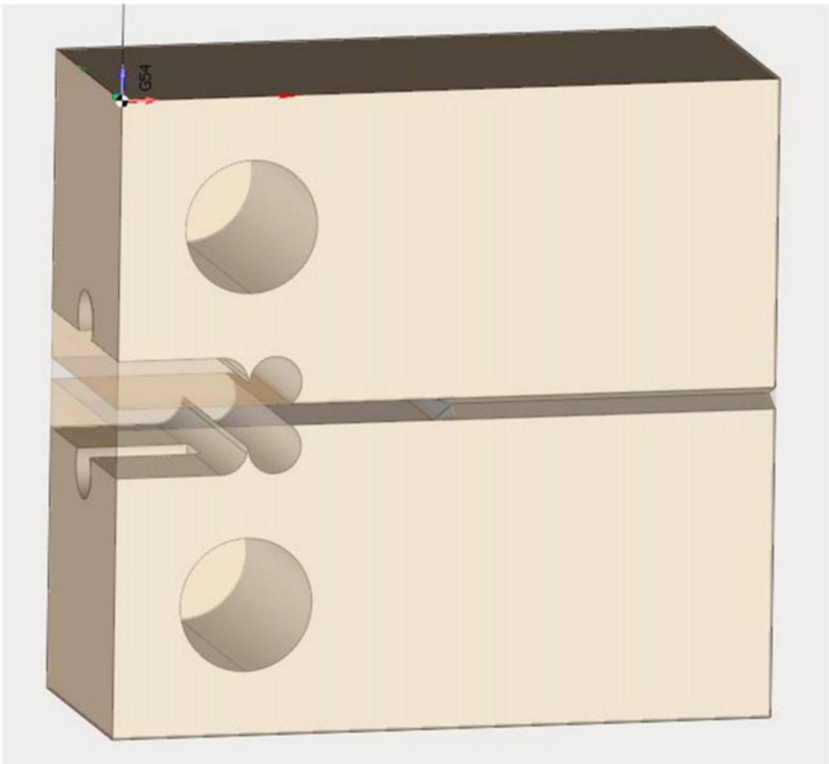

Figure A5-3: 0.5TC(T) Isometric

*** This record was final approved on 12/06/2024 08:42:18. (This statement was added by the PRIME system upon its validation)

Table A5-2: Test specimens

Specimen ID	Thickness Location	Orientation
L-TB1 to L-TB4	3/4T from top	L-T strong
T-LU1 to T-LU6	1/4T from top	T-L weak
T-LB8 (T-LB7 not used)	3/4T from top	T-L weak

Measurements were taken from the specimen fracture surface for precrack and final crack size and specimen side surface photos and scaled using the scale bar.

Tensile properties were taken from WCAP-7373 [A4] which are surveillance program baseline test results with the relevant results shown in Table A5-3.

Table A5-3: Material Properties for Plate W10201-4 [A4]

Orientation	Test Temperature °F	0.2% Yield Strength (ksi)	Ultimate Strength (ksi)
L-T	400	56.4	79.6
L-T	600	57.1	84.0
T-L	400	55.8	77.4
T-L	600	56.2	82.7

*** This record was final approved on 12/06/2024 08:42:18. (This statement was added by the PRIME system upon its validation)

A.6 J-R Curve Test Results

The precracking met the requirements of E1820 [A3], therefore all the precracks were acceptable. T-LB8 failed the A9.9.2.2 a_{0q} R^2 requirement of >0.96 by a small amount (0.93). Regardless of the failure of the a_{0q} positioning criteria, the a_{0q} Δa position was definitively obtained and is positioned as expected through inspection of the blunting line relative to the J-R curve, therefore the determination of J_Q can be determined with certainty even though a fully valid E1820 J_{Ic} measurement was not obtained. Test T-LU6, 2 of the 9 final crack length measurements were short violating the crack straightness criteria of 8.4.5 of E1820 which may affect slightly the J-R curve affecting the C or n value.

Tests L-TB1, L-TB2, T-LU1 and T-LU2 had a large backup rather than following the blunting line and T-LU2 had a crooked precrack. These are not included in the summary table as the results are not reliable.

A.7 Adjustment of Measured J Data to account for Neutron Irradiation

The measured upper-shelf toughness (J) data was adjusted to account for the reduction in toughness due to neutron irradiation. RG1.161 recommends use of NUREG/CR-5265 [A6] or a material-specific justification for plates with S ≥ 0.018%. RG1.161 has an upper limit in sulfur because J-R data for plates with high sulfur content are scarce and the available data showed low toughness, flat J-R curves, and a size effect. The most data available for a high-sulfur A-302B plate are for the V-50 plate as reported in NUREG/CR-5265. The V-50 plate was unusual in that it had a test specimen size effect that has not been observed in other RV material J-R curves and is unique to the V-50 plate. A high content of manganese-sulfide (MnS) inclusions and banded regions of microstructure are believed to be the causes of the unusual specimen size effect observed and the relatively low toughness. The inclusions and banded microstructure are not seen in any of the fracture surfaces of the tested 0.5TC(T) specimens tested from plate W10201-4. In addition, the lowest measured toughness of the W10201-4 plate is higher than the V-50 plate highest values even though the W10201-4 the J-R curve was conducted at 199°C, 117°C higher than the V-50 plate data as shown in Figure A7-1. For these reasons, the V-50 plate is not considered representative and the actual measured toughness of W10201-4 is used with reduction to account for irradiation. This conclusion is consistent with the Palisades and Point Beach equivalent margins analyses [A7] and [A8]. In addition, comparison of test results to another high sulfur plate (S = 0.022%) [A9] tested on 0.5 to 8 inch thick bend bars of a A302B plate shows that the W10201-4 lower bound result, bounds the larger specimens from this 1992 test program.

*** This record was final approved on 12/06/2024 08:42:18. (This statement was added by the PRIME system upon its validation)

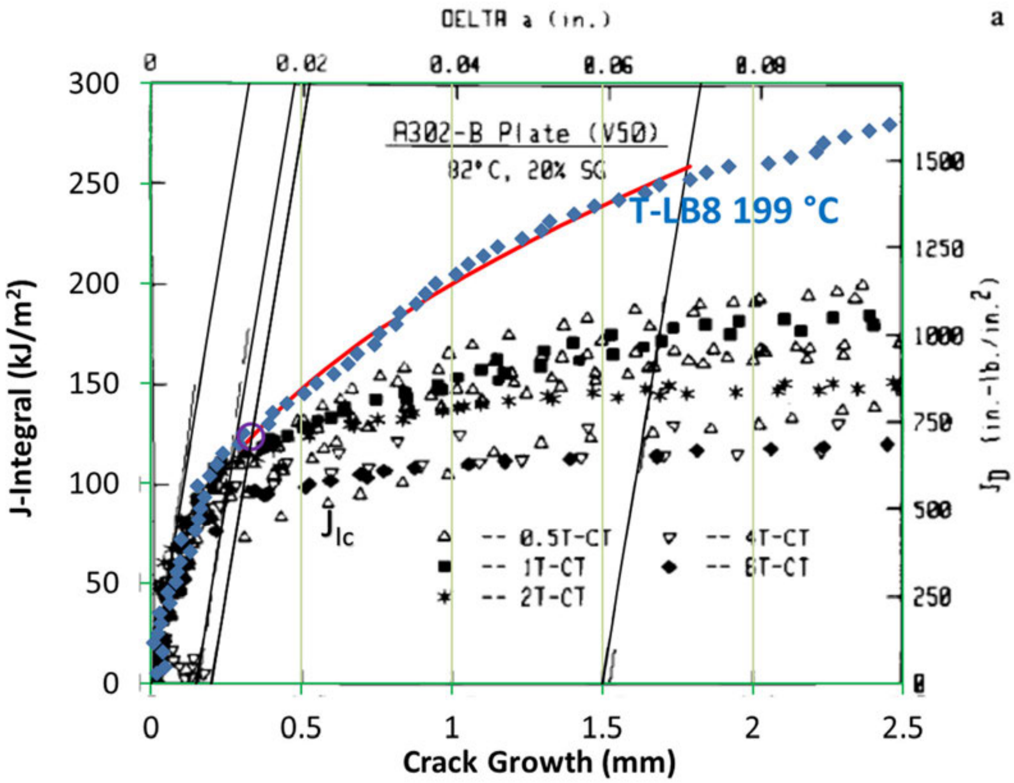

Figure A7-1: Comparison of W10201-4 Plate to V-50 Plate J-R Curve

Two methods are considered to reduce toughness to account for irradiation with the more conservative being chosen:

1. Since Charpy upper-shelf energy (USE) is correlated with J, the reduction according to RG1.99 R2 [A10] is considered in reducing the measured J values, and
2. The reduction according to a more modern USE prediction model [A11] is considered for reduction of the measured J values.

A.7.1 RG1.99 R2 Reduction in USE

RG1.99R2 predicted reduction in USE is calculated in WCAP-18766-NP [A12] and is shown in Table A7-1. The W10201-4 plate falls within the limitations stated in RG1.99R2 section 1.3 and there is no sulfur limitation for predicting USE reduction. As shown in Table 5-2 of WCAP-18766-NP [A12], the W10201-4 plate predicted USE at 1/4T considering the measured USE drop according to RG1.99R2 Position 2.2 is 18%, which is bounded by the 30% calculated from RG1.99R2 Position 1.2. The measured value being bounded by the general RG Position 1.2 model indicates that the higher sulfur content of this plate does not have a deleterious effect on the USE decrease and the Table A7-1 USE drop values can conservatively be applied to the measured J values.

*** This record was final approved on 12/06/2024 08:42:18. (This statement was added by the PRIME system upon its validation)

Table A7-1: Predicted USE for EMA at 70 EFPY for Intermediate Shell Plate W10201-4 [A12]

Vessel Location	Fluence ($\times 10^{19}$ n/cm^2, E > 1.0 MeV)	Projected USE Decrease (%)	Projected SLR USE (ft-lbs)
1/10T	7.077	32%	42.2
1/4T	5.061	30%	43.4

A.7.2 Modern USE Reduction Prediction

Several modern best-estimate USE prediction models were developed by Ogawa et al. for EPRI using 1,177 international RV surveillance program measured changes in USE due to irradiation [A11] and [A13]. The selected models have no significant residual trend with any inputs that include initial USE, fluence, irradiation temperature, copper, nickel, manganese, sulfur, and product form. The "C-1" model developed by EPRI-Ogawa has an associated 2x standard deviation that provides a prediction that bounds at least 95% of the measured USE data that are a function of the predicted USE. The improved model was verified to perform well for the subset of low-USE materials (<100 J), which are of most concern with the EPRI-Ogawa C-1 model bounding 97% of the low-USE measured data. The Ogawa C-1 model included materials in the database with sulfur content up to 0.026% and is therefore applicable to Plate W10201-4 which has 0.019% sulfur. The Ogawa C-1 model is performed with the result shown in Table A7-2.

Table A7-2: Predicted USE Values for EMA at 70 EFPY for Intermediate Shell Plate W10201-4 using Modern Prediction

Vessel Location	Fluence ($\times 10^{19}$ n/cm^2, E > 1.0 MeV)	Projected median USE Decrease (%)	Projected median – 2*SD USE Decrease (%)
1/10T	7.077	12%	28%
1/4T	5.061	11%	28%

These values in Table A7-2 are bounded by the RG1.99R2 predicted decrease shown in Table A7-1, therefore, conservatively, the percent decrease shown in Table A7-1 is applied to the lower bound J-R curve developed in the next section.

A.7.3 Plate W10201-4 Irradiated J-R Curve

The mean and standard deviation (σ) for the 5 T-L tests are calculated for J_{Ic}, C (J at 1 mm) and J at 2.54 mm. The mean - 2σ is calculated for each of these points along the J-R curve and includes J at 0.1 inch since this is used in the EMA. A mean - 2σ lower bound curve was iteratively selected so that the curve lies at or below mean - 2σ at J_{Ic}, 1 mm and 2.54 mm. The lower bound curve is represented by C=184 kJ/m^2, n=0.43 and bounds the lowest measured test and mean - 2σ and is therefore conservatively used for all temperatures between 199 and 288°C at 70 EFPY as shown in Table A7-3.

Table A7-4 shows the decrease of the lower bound J-R curve using the RG1.99R2 decrease.

*** This record was final approved on 12/06/2024 08:42:18. (This statement was added by the PRIME system upon its validation)

Table A7-3: Lower Bound Unirradiated Plate W10201-4 J-R Curve

Orientation, Thickness Location	Test Temperature (°C)	Specimen ID	J_{Ic} (kJ/m^2)	C (J@1mm) (kJ/m^2)	n	J@2.54mm (J@0.1 in) (kJ/m^2)
T-L, 1/4T	288	T-LU3	150	216	0.35	299
	288	T-LU4	174	233	0.30	308
	199	T-LU5	140	203	0.36	284
	199	T-LU6	162	230	0.36	322
T-L, 3/4T	199	T-LB8	123	200	0.44	301
Mean			150	216		303
σ			19.7	15.1		13.7
mean - 2σ			110	186		275
Lower Bound: C=184, n=0.43	199 - 288		110	**184**	**0.43**	275

Table A7-4: Lower Bound Predicted Toughness Values for EMA at 70 EFPY for Intermediate Shell Plate W10201-4

Vessel Location	Fluence[(b)] (x 10^{19} n/cm^2, E > 1.0 MeV)	Projected RG1.99R2 USE Decrease (%)	J_{Ic}		C		n
			kJ/m^2	in-lb/in^2	kJ/m^2	in-lb/in^2	
Unirradiated	**0.0**	**0%**	**110**	627	**184**	4225	0.43
1/10T	7.077	32%	75	426	125	2873	0.43
1/4T	5.061	30%	77	439	129	2958	0.43

A.7.4 Other Beltline Plates

Plate W10201-5 (Heat B-1256-1) also has high sulfur (0.021%) and is predicted to drop below 50 ft-lb USE per WCAP-18766-NP [A12], but is not available in archives for testing. This heat is contained in some of the surveillance capsules that have been tested and Capsule U which is planned for withdrawal and testing in a few years. It is recommended that high S plates W10201-4 and W10201-5 be tested for upper-shelf fracture toughness when Capsule U is withdrawn and tested. There are 2 upper shell plates (W10201-1 and W10201-3) and 2 lower shell plates (W10201-4 and W10201-5) projected to drop below 50 ft-lbs per Table 5-3 of WCAP-18766-NP [A12]. Plate W10201-5 has higher S than the tested plate W10201-4, however the tested W10201-4 plate has the lowest projected USE due to its higher Cu content and lower starting USE, therefore the W10201-4 projected J-R properties are bounding for all the upper and intermediate shell plates. In addition, all 3 of the intermediate shell plates have measured irradiated USE values which when projected using the RG1.99R2 Position 2.2 methodology are bounded by the Position 1.2 projections. Therefore, the RG1.99R2 Position 1.2 projections are conservative and the measured J-R curve projected to SLR fluence can be conservatively used for all the plates.

*** This record was final approved on 12/06/2024 08:42:18. (This statement was added by the PRIME system upon its validation)

A.7.5 Plate W10201-1 and Weld W5214 Irradiated J-R Testing

Upper shell plate W10201-1 weld W5214 were available from the tested Capsule X HAZ specimens irradiated to 4.42×10^{19} n/cm^2 which is significantly higher than either material is projected to reach during SLR [A12]. This plate and weld were machined into 0.16TC(T) specimens and tested mostly in the ductile-brittle transition region. However, one of each was tested slightly above this region and a full J-R curve was generated for each according to ASTM E1820-15 [A3]. The plate result was significantly higher than the measurement capacity of the small specimen and is therefore not a valid measure of J_{Ic}, in addition to a couple of other violations (see Table A7-5 and Figure A7-2). However, it demonstrated very good toughness at this high fluence which is greater than the projected Intermediate Shell Plate W10201-4 toughness at SLR fluence providing support to the projected toughness values reported in Table A7-4. The weld test had a number of test violations primarily due to the small specimen size, therefore the reported J_Q is approximate. However, the J_Q and J-R curve measured values are significantly higher than the projected J-R curve properties for Intermediate Shell Plate W10201-4 toughness at SLR fluence also providing support to the projected toughness values reported in Table A7-4 being lower bound for the RPV. It is noted that the test temperature and fluence are different, so a direct quantitative comparison cannot be made.

Table A7-5: Invalid Toughness Properties of Specimens Irradiated in Capsule X to Fluence of 4.42×10^{19} n/cm^2

Material	Test Temperature (°C)	J_Q (kJ/m^2)	J_{Ic} Validity Violation	C	n	J-R Curve Validity Violation	Specimen ID
Upper shell plate W10201-1	-31	~402[1]	Multiple[1]	~506	~0.35	Multiple[1]	PB
Weld W5214	78	~129[2]	Multiple[2]	~253	~0.55	Multiple[2]	WU

Notes:

1. Significant E1820-15 violations included: Significantly exceeds J_{max} (A8.3.2); Final crack front straightness violation (9.1.4.2); and blunting line crack size measurements exceed noise limit (A9.9.2.2).
2. Significant E1820-15 violations included: Final crack front straightness violation (9.1.4.2); Compliance measured Δa does not agree with optical fracture surface measurement (9.1.5.2); Minor violations included: blunting line crack size measurements exceed noise limit slightly (A9.9.2.2) and initial a straightness (9.1.4.1).

*** This record was final approved on 12/06/2024 08:42:18. (This statement was added by the PRIME system upon its validation)

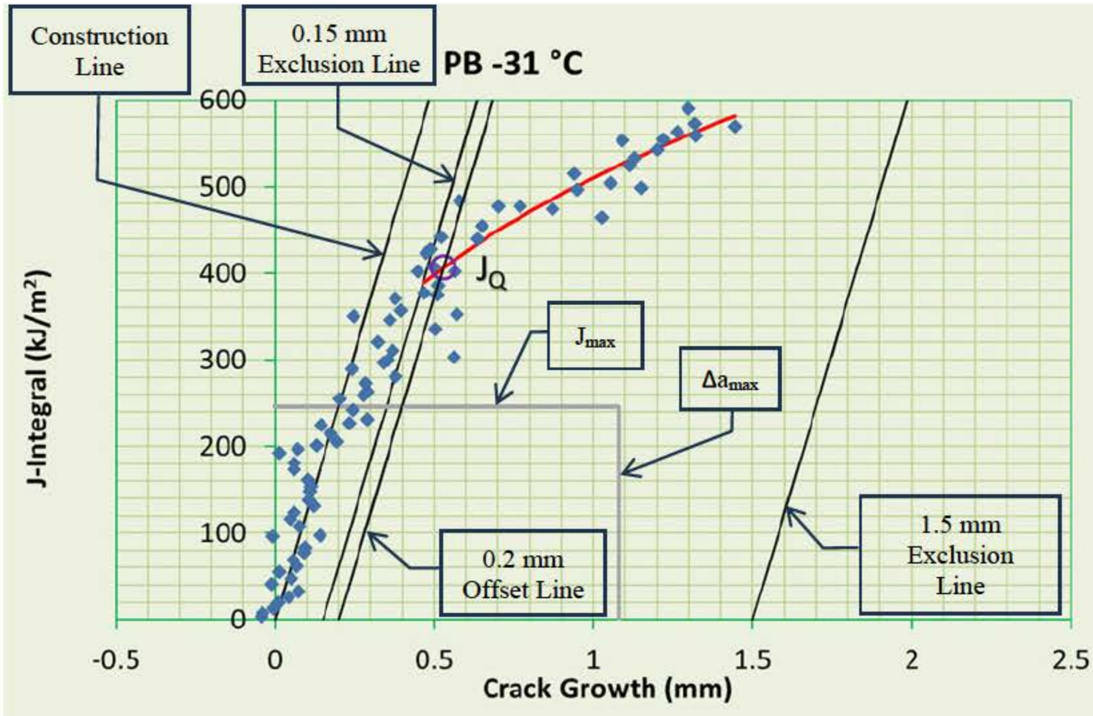

Figure A7-2: Upper Shell Plate W10201-1 J-R Curve with Fluence of 4.42 × 10^{19} n/cm^2

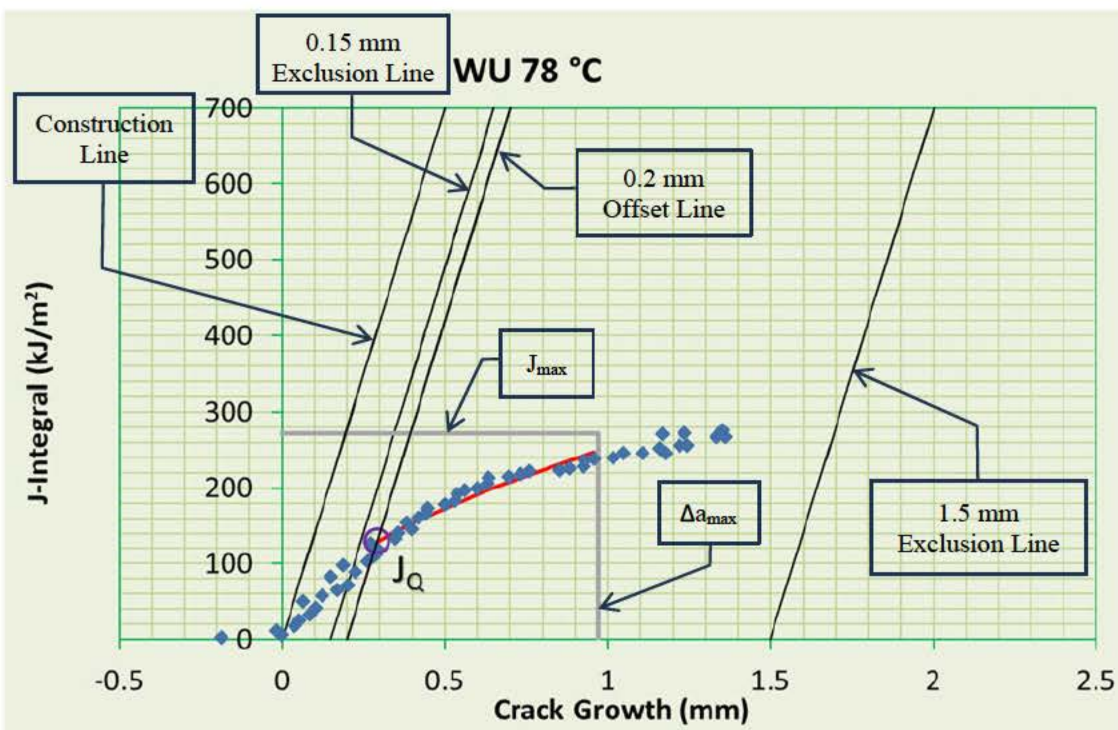

Figure A7-3: Weld W5214 J-R Curve with Fluence of 4.42 × 10^{19} n/cm^2

A.8 Detailed Test Results

Specimen ID	L-TB4			J_Q	255.8	kJ/m^2
Fluence	0	n/cm^2		C1	310.9	
Test Temperature	200	°C		C2	0.26	
Width [W]	25.40	mm		KJ_Q	232.0	Mpa√m
Thickness [B]	12.70	mm		**J-R Curve Valid; A8**		
Tensile Strength	549	MPa			Jmax; A8.3.1	YES
Yield Strength	389	MPa			Δamax; A8.3.2	YES
Net Thickness	9.95	mm		a final crack straightness; 9.1.4.2		YES
Initial adjusted crack length	12.36	mm		**J_{Ic} Valid; A9**		
Initial fatigue crack length (measured)	12.08	mm		a0 crack straightness; 9.1.4.1		YES
Final crack length (calculated)	14.70	mm	Points between exclusion lines; A9.6.6.6 or A9.7			YES
Final crack length (measured)	15.08	mm	Initial crack length agreement; A9.9.2.1			YES
			Initial crack length Adjustment; A9.9.2.2			NO
			Precycle crack length consistency; 8.6.3.1			YES
			Δa predicted vs optical; 9.1.5.2			NO
Sequence	**Peak Load (kN)**	**Peak CMOD (mm)**	**a (mm)**	**Δa (mm)**	**K (MPa√m)**	**J (kJ/m^2)**
1	6.6	0.10	12.40	0.04	34.3	5.6
2	7.9	0.13	12.37	0.01	40.8	8.7
3	9.0	0.15	12.39	0.03	46.6	12.4
4	9.8	0.18	12.36	0.00	50.7	16.7
5	10.4	0.20	12.38	0.02	54.0	21.0
6	10.9	0.23	12.38	0.02	56.4	25.8
7	11.2	0.25	12.37	0.01	58.0	30.9
8	11.4	0.28	12.40	0.04	59.5	35.8
9	11.6	0.31	12.38	0.02	60.4	41.3
10	11.8	0.33	12.40	0.04	61.5	46.3
11	12.0	0.36	12.39	0.03	62.2	51.7
12	12.1	0.38	12.44	0.08	63.3	56.7
13	12.2	0.41	12.44	0.08	63.9	62.1
14	12.3	0.43	12.45	0.09	64.6	67.6
15	12.5	0.46	12.46	0.10	65.3	72.9
16	12.6	0.48	12.46	0.10	65.9	78.6
17	12.7	0.51	12.47	0.11	66.5	84.1
18	12.8	0.53	12.48	0.12	67.1	89.6
19	12.9	0.56	12.47	0.11	67.4	95.5
20	12.9	0.59	12.49	0.13	68.1	100.9
21	13.0	0.61	12.48	0.12	68.4	106.9
22	13.1	0.64	12.50	0.14	69.0	112.5
23	13.2	0.66	12.51	0.15	69.6	118.2
24	13.3	0.69	12.49	0.13	69.8	124.5
25	13.4	0.71	12.52	0.16	70.5	129.9
26	13.4	0.74	12.51	0.15	70.7	136.1
27	13.5	0.76	12.54	0.18	71.1	141.6
28	13.5	0.79	12.54	0.18	71.4	147.6
29	13.5	0.81	12.54	0.18	71.5	153.7
30	13.5	0.84	12.58	0.22	72.0	159.1
31	13.5	0.86	12.59	0.23	71.9	165.0
32	13.5	0.89	12.64	0.28	72.4	170.0
33	13.6	0.92	12.59	0.23	72.1	177.3
34	13.6	0.94	12.49	0.13	71.5	185.5
35	13.7	0.97	12.51	0.15	71.9	191.0
36	13.7	0.99	12.54	0.18	72.2	196.6
37	13.7	1.02	12.58	0.22	72.9	201.6
38	13.7	1.04	12.58	0.22	73.0	207.8
39	13.8	1.07	12.61	0.25	73.4	213.4
40	13.8	1.09	12.66	0.30	73.9	218.4
41	13.8	1.12	12.65	0.29	74.0	224.8
42	13.8	1.14	12.71	0.35	74.4	229.5
43	13.8	1.17	12.74	0.38	74.7	235.1
44	13.8	1.19	12.76	0.40	74.9	240.6
45	13.8	1.22	12.81	0.45	75.4	245.5
46	13.8	1.24	12.82	0.46	75.5	251.5
47	13.8	1.27	12.88	0.52	75.9	256.2
48	13.8	1.30	12.85	0.49	75.7	263.2
49	13.7	1.32	12.91	0.55	75.9	267.9
50	13.6	1.35	12.96	0.60	75.9	272.6
51	13.6	1.37	12.98	0.62	75.7	278.1
52	13.5	1.40	13.06	0.70	76.3	281.8
53	13.4	1.42	13.07	0.71	75.8	287.7
54	13.3	1.45	13.13	0.77	75.8	292.1
55	13.3	1.47	13.17	0.81	75.9	296.9
56	13.2	1.50	13.22	0.86	75.7	301.4
57	13.1	1.52	13.30	0.94	76.0	304.7
58	13.0	1.55	13.31	0.95	75.8	310.7
59	12.9	1.58	13.40	1.04	76.0	313.4
60	12.8	1.60	13.45	1.09	75.9	317.6
61	12.7	1.63	13.49	1.13	75.9	322.2
62	12.7	1.65	13.55	1.19	76.0	325.9
63	12.5	1.68	13.58	1.22	75.5	331.0
64	12.4	1.70	13.69	1.33	75.8	332.6
65	12.3	1.73	13.74	1.38	75.7	336.5
66	12.2	1.75	13.79	1.43	75.3	340.8
67	12.1	1.78	13.85	1.49	75.3	344.5
68	12.0	1.80	13.89	1.53	75.0	348.6
69	11.7	1.83	13.97	1.61	74.3	351.2
70	11.5	1.86	14.07	1.71	73.8	352.7
71	11.1	1.91	14.21	1.85	72.6	358.0
72	10.7	1.96	14.36	2.00	71.9	361.9
73	10.4	2.01	14.56	2.20	71.4	363.8
74	10.1	2.06	14.70	2.34	71.4	368.0

*** This record was final approved on 12/06/2024 08:42:18. (This statement was added by the PRIME system upon its validation)

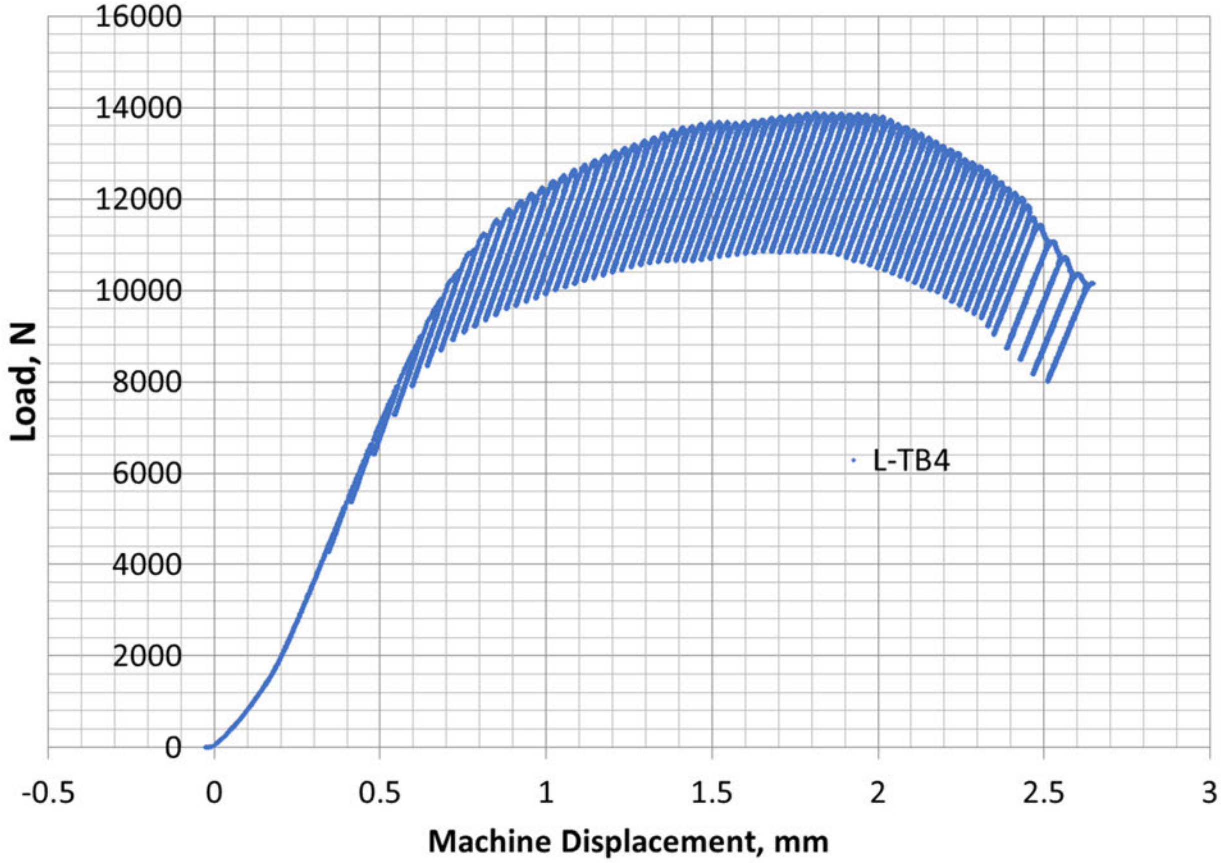

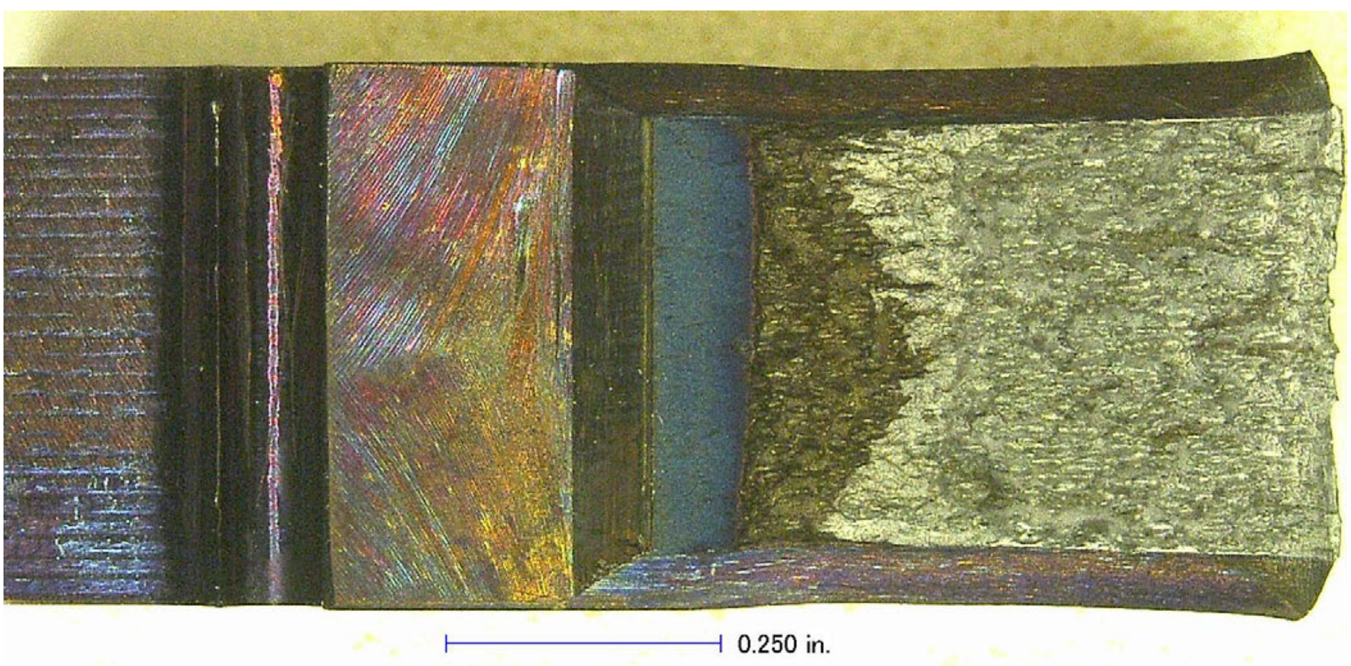

*** This record was final approved on 12/06/2024 08:42:18. (This statement was added by the PRIME system upon its validation)

Specimen ID	L-TB3			J_Q	132.0	kJ/m^2
Fluence	0	n/cm^2		C1	251.2	
Test Temperature	291	°C		C2	0.59	
Width [W]	25.40	mm		KJ_Q	164.2	Mpa√m
Thickness [B]	12.70	mm		**J-R Curve Valid; A8**		
Tensile Strength	580	MPa			Jmax; A8.3.1	YES
Yield Strength	394	MPa			Δamax; A8.3.2	YES
Net Thickness	9.95	mm		a final crack straightness; 9.1.4.2		YES
Initial adjusted crack length	12.13	mm		**J_{Ic} Valid; A9**		
Initial fatigue crack length (measured)	12.08	mm		a0 crack straightness; 9.1.4.1		YES
Final crack length (calculated)	14.38	mm	Points between exclusion lines; A9.6.6.6 or A9.7			YES
Final crack length (measured)	14.69	mm	Initial crack length agreement; A9.9.2.1			YES
			Initial crack length Adjustment; A9.9.2.2			YES
			Precycle crack length consistency; 8.6.3.1			YES
				Δa predicted vs optical; 9.1.5.2		YES
Sequence	**Peak Load (kN)**	**Peak CMOD (mm)**	**a (mm)**	**Δa (mm)**	**K (MPa√m)**	**J (kJ/m^2)**
1	6.5	0.10	12.19	0.06	33.2	5.4
2	7.8	0.13	12.16	0.02	39.2	8.4
3	8.7	0.15	12.17	0.03	44.2	11.8
4	9.5	0.18	12.15	0.02	47.9	15.7
5	10.1	0.20	12.16	0.03	51.0	19.9
6	10.5	0.23	12.14	0.01	53.1	24.4
7	10.9	0.25	12.15	0.02	55.0	28.9
8	11.2	0.28	12.15	0.02	56.4	33.7
9	11.4	0.31	12.15	0.02	57.6	38.5
10	11.6	0.33	12.19	0.06	59.0	43.4
11	11.8	0.36	12.22	0.09	60.1	50.4
12	12.0	0.38	12.25	0.11	61.2	55.4
13	12.1	0.41	12.28	0.14	62.3	60.6
14	12.3	0.43	12.26	0.13	62.9	66.1
15	12.4	0.46	12.30	0.17	64.0	71.2
16	12.6	0.48	12.30	0.16	64.6	76.7
17	12.7	0.51	12.34	0.21	65.6	81.9
18	12.8	0.53	12.33	0.20	66.2	87.6
19	13.0	0.56	12.36	0.22	67.0	93.0
20	13.0	0.59	12.39	0.26	67.8	98.4
21	13.1	0.61	12.39	0.26	68.3	104.2
22	13.2	0.64	12.44	0.31	69.2	109.3
23	13.3	0.66	12.43	0.30	69.6	115.4
24	13.4	0.69	12.45	0.32	70.3	121.0
25	13.5	0.71	12.46	0.33	70.7	126.9
26	13.6	0.74	12.51	0.38	71.5	132.2
27	13.6	0.76	12.54	0.41	72.1	137.8
28	13.7	0.79	12.54	0.40	72.4	144.1
29	13.8	0.81	12.57	0.43	72.9	149.7
30	13.8	0.84	12.59	0.46	73.4	155.4
31	13.8	0.86	12.62	0.48	73.8	161.2
32	13.9	0.89	12.65	0.52	74.3	166.7
33	13.9	0.92	12.66	0.53	74.5	172.7
34	13.9	0.94	12.70	0.57	75.0	178.2
35	13.9	0.97	12.73	0.60	75.4	183.9
36	14.0	0.99	12.75	0.62	75.7	189.9
37	14.0	1.02	12.79	0.66	76.1	195.2
38	14.0	1.04	12.78	0.64	76.0	202.1
39	13.9	1.07	12.82	0.68	76.2	207.5
40	13.9	1.09	12.84	0.70	76.4	213.4
41	14.0	1.12	12.87	0.74	76.8	218.9
42	14.0	1.14	12.92	0.78	77.3	224.0
43	14.0	1.17	12.91	0.78	77.2	230.6
44	13.9	1.19	12.95	0.82	77.4	236.1
45	13.9	1.22	12.98	0.85	77.4	241.5
46	13.8	1.25	13.00	0.87	77.4	247.5
47	13.7	1.27	13.06	0.93	77.4	252.1
48	13.6	1.30	13.11	0.97	77.1	257.3
49	13.5	1.32	13.21	1.08	77.3	260.4
50	13.4	1.35	13.25	1.12	77.2	265.3
51	13.3	1.37	13.30	1.16	77.1	270.2
52	13.3	1.40	13.34	1.21	77.5	275.0
53	13.2	1.42	13.36	1.22	77.3	280.8
54	13.2	1.45	13.42	1.29	77.8	285.0
55	13.2	1.47	13.44	1.31	77.9	290.5
56	13.2	1.50	13.47	1.34	78.1	295.9
57	13.1	1.53	13.54	1.40	78.6	299.8
58	13.1	1.55	13.54	1.40	78.4	306.1
59	13.1	1.58	13.60	1.46	78.8	310.2
60	13.0	1.60	13.60	1.47	78.8	316.2
61	12.8	1.65	13.71	1.57	78.6	325.2
62	12.7	1.70	13.77	1.64	78.6	335.0
63	12.7	1.76	13.84	1.71	78.8	344.8
64	12.5	1.81	13.92	1.79	78.7	353.4
65	12.3	1.86	14.03	1.90	78.6	361.3
66	12.1	1.91	14.13	2.00	78.2	368.8
67	11.8	1.96	14.23	2.09	77.4	376.5
68	11.5	2.01	14.38	2.25	77.2	381.2

*** This record was final approved on 12/06/2024 08:42:18. (This statement was added by the PRIME system upon its validation)

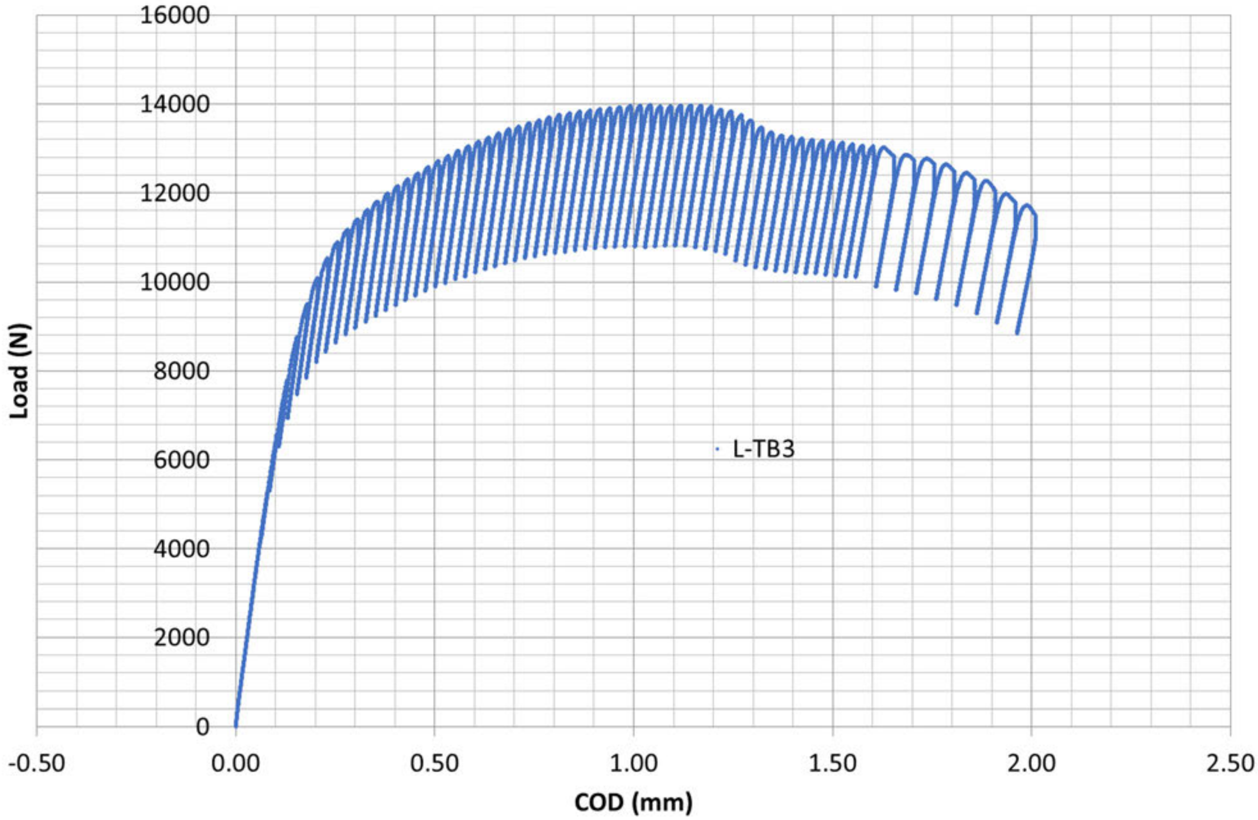

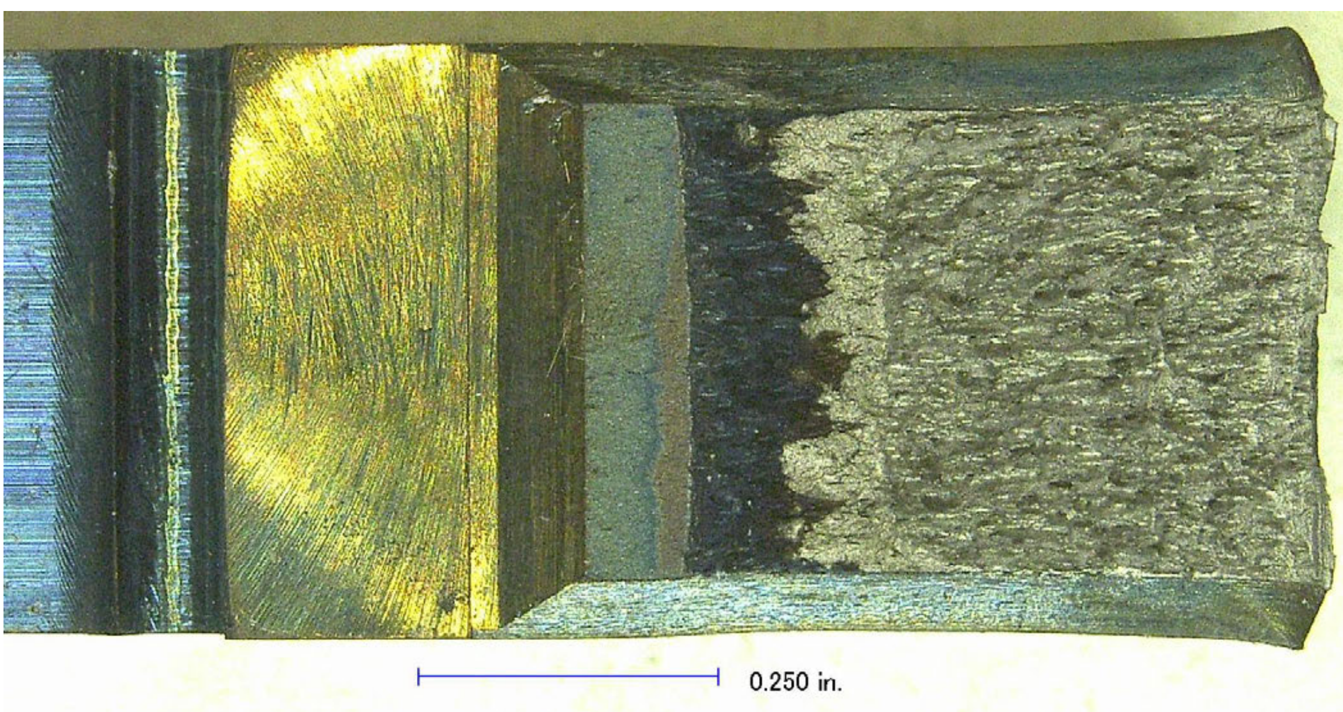

*** This record was final approved on 12/06/2024 08:42:18. (This statement was added by the PRIME system upon its validation)

Specimen ID	T-LU3			J_Q	150.4	kJ/m^2
Fluence	0	n/cm^2		C1	216.4	
Test Temperature	288	°C		C2	0.35	
Width [W]	25.40	mm		KJ_Q	175.3	Mpa√m
Thickness [B]	12.70	mm		**J-R Curve Valid; A8**		
Tensile Strength	571	MPa			Jmax; A8.3.1	YES
Yield Strength	388	MPa			Δamax; A8.3.2	YES
Net Thickness	9.95	mm		a final crack straightness; 9.1.4.2		YES
Initial adjusted crack length	11.89	mm		**J_{Ic} Valid; A9**		
Initial fatigue crack length (measured)	12.08	mm		a0 crack straightness; 9.1.4.1		YES
Final crack length (calculated)	14.71	mm	Points between exclusion lines; A9.6.6.6 or A9.7			YES
Final crack length (measured)	15.30	mm	Initial crack length agreement; A9.9.2.1			YES
			Initial crack length Adjustment; A9.9.2.2			YES
			Precycle crack length consistency; 8.6.3.1			YES
			Δa predicted vs optical; 9.1.5.2			YES

Sequence	Peak Load (kN)	Peak CMOD (mm)	a (mm)	Δa (mm)	K (MPa√m)	J (kJ/m^2)
1	6.5	0.10	11.96	0.07	32.2	5.1
2	7.7	0.13	11.94	0.05	37.8	8.1
3	8.6	0.15	11.93	0.04	42.4	11.7
4	9.3	0.18	11.90	0.01	45.7	15.6
5	9.9	0.20	11.93	0.04	48.5	19.6
6	10.3	0.23	11.89	0.00	50.3	24.1
7	10.6	0.25	11.89	0.00	51.9	28.5
8	10.9	0.28	11.91	0.02	53.3	33.1
9	11.1	0.30	11.87	-0.02	54.2	38.0
10	11.3	0.33	11.94	0.05	55.6	42.5
11	11.5	0.36	11.90	0.01	56.3	47.6
12	11.6	0.38	11.97	0.07	57.6	52.1
13	11.8	0.41	11.98	0.09	58.5	57.1
14	12.0	0.43	11.98	0.09	59.2	62.3
15	12.1	0.46	12.00	0.11	60.0	67.2
16	12.2	0.48	11.99	0.10	60.6	72.6
17	12.3	0.51	12.04	0.15	61.5	77.5
18	12.5	0.53	12.04	0.15	62.1	82.8
19	12.6	0.56	12.06	0.17	62.8	88.1
20	12.7	0.58	12.09	0.20	63.6	93.3
21	12.8	0.61	12.08	0.19	64.0	99.0
22	12.9	0.63	12.12	0.23	64.8	104.0
23	12.9	0.66	12.11	0.22	65.0	109.8
24	13.0	0.69	12.11	0.22	65.4	115.4
25	13.1	0.71	12.14	0.25	65.9	120.8
26	13.1	0.74	12.15	0.26	66.2	126.3
27	13.2	0.76	12.20	0.31	66.9	131.2
28	13.2	0.79	12.19	0.30	66.9	137.2
29	13.2	0.81	12.22	0.33	67.3	142.5
30	13.2	0.84	12.27	0.38	67.8	147.5
31	13.3	0.86	12.26	0.37	67.9	153.5
32	13.3	0.89	12.32	0.43	68.5	158.3
33	13.3	0.91	12.36	0.47	68.9	163.4
34	13.3	0.94	12.38	0.49	69.2	168.9
35	13.4	0.96	12.39	0.50	69.5	174.5
36	13.4	0.99	12.44	0.55	70.0	179.5
37	13.4	1.02	12.53	0.64	70.7	183.8
38	13.3	1.04	12.55	0.66	70.7	189.2
39	13.3	1.07	12.61	0.72	71.1	194.1
40	13.3	1.09	12.64	0.75	71.3	199.3
41	13.3	1.12	12.69	0.80	71.4	204.2
42	13.2	1.14	12.77	0.88	71.9	208.3
43	13.2	1.17	12.80	0.91	72.0	213.5
44	13.1	1.19	12.86	0.97	72.2	218.1
45	13.1	1.22	12.93	1.04	72.5	222.3
46	13.0	1.24	12.97	1.08	72.6	227.2
47	13.0	1.27	13.02	1.13	72.7	232.0
48	12.7	1.30	13.05	1.16	71.6	237.3
49	12.4	1.32	13.20	1.30	71.3	239.0
50	12.2	1.35	13.28	1.38	70.8	242.6
51	12.0	1.37	13.36	1.47	70.2	246.0
52	11.8	1.40	13.54	1.65	70.6	246.1
53	11.5	1.42	13.63	1.74	69.6	249.4
54	11.3	1.45	13.76	1.87	69.4	251.0
55	10.9	1.47	13.87	1.98	68.4	253.1
56	10.8	1.50	13.99	2.10	68.5	254.6
57	10.0	1.55	14.26	2.37	66.3	256.8
58	9.7	1.60	14.48	2.59	66.3	259.6
59	9.5	1.65	14.71	2.82	66.7	261.8

*** This record was final approved on 12/06/2024 08:42:18. (This statement was added by the PRIME system upon its validation)

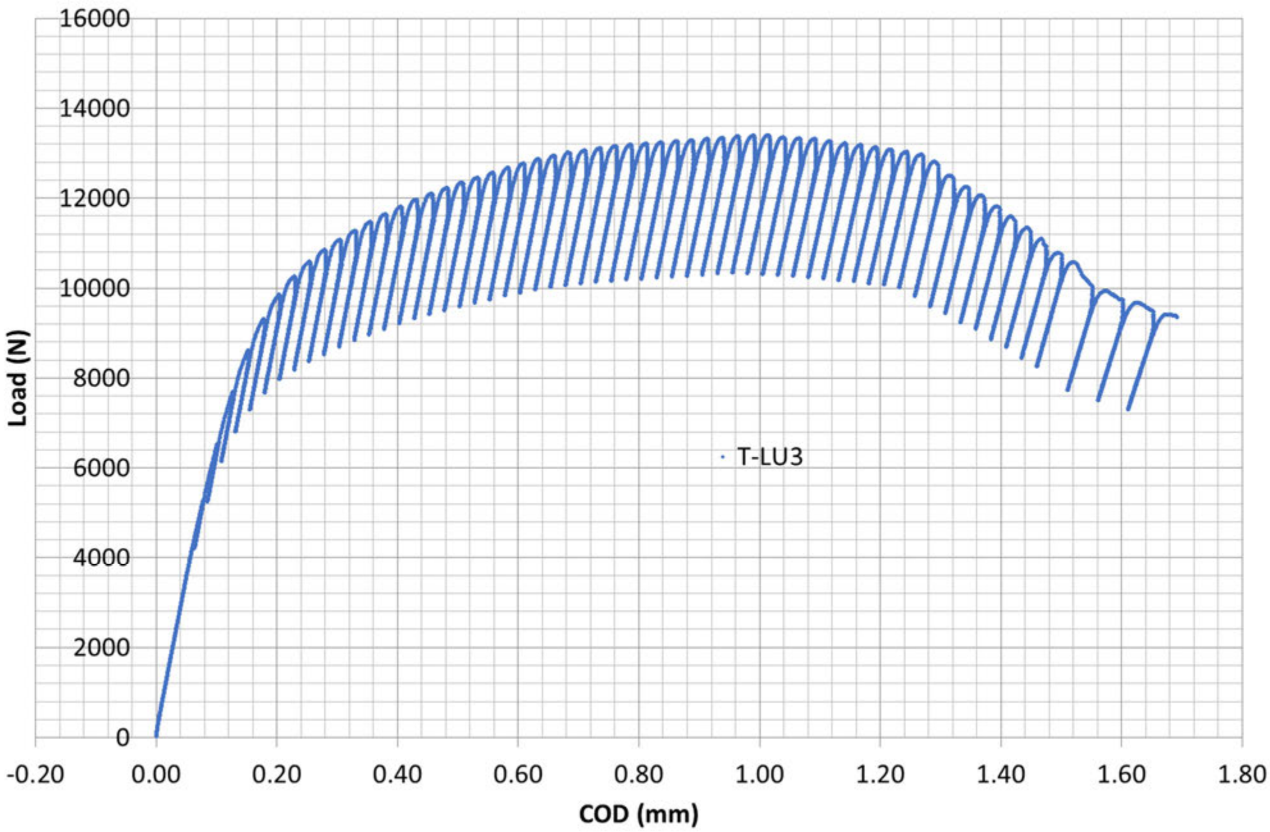

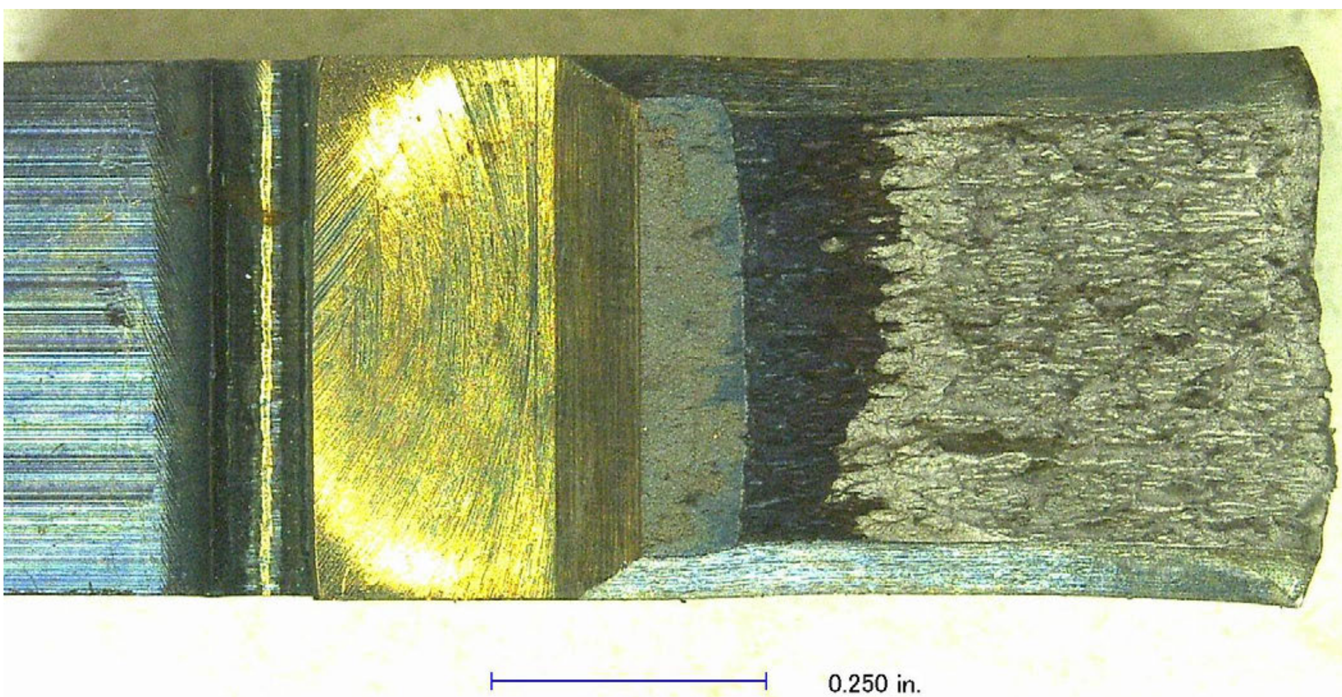

*** This record was final approved on 12/06/2024 08:42:18. (This statement was added by the PRIME system upon its validation)

Specimen ID	T-LU4			J_Q	173.6	kJ/m^2
Fluence	0	n/cm^2		C1	232.7	
Test Temperature	288	°C		C2	0.30	
Width [W]	25.4	mm		KJ_Q	188.4	Mpa√m
Thickness [B]	12.70	mm		**J-R Curve Valid; A8**		
Tensile Strength	571	MPa			Jmax; A8.3.1	YES
Yield Strength	388	MPa			Δamax; A8.3.2	YES
Net Thickness	9.95	mm			a final crack straightness; 9.1.4.2	Minor
Initial adjusted crack length	11.62	mm		**J_{Ic} Valid; A9**		
Initial fatigue crack length (measured)	12.08	mm			a0 crack straightness; 9.1.4.1	YES
Final crack length (calculated)	14.17	mm			Points between exclusion lines; A9.6.6.6 or A9.7	YES
Final crack length (measured)	14.98	mm			Initial crack length agreement; A9.9.2.1	YES
					Initial crack length Adjustment; A9.9.2.2	YES
					Precycle crack length consistency; 8.6.3.1	YES
					Δa predicted vs optical; 9.1.5.2	YES
Sequence	**Peak Load (kN)**	**Peak CMOD (mm)**	**a (mm)**	**Δa (mm)**	**K (MPa√m)**	**J (kJ/m^2)**
1	6.6	0.10	11.71	0.09	31.9	5.0
2	7.9	0.12	11.69	0.06	37.8	8.1
3	8.9	0.15	11.68	0.05	42.7	11.6
4	9.7	0.17	11.69	0.07	46.5	15.6
5	10.3	0.20	11.66	0.03	49.3	19.9
6	10.8	0.22	11.60	-0.02	51.2	24.6
7	11.2	0.25	11.63	0.01	53.1	29.1
8	11.4	0.27	11.61	-0.01	54.3	34.0
9	11.7	0.30	11.63	0.01	55.5	38.7
10	11.9	0.33	11.62	-0.01	56.5	43.8
11	12.1	0.35	11.65	0.03	57.6	48.7
12	12.3	0.38	11.67	0.04	58.6	53.7
13	12.4	0.40	11.68	0.06	59.6	58.9
14	12.6	0.43	11.69	0.07	60.4	64.1
15	12.8	0.45	11.69	0.06	61.1	69.6
16	12.9	0.48	11.73	0.10	62.1	74.7
17	13.0	0.50	11.73	0.11	62.8	80.1
18	13.2	0.53	11.71	0.09	63.2	85.9
19	13.3	0.55	11.75	0.13	64.0	91.1
20	13.4	0.58	11.76	0.14	64.6	96.7
21	13.5	0.61	11.79	0.17	65.4	102.0
22	13.6	0.63	11.81	0.18	66.0	107.6
23	13.7	0.66	11.77	0.15	66.2	114.0
24	13.8	0.68	11.84	0.22	67.2	118.9
25	13.9	0.71	11.82	0.20	67.5	125.0
26	14.0	0.73	11.86	0.23	68.1	130.4
27	14.0	0.76	11.84	0.22	68.3	136.7
28	14.1	0.78	11.87	0.24	68.8	142.3
29	14.1	0.81	11.90	0.28	69.3	147.8
30	14.2	0.83	11.89	0.27	69.4	154.1
31	14.2	0.86	11.94	0.32	70.0	159.2
32	14.2	0.88	11.96	0.34	70.4	164.9
33	14.3	0.91	11.96	0.34	70.5	171.1
34	14.3	0.94	12.04	0.42	71.2	175.7
35	14.3	0.96	12.08	0.45	71.6	181.3
36	14.3	0.99	12.13	0.51	72.1	186.4
37	14.3	1.01	12.16	0.54	72.5	191.9
38	14.3	1.04	12.20	0.57	72.7	197.4
39	14.3	1.06	12.26	0.63	73.2	202.3
40	14.3	1.09	12.27	0.64	73.0	208.6
41	14.2	1.11	12.35	0.73	73.2	212.6
42	14.1	1.14	12.38	0.76	73.1	218.2
43	14.0	1.16	12.46	0.84	73.3	222.5
44	13.9	1.19	12.54	0.92	73.5	226.6
45	13.7	1.22	12.62	1.00	73.3	230.8
46	13.6	1.24	12.67	1.05	73.1	235.7
47	13.5	1.27	12.75	1.12	73.0	239.8
48	13.3	1.29	12.79	1.17	72.7	244.5
49	13.2	1.32	12.87	1.25	72.8	248.4
50	13.1	1.34	12.92	1.30	72.7	252.9
51	13.0	1.37	12.99	1.37	72.7	257.1
52	12.8	1.39	13.08	1.45	72.5	260.5
53	12.7	1.42	13.14	1.52	72.2	264.4
54	12.5	1.44	13.22	1.60	71.8	267.9
55	12.3	1.47	13.31	1.69	71.8	270.9
56	12.2	1.49	13.38	1.75	71.7	274.6
57	12.1	1.52	13.42	1.79	71.6	279.0
58	12.1	1.55	13.50	1.88	72.0	282.0
59	11.9	1.60	13.59	1.96	71.4	290.9
60	11.7	1.65	13.68	2.06	71.4	298.7
61	11.5	1.70	13.83	2.21	71.3	304.7
62	11.1	1.75	13.98	2.36	70.8	310.2
63	10.7	1.80	14.17	2.55	69.7	313.9

*** This record was final approved on 12/06/2024 08:42:18. (This statement was added by the PRIME system upon its validation)

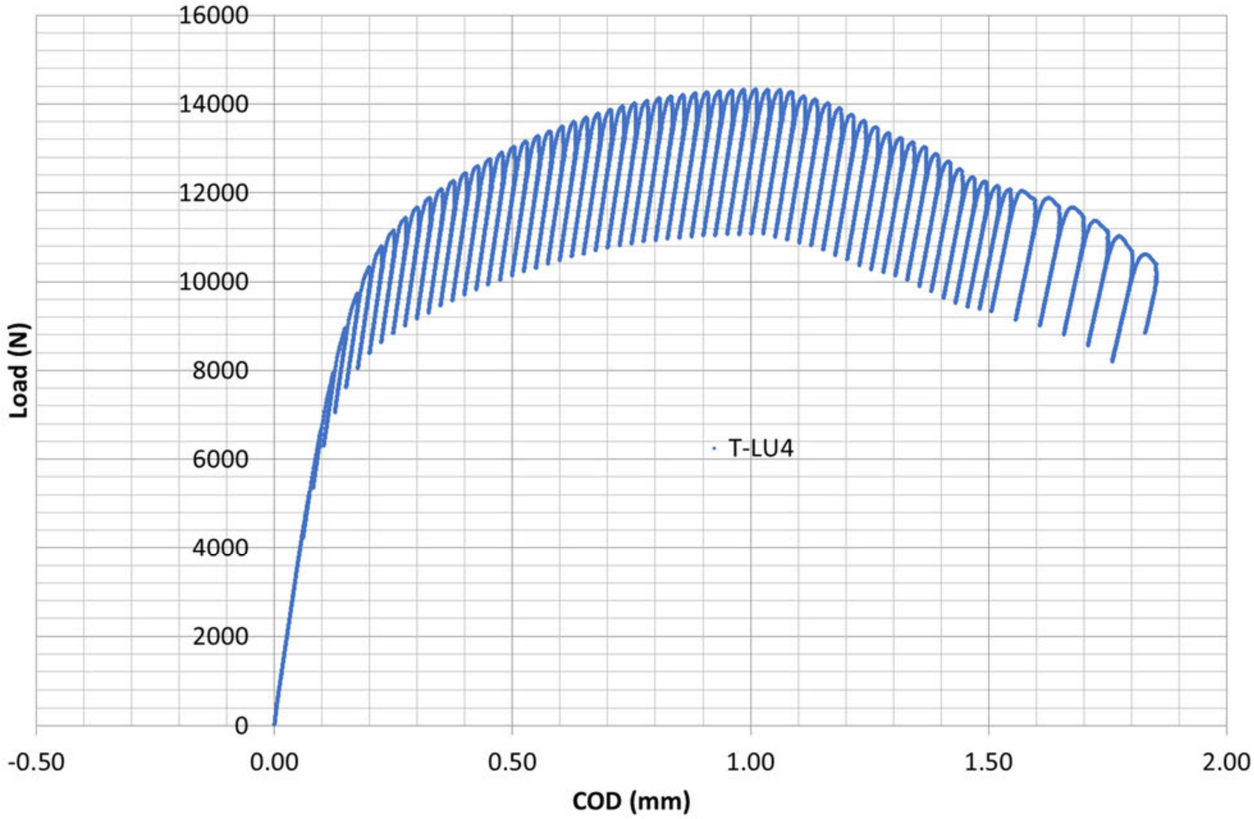

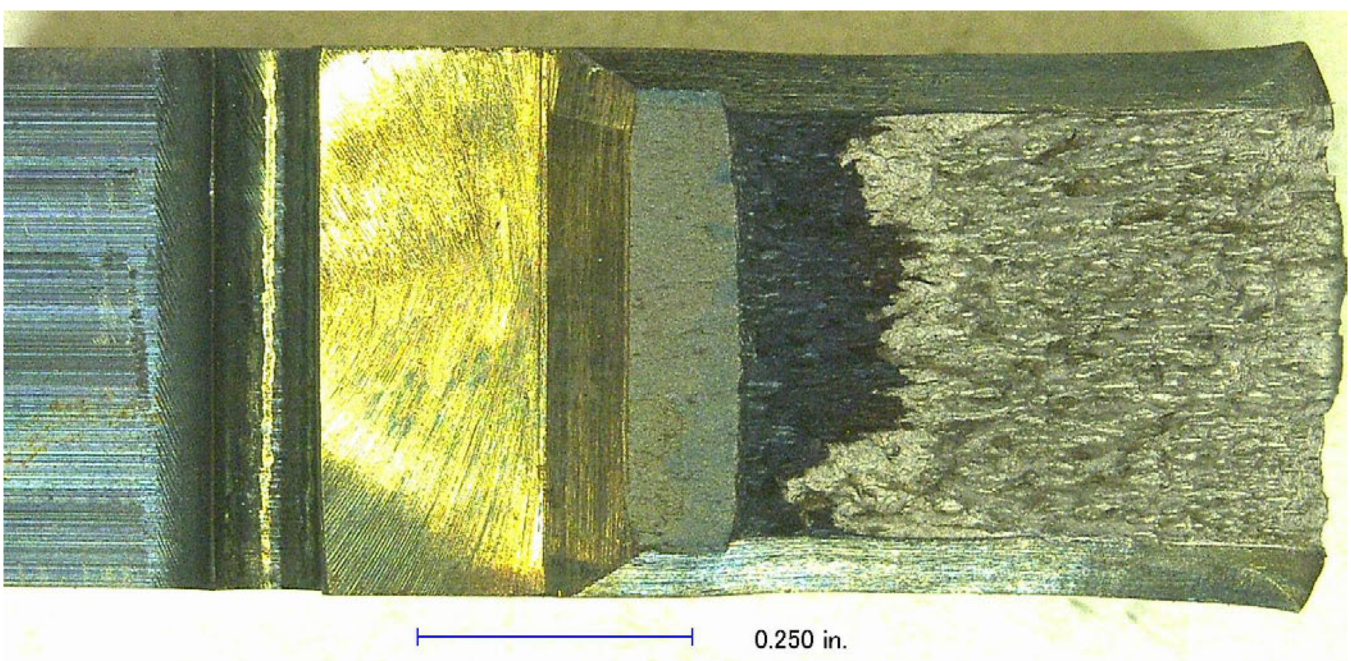

*** This record was final approved on 12/06/2024 08:42:18. (This statement was added by the PRIME system upon its validation)

Specimen ID	T-LU5			J_Q	140.2	kJ/m^2
Fluence	0	n/cm^2		C1	203.3	
Test Temperature	199	°C		C2	0.36	
Width [W]	25.40	mm		KJ_Q	171.8	Mpa√m
Thickness [B]	12.70	mm		**J-R Curve Valid; A8**		
Tensile Strength	534	MPa			Jmax; A8.3.1	YES
Yield Strength	385	MPa			Δamax; A8.3.2	YES
Net Thickness	9.95	mm			a final crack straightness; 9.1.4.2	Minor
Initial adjusted crack length	11.72	mm		**J_{Ic} Valid; A9**		
Initial fatigue crack length (measured)	12.08	mm			a0 crack straightness; 9.1.4.1	YES
Final crack length (calculated)	14.35	mm			Points between exclusion lines; A9.6.6.6 or A9.7	YES
Final crack length (measured)	14.87	mm			Initial crack length agreement; A9.9.2.1	YES
					Initial crack length Adjustment; A9.9.2.2	YES
					Precycle crack length consistency; 8.6.3.1	YES
					Δa predicted vs optical; 9.1.5.2	YES

Sequence	**Peak Load (kN)**	**Peak CMOD (mm)**	**a (mm)**	**Δa (mm)**	**K (MPa√m)**	**J (kJ/m^2)**
1	6.7	0.09	11.73	0.02	32.0	4.9
2	8.0	0.12	11.70	-0.01	38.5	8.0
3	9.2	0.14	11.75	0.04	44.3	11.7
4	10.0	0.17	11.73	0.01	48.2	15.8
5	10.6	0.20	11.71	0.00	51.1	20.2
6	11.1	0.22	11.74	0.03	53.5	24.8
7	11.4	0.25	11.71	-0.01	54.8	29.9
8	11.6	0.27	11.76	0.04	56.2	34.8
9	11.8	0.30	11.75	0.03	57.1	39.9
10	12.0	0.33	11.77	0.05	58.0	44.9
11	12.1	0.35	11.79	0.07	58.8	49.8
12	12.3	0.38	11.79	0.08	59.5	55.0
13	12.4	0.40	11.83	0.11	60.2	60.0
14	12.5	0.43	11.81	0.09	60.7	65.6
15	12.6	0.45	11.83	0.12	61.4	70.7
16	12.7	0.48	11.83	0.11	61.8	76.2
17	12.8	0.50	11.80	0.09	62.2	81.8
18	12.9	0.53	11.85	0.13	62.8	86.9
19	13.0	0.55	11.82	0.11	63.2	92.7
20	13.1	0.58	11.86	0.15	63.8	97.9
21	13.1	0.60	11.89	0.17	64.2	103.2
22	13.1	0.63	11.89	0.17	64.4	108.8
23	13.2	0.66	11.94	0.22	65.0	113.8
24	13.2	0.68	11.93	0.22	65.1	119.5
25	13.3	0.71	11.97	0.26	65.7	124.7
26	13.3	0.73	12.00	0.28	66.0	130.2
27	13.3	0.76	12.01	0.29	66.3	135.8
28	13.4	0.78	12.07	0.36	67.0	140.6
29	13.4	0.81	12.10	0.38	67.3	146.0
30	13.4	0.83	12.13	0.42	67.5	151.2
31	13.4	0.86	12.17	0.46	67.8	156.3
32	13.4	0.88	12.20	0.48	67.9	161.7
33	13.3	0.91	12.29	0.58	68.4	165.8
34	13.2	0.93	12.33	0.61	68.3	171.1
35	13.2	0.96	12.39	0.68	68.4	175.5
36	13.1	0.99	12.44	0.73	68.5	180.3
37	13.1	1.01	12.47	0.75	68.5	185.5
38	13.0	1.04	12.55	0.84	68.9	189.7
39	12.9	1.06	12.59	0.88	68.8	194.6
40	12.8	1.09	12.66	0.95	68.9	198.8
41	12.7	1.11	12.70	0.99	68.6	203.7
42	12.6	1.14	12.81	1.10	68.8	206.9
43	12.5	1.16	12.91	1.20	69.1	210.2
44	12.5	1.19	12.93	1.21	69.0	215.5
45	12.4	1.21	13.04	1.32	69.9	218.3
46	12.4	1.24	13.08	1.37	70.1	223.1
47	12.3	1.27	13.17	1.45	70.4	226.7
48	12.3	1.29	13.24	1.52	70.7	230.3
49	12.2	1.32	13.24	1.53	70.6	236.0
50	12.2	1.34	13.30	1.58	70.8	240.3
51	12.1	1.37	13.33	1.62	70.7	245.1
52	12.0	1.39	13.38	1.66	70.7	249.4
53	12.0	1.42	13.45	1.73	70.9	253.2
54	11.9	1.44	13.47	1.76	70.6	258.0
55	11.6	1.47	13.57	1.86	70.0	260.8
56	11.4	1.49	13.60	1.89	68.8	265.4
57	11.2	1.52	13.73	2.02	68.6	266.8
58	11.0	1.54	13.87	2.16	68.8	267.7
59	10.9	1.57	13.95	2.24	68.8	270.5
60	10.5	1.62	14.12	2.41	68.2	275.4
61	10.4	1.67	14.21	2.50	68.0	282.7
62	10.2	1.72	14.35	2.64	67.9	288.2

*** This record was final approved on 12/06/2024 08:42:18. (This statement was added by the PRIME system upon its validation)

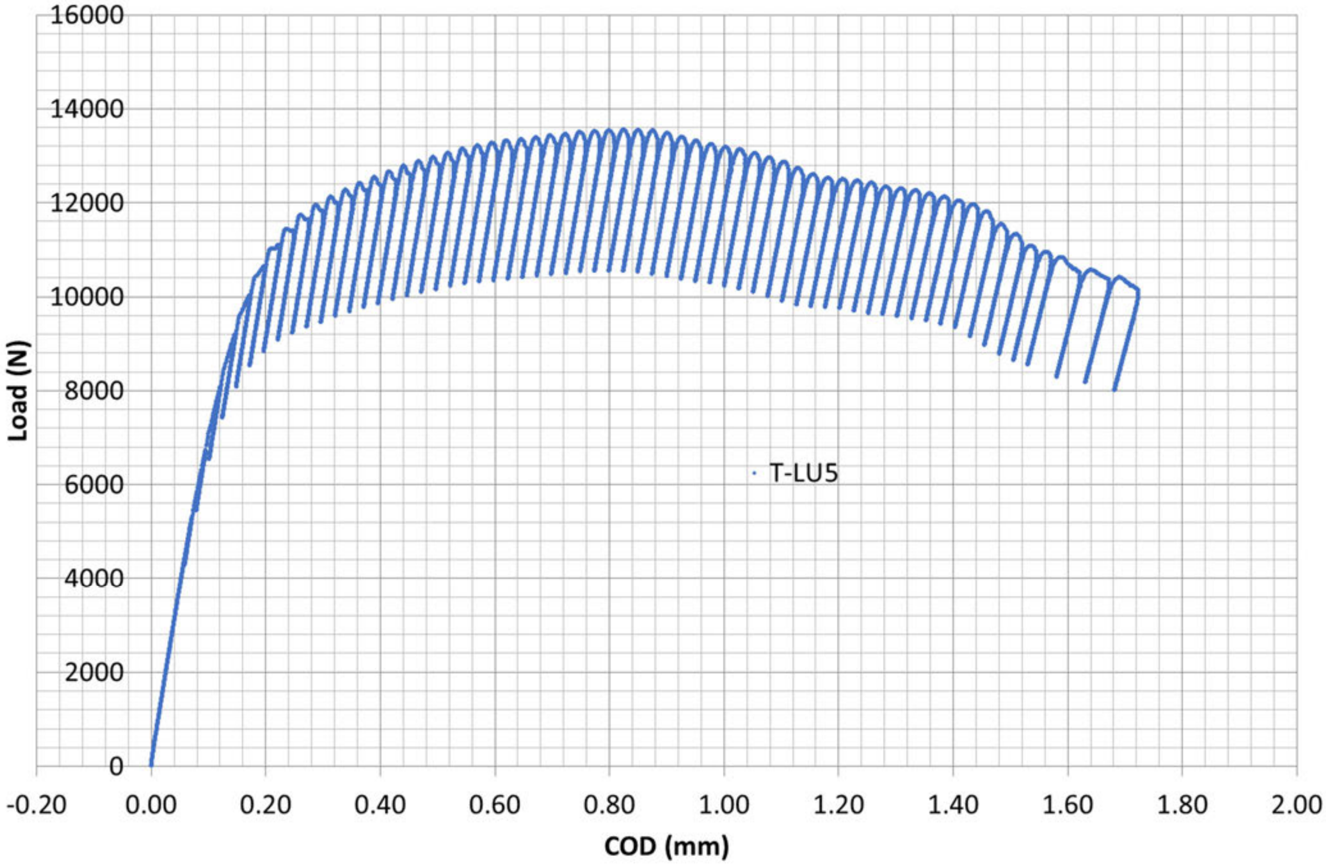

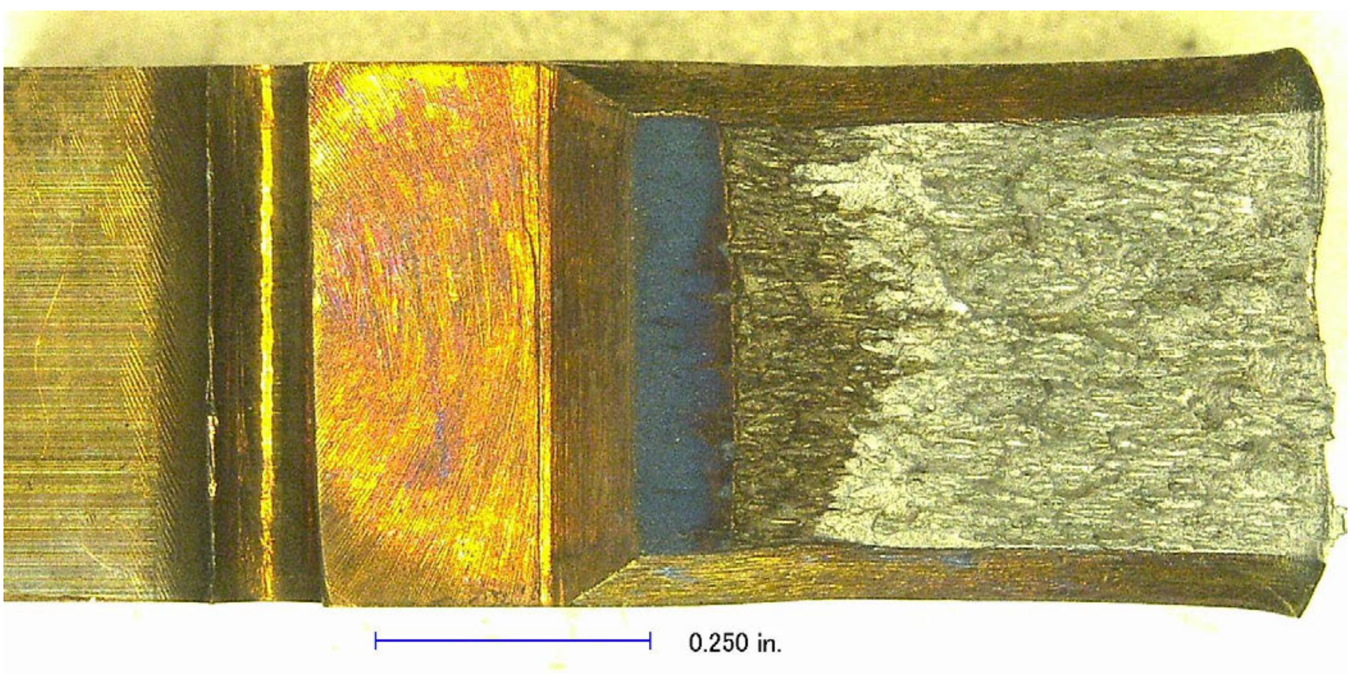

*** This record was final approved on 12/06/2024 08:42:18. (This statement was added by the PRIME system upon its validation)

Specimen ID	T-LU6			J_Q	161.8	kJ/m^2
Fluence	0	n/cm^2		C1	229.8	
Test Temperature	199	°C		C2	0.36	
Width [W]	25.40	mm		KJ_Q	184.5	Mpa√m
Thickness [B]	12.70	mm		**J-R Curve Valid; A8**		
Tensile Strength	534	MPa			Jmax; A8.3.1	YES
Yield Strength	385	MPa			Δamax; A8.3.2	YES
Net Thickness	9.95	mm		a final crack straightness; 9.1.4.2		Minor
Initial adjusted crack length	11.67	mm		**J_{Ic} Valid; A9**		
Initial fatigue crack length (measured)	12.08	mm		a0 crack straightness; 9.1.4.1		YES
Final crack length (calculated)	14.33	mm	Points between exclusion lines; A9.6.6.6 or A9.7			YES
Final crack length (measured)	14.93	mm	Initial crack length agreement; A9.9.2.1			YES
			Initial crack length Adjustment; A9.9.2.2			YES
			Precycle crack length consistency; 8.6.3.1			YES
			Δa predicted vs optical; 9.1.5.2			YES
Sequence	**Peak Load (kN)**	**Peak CMOD (mm)**	**a (mm)**	**Δa (mm)**	**K (MPa√m)**	**J (kJ/m^2)**
1	6.7	0.09	11.70	0.02	32.1	4.9
2	8.1	0.12	11.73	0.05	38.8	8.0
3	9.2	0.14	11.72	0.05	44.3	11.7
4	10.1	0.17	11.70	0.03	48.3	15.9
5	10.7	0.20	11.70	0.02	51.1	20.3
6	11.1	0.22	11.70	0.03	53.4	24.9
7	11.5	0.25	11.69	0.02	55.0	29.8
8	11.7	0.27	11.68	0.00	56.0	34.9
9	11.9	0.30	11.69	0.02	57.1	40.0
10	12.1	0.32	11.71	0.03	58.0	44.9
11	12.2	0.35	11.71	0.03	58.7	50.0
12	12.4	0.37	11.75	0.08	59.7	55.0
13	12.5	0.40	11.75	0.08	60.2	60.3
14	12.6	0.42	11.76	0.08	60.8	65.6
15	12.7	0.45	11.78	0.11	61.5	70.8
16	12.8	0.48	11.77	0.09	61.9	76.4
17	12.9	0.50	11.80	0.13	62.7	81.5
18	13.0	0.53	11.81	0.13	63.2	87.0
19	13.1	0.55	11.84	0.16	63.8	92.3
20	13.2	0.58	11.85	0.18	64.4	97.7
21	13.3	0.60	11.86	0.19	64.8	103.4
22	13.4	0.63	11.88	0.20	65.4	108.8
23	13.4	0.65	11.86	0.19	65.5	114.8
24	13.5	0.68	11.89	0.21	66.1	120.2
25	13.5	0.70	11.90	0.23	66.4	125.8
26	13.6	0.73	11.92	0.25	66.9	131.3
27	13.7	0.75	11.98	0.30	67.6	136.4
28	13.7	0.78	11.95	0.28	67.6	142.7
29	13.8	0.81	11.99	0.32	68.2	147.9
30	13.8	0.83	12.00	0.33	68.3	153.8
31	13.8	0.86	12.02	0.35	68.7	159.3
32	13.8	0.88	12.06	0.39	69.0	164.5
33	13.8	0.91	12.07	0.39	68.9	170.5
34	13.8	0.93	12.15	0.48	69.6	174.8
35	13.8	0.96	12.18	0.51	69.8	180.3
36	13.8	0.98	12.23	0.56	70.1	185.4
37	13.8	1.01	12.28	0.60	70.5	190.3
38	13.7	1.03	12.31	0.63	70.7	195.8
39	13.7	1.06	12.35	0.68	71.1	200.7
40	13.7	1.09	12.41	0.74	71.5	205.6
41	13.7	1.11	12.44	0.77	71.5	210.8
42	13.7	1.14	12.52	0.85	72.1	214.9
43	13.6	1.16	12.55	0.88	72.1	220.3
44	13.5	1.19	12.63	0.95	72.3	224.6
45	13.4	1.21	12.66	0.99	71.8	229.8
46	13.3	1.24	12.71	1.04	71.8	234.5
47	13.2	1.26	12.78	1.11	71.9	238.6
48	13.1	1.29	12.84	1.17	71.8	243.0
49	13.0	1.31	12.92	1.25	71.7	246.7
50	12.9	1.34	12.96	1.29	71.7	251.5
51	12.8	1.37	13.02	1.35	71.8	255.7
52	12.7	1.39	13.10	1.43	72.1	259.2
53	12.6	1.42	13.14	1.47	71.5	263.9
54	12.5	1.44	13.24	1.57	71.9	266.7
55	12.4	1.47	13.28	1.60	71.8	271.5
56	12.3	1.49	13.33	1.66	71.8	275.4
57	12.2	1.52	13.37	1.70	71.7	280.1
58	12.1	1.54	13.42	1.75	71.5	284.2
59	12.0	1.57	13.51	1.84	71.7	286.8
60	11.9	1.59	13.53	1.86	71.3	291.8
61	11.3	1.65	13.68	2.00	69.0	298.3
62	11.0	1.70	13.82	2.14	68.2	304.0
63	10.6	1.75	13.99	2.32	67.3	308.2
64	10.3	1.80	14.14	2.46	67.0	312.9
65	10.0	1.85	14.33	2.65	66.5	315.9

*** This record was final approved on 12/06/2024 08:42:18. (This statement was added by the PRIME system upon its validation)

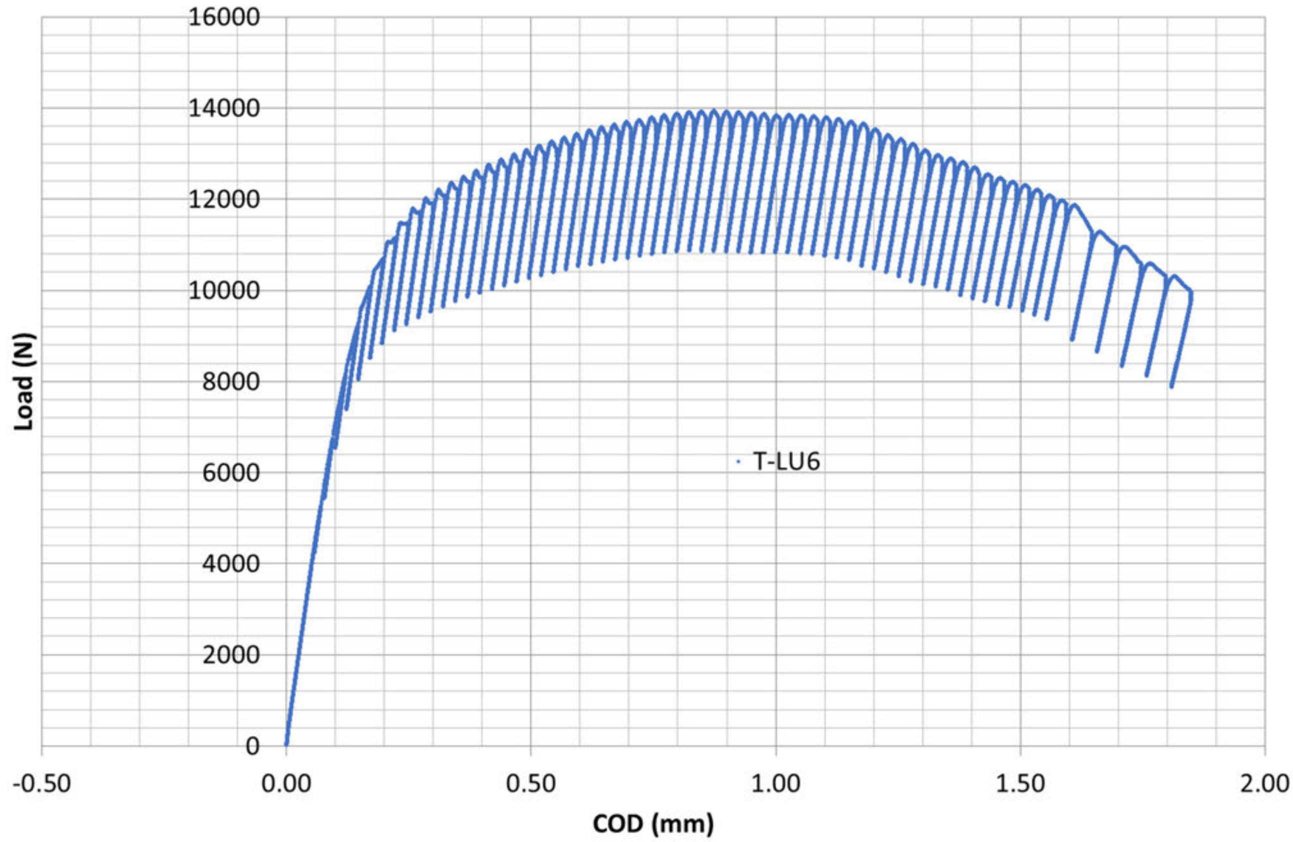

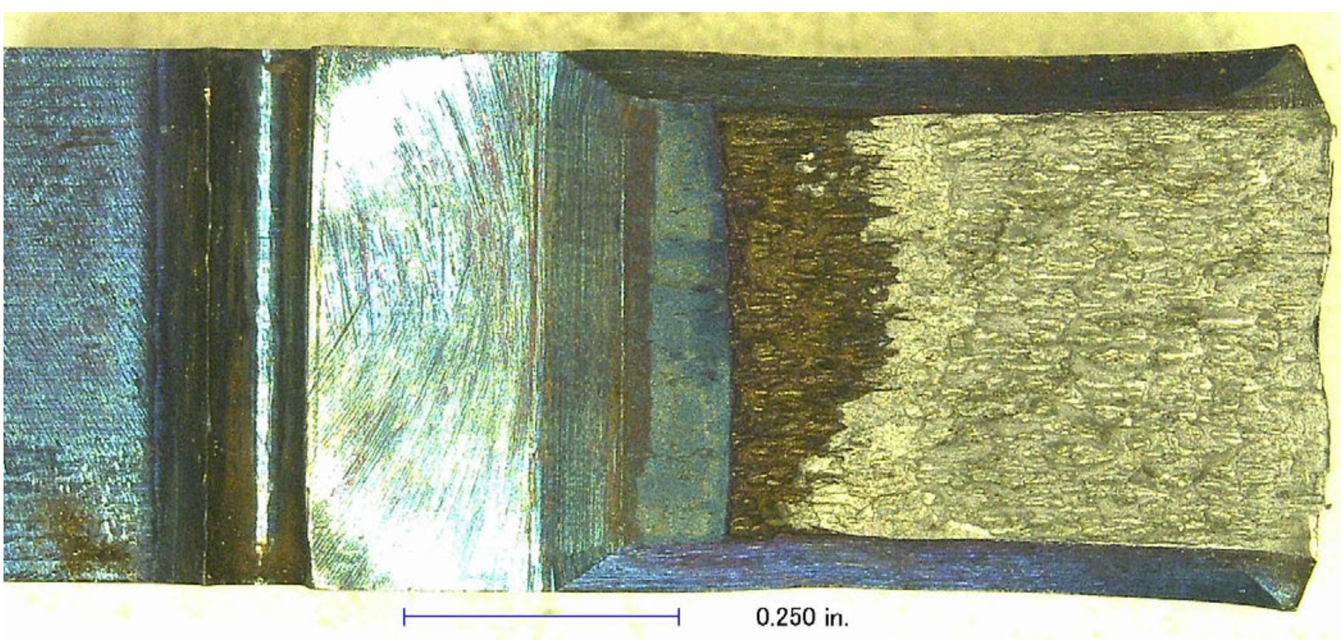

*** This record was final approved on 12/06/2024 08:42:18. (This statement was added by the PRIME system upon its validation)

Specimen ID	T-LB8			J_Q	123.0	kJ/m^2
Fluence	0	n/cm^2		C1	199.7	
Test Temperature	199	°C		C2	0.44	
Width [W]	25.40	mm		KJ_Q	160.9	Mpa√m
Thickness [B]	12.70	mm		**J-R Curve Valid; A8**		
Tensile Strength	534	MPa			Jmax; A8.3.1	YES
Yield Strength	385	MPa			Δamax; A8.3.2	YES
Net Thickness	9.95	mm		a final crack straightness; 9.1.4.2		YES
Initial adjusted crack length	11.81	mm		**J_{Ic} Valid; A9**		
Initial fatigue crack length (measured)	12.08	mm		a0 crack straightness; 9.1.4.1		YES
Final crack length (calculated)	14.63	mm	Points between exclusion lines; A9.6.6.6 or A9.7			YES
Final crack length (measured)	15.23	mm	Initial crack length agreement; A9.9.2.1			YES
			Initial crack length Adjustment; A9.9.2.2			Minor
			Precycle crack length consistency; 8.6.3.1			YES
			Δa predicted vs optical; 9.1.5.2			YES
Sequence	**Peak Load (kN)**	**Peak CMOD (mm)**	**a (mm)**	**Δa (mm)**	**K (MPa√m)**	**J (kJ/m^2)**
1	6.7	0.10	11.83	0.02	32.4	5.0
2	8.0	0.12	11.85	0.04	39.0	8.1
3	9.1	0.15	11.80	0.00	44.3	11.8
4	10.0	0.18	11.85	0.04	48.8	15.9
5	10.6	0.20	11.82	0.01	51.7	20.4
6	11.1	0.23	11.83	0.02	54.1	25.0
7	11.4	0.25	11.84	0.03	55.7	29.8
8	11.7	0.28	11.84	0.03	56.9	35.0
9	11.9	0.30	11.87	0.06	58.0	40.0
10	12.0	0.33	11.86	0.06	58.8	45.2
11	12.2	0.36	11.89	0.08	59.8	50.2
12	12.3	0.38	11.89	0.09	60.3	55.5
13	12.4	0.41	11.90	0.10	61.0	60.6
14	12.6	0.43	11.94	0.13	61.9	65.8
15	12.6	0.46	11.90	0.10	62.1	71.5
16	12.7	0.48	11.95	0.15	62.9	76.5
17	12.8	0.51	11.96	0.16	63.4	81.9
18	12.9	0.53	11.97	0.16	63.8	87.4
19	13.0	0.56	11.99	0.18	64.4	92.9
20	13.0	0.58	11.96	0.16	64.4	98.7
21	13.1	0.61	12.00	0.20	65.0	104.0
22	13.1	0.63	12.03	0.22	65.3	109.3
23	13.1	0.66	12.05	0.24	65.4	114.8
24	13.1	0.69	12.10	0.29	65.8	119.7
25	13.1	0.71	12.11	0.31	65.7	125.3
26	13.1	0.74	12.20	0.39	66.3	129.7
27	13.1	0.76	12.21	0.41	66.4	135.1
28	13.0	0.79	12.26	0.45	66.6	140.1
29	13.0	0.81	12.31	0.51	66.9	144.9
30	13.0	0.84	12.36	0.55	67.1	150.1
31	13.0	0.86	12.41	0.61	67.6	154.8
32	13.0	0.89	12.46	0.65	68.0	159.7
33	13.0	0.91	12.49	0.68	68.2	164.9
34	13.0	0.94	12.55	0.74	68.6	169.5
35	13.0	0.96	12.56	0.76	68.7	175.0
36	12.9	0.99	12.62	0.82	69.1	179.8
37	12.9	1.02	12.63	0.83	69.1	185.2
38	12.9	1.04	12.69	0.88	69.5	190.0
39	12.9	1.07	12.72	0.91	69.7	195.1
40	12.8	1.09	12.75	0.95	69.5	200.2
41	12.8	1.12	12.82	1.01	69.9	204.4
42	12.7	1.14	12.86	1.05	69.8	209.4
43	12.6	1.17	12.91	1.11	69.8	213.9
44	12.5	1.19	12.96	1.15	69.7	218.5
45	12.4	1.22	13.04	1.23	69.6	222.2
46	12.3	1.24	13.10	1.30	69.8	226.3
47	12.3	1.27	13.13	1.33	69.7	231.2
48	12.1	1.30	13.21	1.41	69.7	234.8
49	12.0	1.32	13.28	1.47	69.5	238.5
50	11.9	1.35	13.36	1.56	69.4	241.9
51	11.7	1.37	13.45	1.64	69.3	245.1
52	11.5	1.40	13.50	1.69	68.6	249.2
53	11.4	1.42	13.60	1.79	68.9	251.7
54	11.3	1.45	13.65	1.85	68.9	255.6
55	11.2	1.47	13.73	1.92	68.8	258.7
56	11.1	1.50	13.86	2.05	69.2	260.1
57	11.0	1.52	13.93	2.13	69.2	263.2
58	10.9	1.55	14.02	2.21	69.4	265.8
59	10.8	1.57	14.04	2.23	69.2	270.4
60	10.7	1.60	14.11	2.31	69.1	273.5
61	10.6	1.63	14.19	2.39	69.0	276.1
62	10.4	1.65	14.26	2.45	68.8	279.2
63	10.0	1.70	14.50	2.69	68.0	281.1
64	9.7	1.75	14.63	2.83	67.8	286.5

*** This record was final approved on 12/06/2024 08:42:18. (This statement was added by the PRIME system upon its validation)

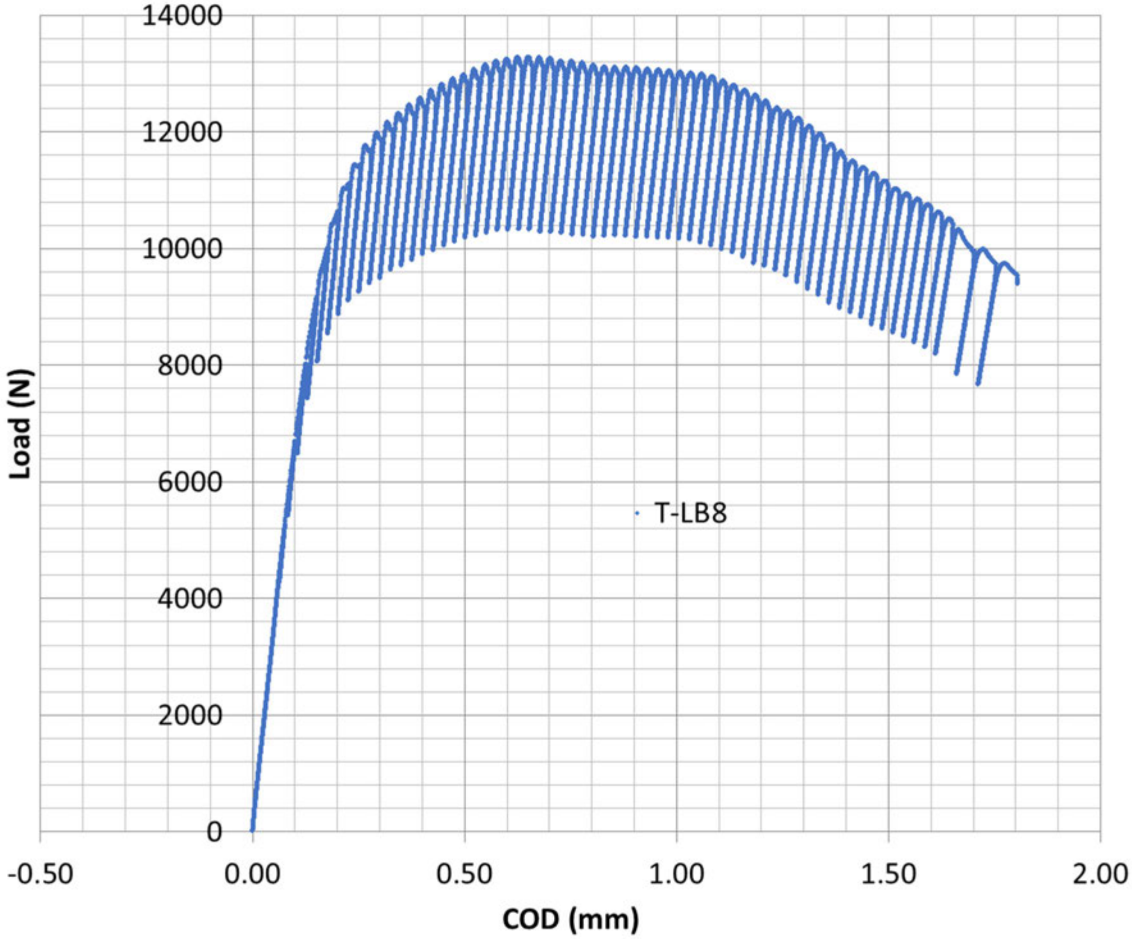

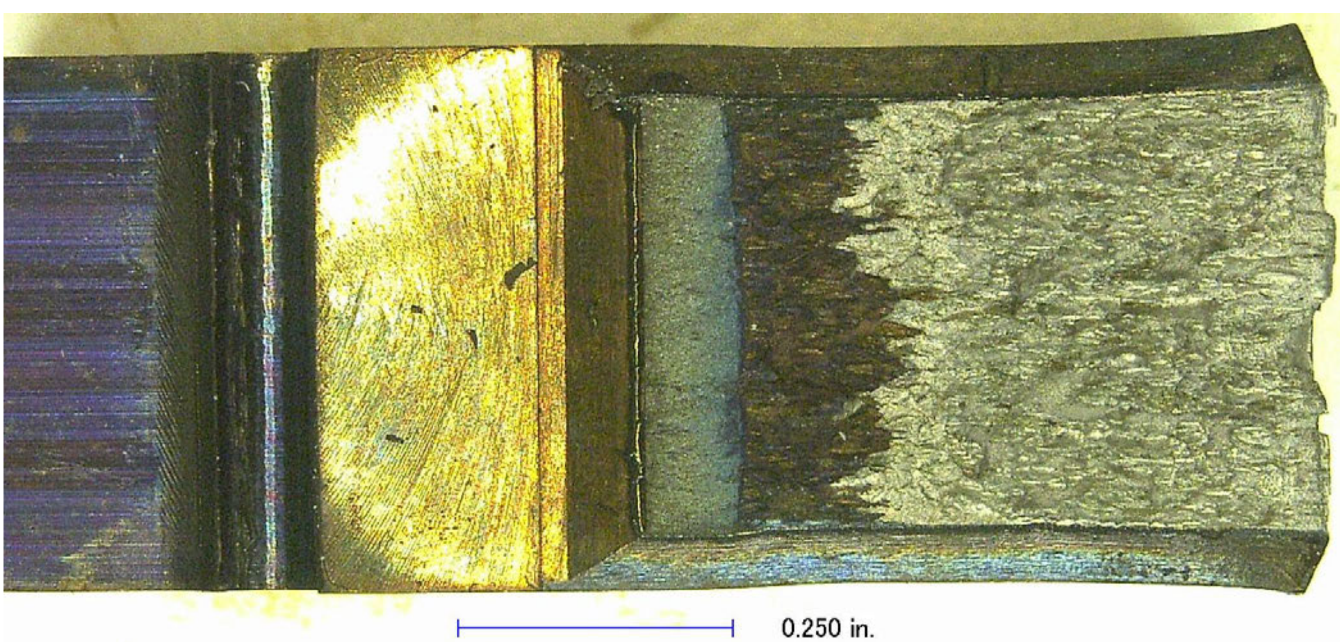

*** This record was final approved on 12/06/2024 08:42:18. (This statement was added by the PRIME system upon its validation)

Specimen ID	PB			J_Q	402.3	kJ/m^2
Fluence	4.42	n/cm^2		C1	505.7	
Test Temperature	-31	°C		C2	0.35	
Width [W]	8.48	mm		KJ_Q	301.7	Mpa√m
Thickness [B]	3.96	mm		**J-R Curve Valid; A8**		
Tensile Strength	685	MPa		Jmax; A8.3.1		NO
Yield Strength	554	MPa		Δamax; A8.3.2		YES
Net Thickness	3.96	mm		a final crack straightness; 9.1.4.2		NO
Initial adjusted crack length	4.25	mm		**J_{Ic} Valid; A9**		
Initial fatigue crack length (measured)	4.12	mm		a0 crack straightness; 9.1.4.1		YES
Final crack length (calculated)	5.69	mm	Points between exclusion lines; A9.6.6.6 or A9.7			YES
Final crack length (measured)	5.63	mm	Initial crack length agreement; A9.9.2.1			YES
			Initial crack length Adjustment; A9.9.2.2			NO
			Precycle crack length consistency; 8.6.3.1			YES
			Δa predicted vs optical; 9.1.5.2			YES
Sequence	**Peak Load (kN)**	**Peak CMOD (mm)**	**a (mm)**	**Δa (mm)**	**K (MPa√m)**	**J (kJ/m^2)**
1	1.0	0.05	4.20	-0.04	26.6	3.1
2	1.4	0.07	4.20	-0.04	37.8	7.4
3	1.8	0.10	4.24	0.00	46.6	12.6
4	2.0	0.12	4.25	0.01	51.9	19.1
5	2.0	0.15	4.29	0.04	54.8	26.0
6	2.1	0.17	4.32	0.07	56.4	32.3
7	2.1	0.20	4.23	-0.01	55.6	40.4
8	2.1	0.22	4.30	0.05	57.3	46.7
9	2.1	0.25	4.26	0.01	57.2	54.2
10	2.2	0.27	4.31	0.07	58.8	60.9
11	2.2	0.30	4.30	0.05	59.1	68.0
12	2.2	0.33	4.34	0.09	60.6	76.6
13	2.2	0.35	4.34	0.10	61.1	82.5
14	2.2	0.38	4.24	-0.01	59.1	95.0
15	2.3	0.40	4.38	0.14	62.9	96.1
16	2.3	0.43	4.32	0.08	61.9	107.2
17	2.3	0.45	4.29	0.04	61.6	114.8
18	2.3	0.47	4.30	0.06	62.1	122.6
19	2.3	0.51	4.36	0.12	63.9	130.1
20	2.3	0.52	4.35	0.10	64.1	136.9
21	2.3	0.56	4.35	0.11	64.2	146.8
22	2.3	0.57	4.36	0.11	64.6	152.1
23	2.4	0.60	4.35	0.10	64.7	160.2
24	2.4	0.62	4.30	0.06	64.0	171.9
25	2.4	0.65	4.30	0.06	64.2	179.3
26	2.4	0.67	4.26	0.01	63.2	191.0
27	2.4	0.70	4.31	0.07	64.8	195.1
28	2.4	0.73	4.37	0.13	66.1	199.5
29	2.4	0.75	4.44	0.19	67.7	204.0
30	2.4	0.78	4.42	0.17	67.3	213.1
31	2.4	0.80	4.39	0.14	66.6	223.0
32	2.4	0.83	4.47	0.23	69.0	225.2
33	2.4	0.85	4.53	0.29	70.7	229.6
34	2.4	0.87	4.49	0.24	69.3	239.6
35	2.4	0.90	4.44	0.20	68.2	252.1
36	2.4	0.93	4.52	0.28	70.2	256.6
37	2.4	0.95	4.53	0.29	70.6	261.3
38	2.4	0.98	4.53	0.28	70.3	271.1
39	2.4	1.01	4.48	0.24	68.6	286.2
40	2.4	1.02	4.62	0.38	72.2	278.2
41	2.3	1.06	4.58	0.34	70.8	293.7
42	2.3	1.07	4.60	0.35	71.2	297.0
43	2.3	1.11	4.61	0.37	71.5	307.7
44	2.3	1.12	4.56	0.32	70.1	317.9
45	2.3	1.15	4.81	0.56	77.3	300.8
46	2.3	1.18	4.49	0.24	67.8	347.5
47	2.3	1.21	4.60	0.36	70.8	342.6
48	2.3	1.23	4.75	0.50	75.0	332.9
49	2.3	1.25	4.64	0.39	71.7	353.5
50	2.3	1.28	4.62	0.38	70.8	367.5
51	2.3	1.31	4.81	0.57	75.9	349.8
52	2.3	1.34	4.71	0.47	72.4	373.7
53	2.3	1.35	4.75	0.51	73.7	371.9
54	2.2	1.38	4.76	0.51	71.2	383.0
55	2.3	1.40	4.69	0.45	71.6	398.1
56	2.3	1.44	4.74	0.50	72.3	403.3
57	2.2	1.45	4.81	0.56	73.0	398.9
58	2.2	1.47	4.72	0.47	71.5	419.9
59	2.2	1.49	4.73	0.49	72.0	424.5
60	2.2	1.55	4.76	0.52	70.4	438.1
61	2.1	1.60	4.88	0.63	70.8	436.1
62	2.1	1.66	4.89	0.65	70.3	451.1
63	2.0	1.71	4.82	0.58	65.8	479.0
64	2.0	1.76	4.95	0.70	70.8	472.9
65	2.0	1.80	5.01	0.77	72.1	473.6
66	1.9	1.85	5.12	0.87	70.8	469.5
67	1.9	1.92	5.27	1.03	76.5	460.7
68	1.8	1.97	5.19	0.95	71.9	492.3
69	1.8	2.02	5.18	0.94	70.3	510.2
70	1.8	2.06	5.30	1.06	72.8	499.4
71	1.7	2.11	5.40	1.15	72.9	494.8
72	1.7	2.17	5.36	1.12	70.8	519.9
73	1.6	2.22	5.37	1.13	70.4	529.0
74	1.5	2.25	5.34	1.09	64.8	549.0
75	1.6	2.31	5.45	1.20	70.7	538.5
76	1.6	2.36	5.47	1.22	70.3	549.4
77	1.5	2.43	5.51	1.26	70.1	557.8
78	1.5	2.47	5.57	1.32	71.6	554.0
79	1.4	2.52	5.56	1.32	66.7	568.0
80	1.4	2.56	5.54	1.30	67.8	585.2
81	1.4	2.63	5.69	1.45	71.8	564.5

*** This record was final approved on 12/06/2024 08:42:18. (This statement was added by the PRIME system upon its validation)

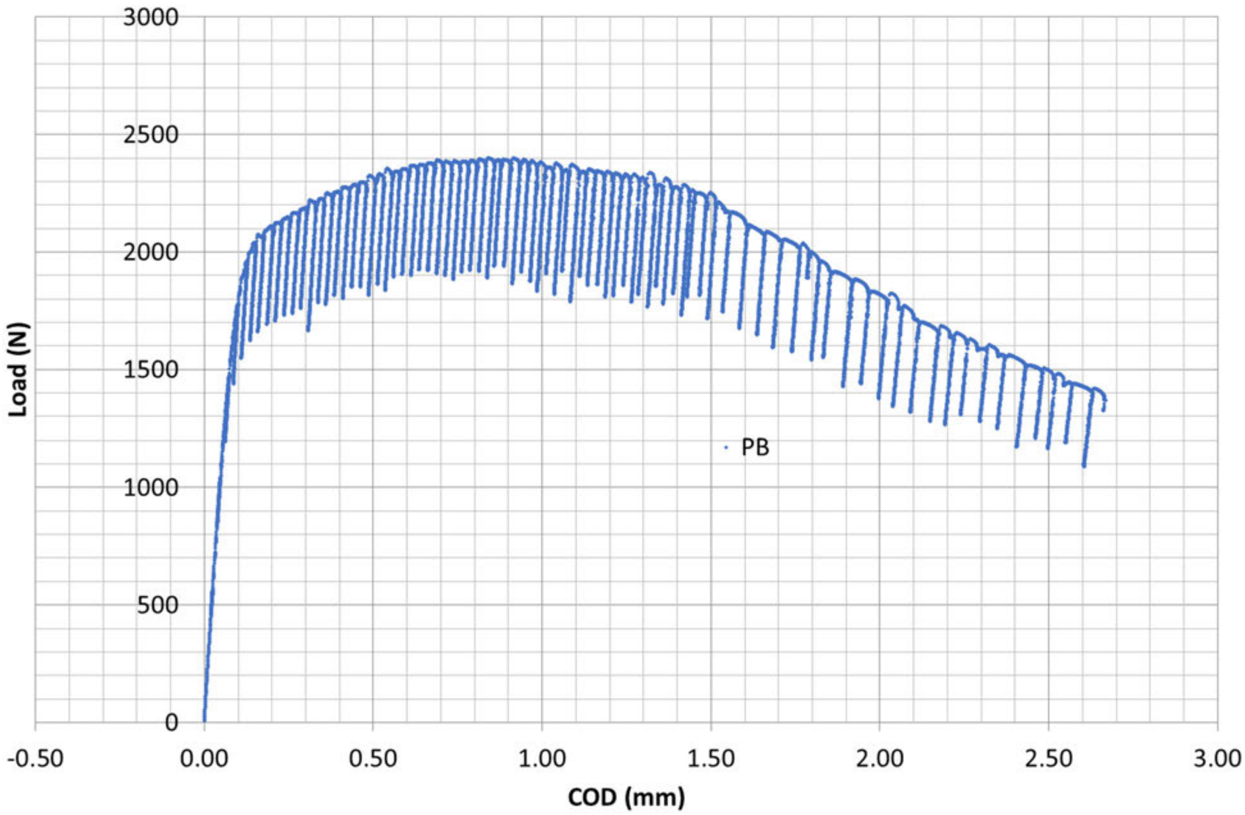

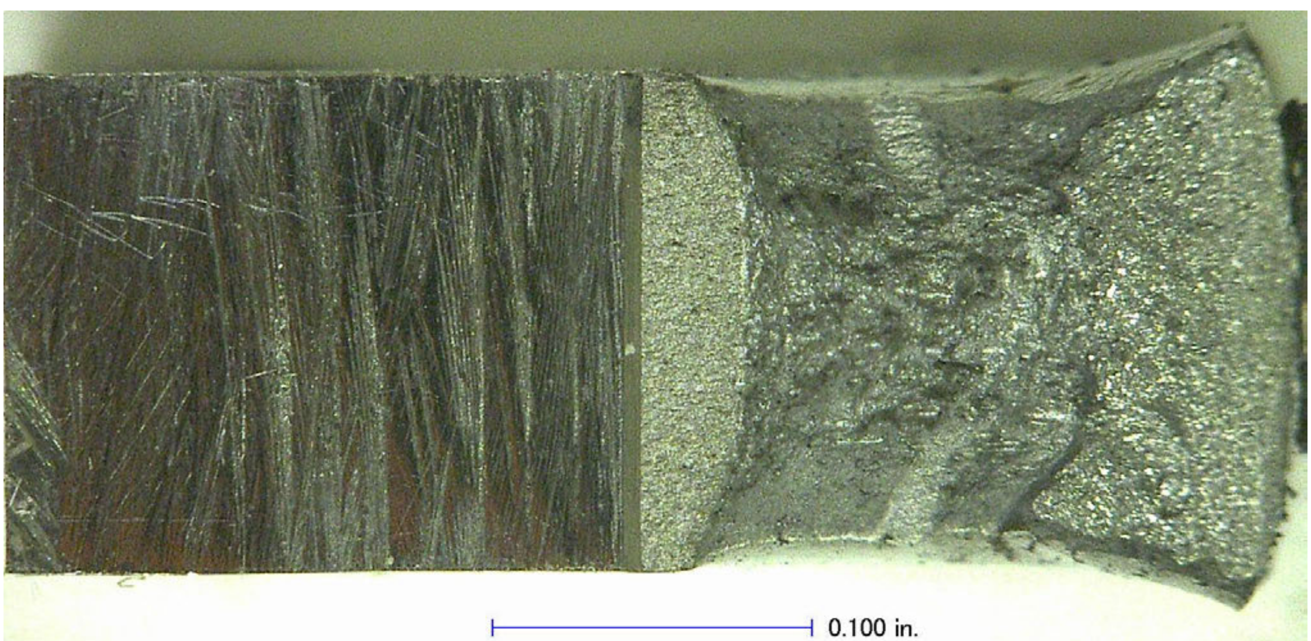

*** This record was final approved on 12/06/2024 08:42:18. (This statement was added by the PRIME system upon its validation)

Specimen ID	WU			J_Q	129.2	kJ/m^2
Fluence	4.42	n/cm^2		C1	252.7	
Test Temperature	78	°C		C2	0.55	
Width [W]	8.3	mm		KJ_Q	168.1	Mpa√m
Thickness [B]	3.96	mm		**J-R Curve Valid; A8**		
Tensile Strength	746	MPa			Jmax; A8.3.1	YES
Yield Strength	650	MPa			Δamax; A8.3.2	YES
Net Thickness	3.96	mm		a final crack straightness; 9.1.4.2		NO
Initial adjusted crack length	4.25	mm		**J_{Ic} Valid; A9**		
Initial fatigue crack length (measured)	4.44	mm		a0 crack straightness; 9.1.4.1		Minor
Final crack length (calculated)	5.61	mm	Points between exclusion lines; A9.6.6.6 or A9.7			YES
Final crack length (measured)	6.02	mm	Initial crack length agreement; A9.9.2.1			YES
			Initial crack length Adjustment; A9.9.2.2			Minor
			Precycle crack length consistency; 8.6.3.1			YES
				Δa predicted vs optical; 9.1.5.2		NO
Sequence	**Peak Load (kN)**	**Peak CMOD (mm)**	**a (mm)**	**Δa (mm)**	**K (MPa√m)**	**J (kJ/m^2)**
1	1.0	0.04	*	*	*	*
2	1.4	0.07	4.24	0.00	38.0	6.4
3	1.7	0.09	4.23	-0.02	47.3	12.1
4	2.0	0.12	4.28	0.04	55.5	18.4
5	2.1	0.14	4.30	0.05	60.4	25.6
6	2.2	0.17	4.33	0.08	63.6	33.2
7	2.3	0.19	4.35	0.10	65.2	41.1
8	2.3	0.22	4.31	0.07	64.7	50.1
9	2.3	0.25	4.37	0.12	66.2	57.8
10	2.3	0.27	4.41	0.17	67.1	64.9
11	2.3	0.30	4.45	0.20	67.8	72.2
12	2.3	0.32	4.39	0.15	66.3	82.8
13	2.3	0.35	4.47	0.23	68.0	88.8
14	2.2	0.37	4.43	0.19	66.2	98.2
15	2.2	0.40	4.51	0.26	67.5	103.4
16	2.2	0.43	4.53	0.29	67.3	111.9
17	2.2	0.45	4.54	0.30	66.8	118.0
18	2.1	0.47	4.52	0.27	65.6	127.2
19	2.1	0.50	4.59	0.35	66.8	132.6
20	2.1	0.53	4.60	0.36	66.1	140.9
21	2.1	0.55	4.64	0.40	66.3	145.6
22	2.0	0.58	4.63	0.38	65.2	154.8
23	2.0	0.61	4.66	0.42	65.6	160.3
24	2.0	0.63	4.69	0.45	65.6	166.8
25	2.0	0.65	4.69	0.45	65.1	173.3
26	2.0	0.68	4.75	0.50	65.9	177.7
27	1.9	0.71	4.78	0.53	65.4	183.3
28	1.9	0.74	4.78	0.54	64.4	192.0
29	1.9	0.76	4.81	0.56	64.2	197.2
30	1.8	0.78	4.84	0.60	64.4	200.1
31	1.8	0.81	4.88	0.63	64.1	205.2
32	1.8	0.83	4.88	0.63	63.0	212.9
33	1.7	0.86	4.94	0.70	63.8	214.8
34	1.7	0.89	4.98	0.74	63.7	218.7
35	1.7	0.91	5.01	0.76	63.6	222.1
36	1.6	0.94	5.10	0.85	65.4	223.1
37	1.6	0.96	5.13	0.88	65.4	225.7
38	1.6	0.98	5.17	0.93	65.6	228.7
39	1.6	1.01	5.18	0.93	64.4	236.4
40	1.5	1.03	5.20	0.96	64.2	238.9
41	1.5	1.06	5.26	1.02	65.0	240.2
42	1.5	1.09	5.29	1.05	64.8	245.6
43	1.4	1.12	5.35	1.11	65.4	246.0
44	1.4	1.14	5.42	1.18	66.8	245.4
45	1.4	1.16	5.41	1.16	65.3	252.0
46	1.4	1.20	5.47	1.22	65.7	255.8
47	1.3	1.21	5.49	1.24	65.6	255.4
48	1.3	1.24	5.41	1.17	61.8	271.1
49	1.3	1.27	5.48	1.24	63.0	271.9
50	1.3	1.31	5.58	1.34	65.6	267.3
51	1.3	1.32	5.61	1.36	65.7	267.2
52	1.2	1.35	5.60	1.35	62.3	275.4

*** This record was final approved on 12/06/2024 08:42:18. (This statement was added by the PRIME system upon its validation)

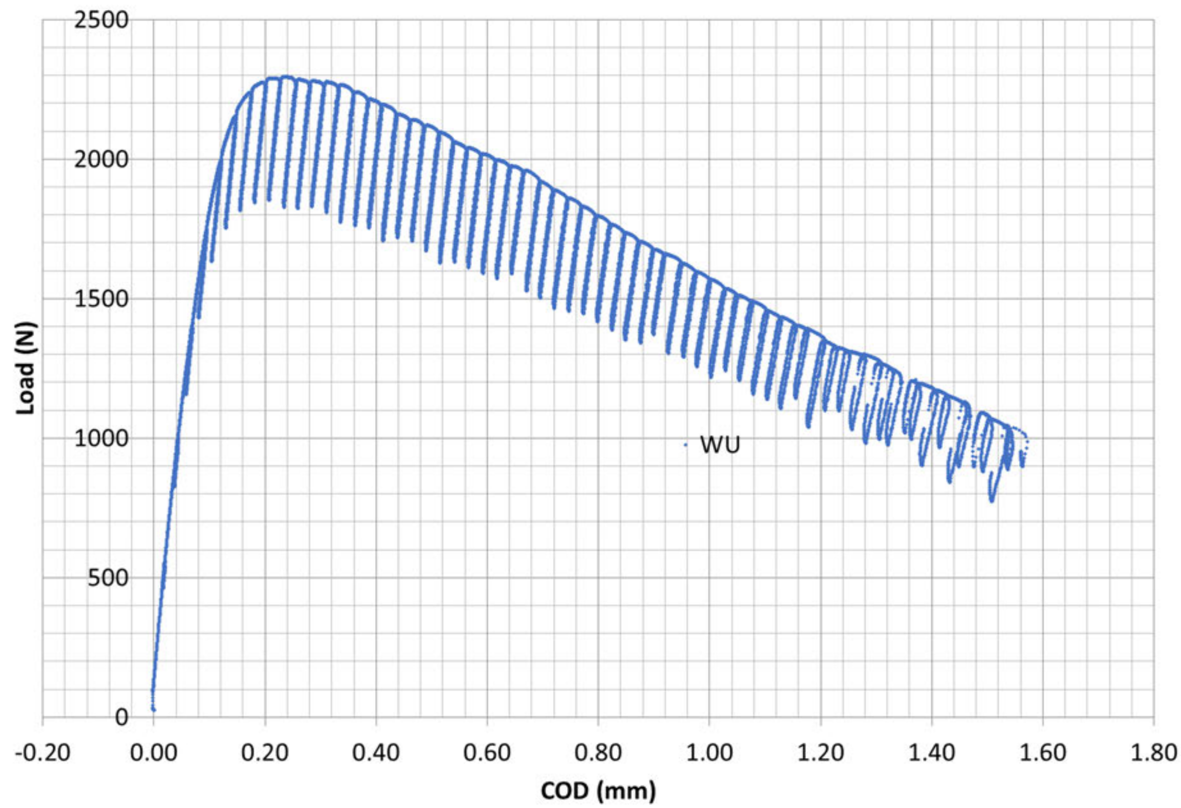

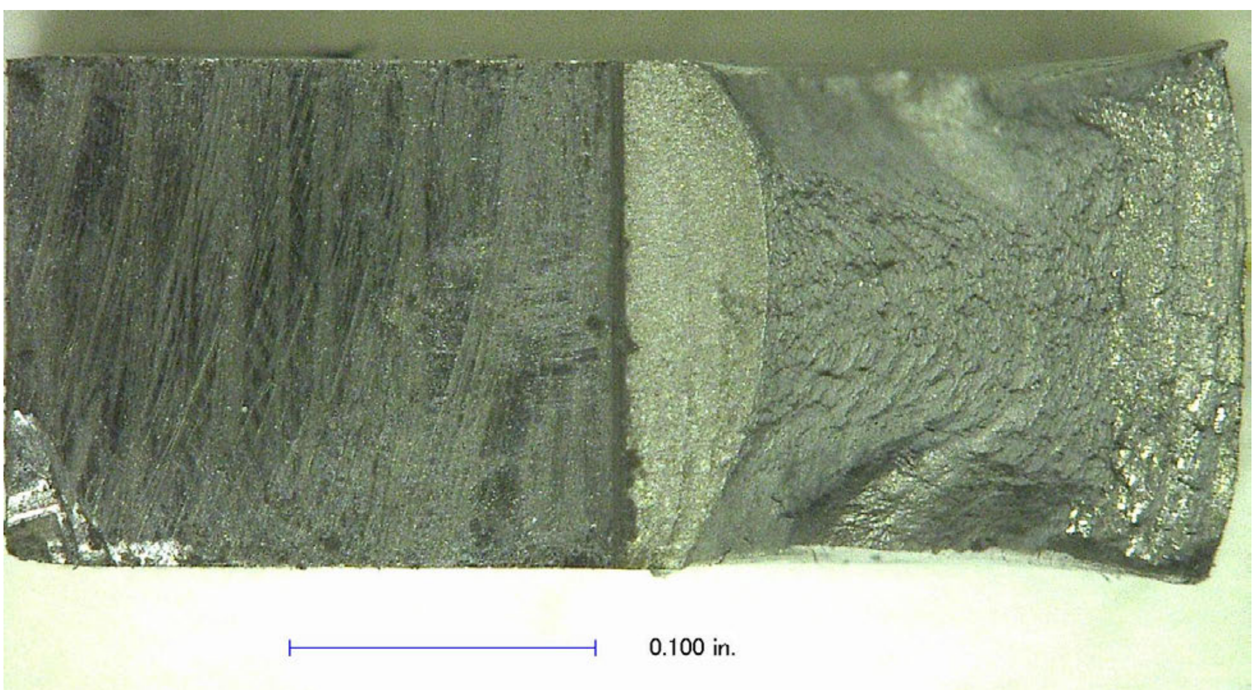

*** This record was final approved on 12/06/2024 08:42:18. (This statement was added by the PRIME system upon its validation)

This page was added to the quality record by the PRIME system upon its validation and shall not be considered in the page numbering of this document.

Approval Information
Author Approval Hall Gordon Z Dec-05-2024 15:04:40
Author Approval Hall J Brian Dec-05-2024 15:14:52
Verifier Approval Hall Gordon Z Dec-05-2024 15:16:52
Verifier Approval Ganta B Reddy Dec-05-2024 17:14:37
Reviewer Approval Demers Thomas E Dec-06-2024 07:55:11
Manager Approval Delport Gerrie W Dec-06-2024 08:42:18

Files approved on Dec-06-2024

*** This record was final approved on 12/06/2024 08:42:18. (This statement was added by the PRIME system upon its validation)